# A Novel Pneumatic Curvilinear Actuator and an Active Gravity Compensation Mechanism for a Gas Powered Above Elbow Prosthesis

Design of a pneumatic actuated elbow mechanism for above elbow prosthesis

A.Sooryanarain

## A Novel Pneumatic Curvilinear Actuator and an Active Gravity Compensation Mechanism for a Gas Powered Above Elbow Prosthesis

Design of a pneumatic actuated elbow mechanism for above elbow prosthesis

Ву

A.Sooryanarain

To obtain the degree of Master of Science At the Delft University of Technology, To be defended publicly on Friday 22nd July, 2016

Student number: 4252241 Thesis committee: Prof.dr.F.C.T.van der Helm Dr. ir. D.H.Plettenburg Dr.ir.J.F.L.Goosen

THE TRUTH IS, MOST OF US DISCOVE	R WHERE WE ARE HEADING WHEN WE ARRIVECalvin, in Calvin and Hobbes by Bill Watterson

### **Preface**

This is my thesis report that comprises of the results of my research on Pneumatically Actuated Elbow Unit for an Above Elbow Prosthesis. As part of the DIPO group's new venture, the goal of this project was to see if a lighter pneumatic powered elbow unit could be designed to replace the commercially available electrical elbow units.

The journey I went through during the whole thesis process was a rollercoaster. I 1<sup>st</sup> started my thesis on the topic of Reciprocating Gait Orthosis (RGO). Sadly that didn't go that well; few months after starting the project, I fell ill. It took about a year for me to completely recover, both physically and psychologically. After recovery, I wanted to turn over a new leaf, and this project was that new leaf. I am glad I had a fresh start with a different topic, because of which, now I have come up this new type of fluidic actuator. On the other hand, it is funny when I come to think of it now; I can also use my current concept with the previous topic too.

I would like to thank my supervisor, Dick Plettenburg, along with Jan van Frankenhuyzen and the people from the 3ME workshop for their guidance and support throughout my master thesis project. Special thanks to Just Herder, Milton Aguirre and Jack Schorsch for sharing me some insights and clarifying my doubts on few topics. Thanks to all the other people who helped me to make it this far. **W**/\_

Aravindan Sooryanarain July 14 2016

### Report Outline

This report presents the results of my MSc. Thesis assignment. The report contains an introduction chapter, followed by a scientific paper and design paper. There are additionally, six Appendices for extra background information. The scientific papers contain few sections/lines that are repeated from the introductory chapter, as these papers were written with the intent to be an independent entity and not a continuation of a previous chapter.

Chapter 1 is a brief introduction to the field of upper limb prosthesis; the prime focus is about transhumeral prosthesis. The chapter enumerates the different types of transhumeral prostheses; also discusses the various choices a prosthetic user makes and the rejection rate of the transhumeral prosthesis. In the end, the chapter the design goal of this project is set after defining the problem.

Chapter 2 is the scientific paper about the design and testing of a novel pneumatic curvilinear actuator. The curvilinear actuator is proposed to be used for the elbow unit's primary actuator. The paper provides a summary of the underlying theory and working principle of the proposed curvilinear actuator. The curvilinear actuator was 3D printed. The paper also contains the results of the bench test of the newly proposed curvilinear actuator.

Chapter 3 is a design paper, it provides the basic insight about gravity compensators and the design of a active gravity compensator using a pneumatic multiplex actuator. The paper also gives a brief explanation about the basic theory of the multiplex actuator and also about the locking mechanism used. The active gravity compensator was designed to meet the load and spatial constraints of the elbow unit. Only the theory and 3D modeling of the gravity compensator was done part of the paper. The testing of the active gravity compensator needs to be done for future work.

Chapter 4 is the Appendix of the thesis report. It contains the additional information of the whole design process that were not included in the two paper, some parts of it might have repeating elements from the paper, but this for telling how the addition data is achieved. Appendix A is about the overall design approach of this project. Appendix B is about the design of a outer shell used for the elbow prosthesis. Appendix C and D talks about the design algorithm used to design the active gravity compensator and curvilinear actuator. Then the Matlab code for the optimization algorithm is given in appendix E and F. At the end of the Appendix there is a reference section for the references that were used in the Appendix.

Finally, Chapter 5 is the literature review. This literature review is not related to pneumatic elbow prostheses, rather it was the literature review about reciprocating gait orthosis, in which I worked earlier, but then I changed the topic and started working on this.

## Contents

PREFACE	VII
REPORT OUTLINE	ıx
INTRODUCTION	ERROR! BOOKMARK NOT DEFINED.
UPPER LIMB LOSS	3
UPPER LIMB PROSTHESIS	3
	3
REJECTION RATES	4
USER'S CHOICE	5
User's Concern	5
FLUID ACTUATED TRANSHUMERAL PROSTHESIS	6
Problem Definition	6
FORCE ANALYSIS	6
	7
Goal	8
Reference	8
SCIENTIFIC PAPER	ERROR! BOOKMARK NOT DEFINED.
NOVEL PNEUMATIC CURVILINEAR ACTUATOR I	FOR A GAS POWERED ELBOW UNIT13
I. INTRODUCTION	13
II. MATERIALS AND METHOD	13
a. Design criteria	
b. Basic theory	
c. Experimental setup	
d. Test Protocol	
e. Data Analysis	
	18
VI. REFERENCE	
DESIGN PAPER	ERROR! BOOKMARK NOT DEFINED.
	MPENSATION MECHANISM FOR A GAS POWERED
ABOVE ELBOW PROSTHESIS	23
I. Introduction	23
II. MATERIALS AND METHOD	24
a. Design criteria	24
J , ,	24
	24
	25
,	25
e.i. Pneumatic multiplex cylinder	26

e.	ii. Design optimization	26
f.	Locking mechanism	27
III.	RESULTS	27
a.	. Gravity compensation mechanism	27
b.	. Braking Mechanism	29
IV.	DISCUSSION	29
٧.	DESIGN SUMMARY	30
VI.	Reference	30
APPE	ENDIX ERROR! BOOKMAF	RK NOT DEFINED.
APPE	ENDIX A: DESIGN PROCESS OF A PNEUMATIC ELBOW UNIT	35
APPE	ENDIX B: OUTER SHELL	36
APPE	ENDIX C: GRAVITY COMPENSATOR DESIGN	38
a.	Spring Design	39
b.	Pneumatic multiplex cylinder Design	39
C.	Design optimization algorithm	40
APPE	ENDIX D: CURVILINEAR ACTUATOR DESIGN AND TESTING	46
a.	. Design algorithm	46
b.		
ΔPPF	,	50
	ENDIX E: MATLAB CODE FOR ACTIVE GRAVITY COMPENSATOR	
APPE	ENDIX E: MATLAB CODE FOR ACTIVE GRAVITY COMPENSATOR	57
APPE APPE	ENDIX E: MATLAB CODE FOR ACTIVE GRAVITY COMPENSATORENDIX F: MATLAB CODE FOR CURVILINEAR ACTUATOR	57 59
APPE APPE	ENDIX E: MATLAB CODE FOR ACTIVE GRAVITY COMPENSATOR	57 59
APPE APPE LITER	ENDIX E: MATLAB CODE FOR ACTIVE GRAVITY COMPENSATORENDIX F: MATLAB CODE FOR CURVILINEAR ACTUATOR	57 59 RK NOT DEFINED.
APPE APPE LITER RECIF	ENDIX E: MATLAB CODE FOR ACTIVE GRAVITY COMPENSATORENDIX F: MATLAB CODE FOR CURVILINEAR ACTUATORENDIX: REFERENCES	5759 RK NOT DEFINED. RK NOT DEFINED.
APPE APPE LITER RECIF	ENDIX E: MATLAB CODE FOR ACTIVE GRAVITY COMPENSATOR ENDIX F: MATLAB CODE FOR CURVILINEAR ACTUATOR ENDIX: REFERENCES ERATURE REVIEW	5759 RK NOT DEFINED. RK NOT DEFINED64
APPE APPE LITER RECIF KEYW ABST	ENDIX E: MATLAB CODE FOR ACTIVE GRAVITY COMPENSATOR ENDIX F: MATLAB CODE FOR CURVILINEAR ACTUATOR ENDIX: REFERENCES	5759 RK NOT DEFINED. RK NOT DEFINED64
APPE APPE LITER RECIF KEYW ABST INTRO	ENDIX E: MATLAB CODE FOR ACTIVE GRAVITY COMPENSATOR ENDIX F: MATLAB CODE FOR CURVILINEAR ACTUATOR ENDIX: REFERENCES  RATURE REVIEW  ERROR! BOOKMAF PROCATING GAIT ORTHOSIS  TRACT	5759 RK NOT DEFINED. RK NOT DEFINED6465
APPE APPE LITER RECIF KEYW ABST INTRO	ENDIX E: MATLAB CODE FOR ACTIVE GRAVITY COMPENSATOR  ENDIX F: MATLAB CODE FOR CURVILINEAR ACTUATOR  ENDIX: REFERENCES  RATURE REVIEW  ERROR! BOOKMAF  WORDS  TRACT  RODUCTION	5759 RK NOT DEFINED. RK NOT DEFINED6465
APPE LITER RECIF KEYW ABST INTRO GOAL BACK	ENDIX E: MATLAB CODE FOR ACTIVE GRAVITY COMPENSATOR ENDIX F: MATLAB CODE FOR CURVILINEAR ACTUATOR ENDIX: REFERENCES  RATURE REVIEW  ERROR! BOOKMAF  PROCATING GAIT ORTHOSIS  TRACT  RODUCTION  KGROUND  AL  KGROUND	5759 RK NOT DEFINED646566
APPE APPE LITER RECIF KEYW ABST INTRO GOAI BACK PC LO	ENDIX E: MATLAB CODE FOR ACTIVE GRAVITY COMPENSATOR  ENDIX F: MATLAB CODE FOR CURVILINEAR ACTUATOR  ENDIX: REFERENCES  RATURE REVIEW  ERROR! BOOKMAF  PROCATING GAIT ORTHOSIS  ERROR! BOOKMAF  WORDS  TRACT  RODUCTION  AL  KGROUND  araplegia  ower Limb Orthosis	5759 RK NOT DEFINED64656666
APPE APPE LITER RECIF KEYW ABST INTRO GOAL BACK PC LO METH	ENDIX E: MATLAB CODE FOR ACTIVE GRAVITY COMPENSATOR  ENDIX: REFERENCES  RATURE REVIEW  ERROR! BOOKMAF  PROCATING GAIT ORTHOSIS  ERROR! BOOKMAF  WORDS  TRACT  RODUCTION  AL  KGROUND  araplegia  ower Limb Orthosis  THODS	5759 RK NOT DEFINED6465666666
APPE APPE LITER RECIF KEYW ABST INTRO GOAL BACK PC LO METI	ENDIX E: MATLAB CODE FOR ACTIVE GRAVITY COMPENSATOR ENDIX F: MATLAB CODE FOR CURVILINEAR ACTUATOR ENDIX: REFERENCES  RATURE REVIEW  ERROR! BOOKMAF  PROCATING GAIT ORTHOSIS  ERROR! BOOKMAF  WORDS  TRACT  RODUCTION  AL  KGROUND  Graplegia  Ower Limb Orthosis  FHODS.  BERROR! BOOKMAF  FOR ACTIVE GRAVITY COMPENSATOR  ERROR! BOOKMAF  FOR ACTIVE GRAVITY COMPENSATOR  ERR	5759 RK NOT DEFINED6465666666
APPE APPE LITER RECIF KEYW ABST INTRO GOAI BACK PC LO METI Se Se	ENDIX F: MATLAB CODE FOR ACTIVE GRAVITY COMPENSATOR  ENDIX F: MATLAB CODE FOR CURVILINEAR ACTUATOR  ENDIX: REFERENCES  RATURE REVIEW  ERROR! BOOKMAF  PROCATING GAIT ORTHOSIS  FRACT  RODUCTION  AL  KGROUND  araplegia  ower Limb Orthosis  HODS.  eearch Methodology.  election Criteria	5759 RK NOT DEFINED646566666666
APPE APPE LITER RECIF KEYW ABST INTRO GOAL BACK PC LO METH See GO	ENDIX E: MATLAB CODE FOR ACTIVE GRAVITY COMPENSATOR  ENDIX F: MATLAB CODE FOR CURVILINEAR ACTUATOR  ENDIX: REFERENCES  ERATURE REVIEW  ERROR! BOOKMAF  PROCATING GAIT ORTHOSIS  ERROR! BOOKMAF  WORDS  TRACT  GODUCTION  AL  KGROUND  araplegia  ower Limb Orthosis  THODS.  election Criteria  Gathered Data	5759 RK NOT DEFINED6465656666666666
APPE APPE LITER RECIF KEYW ABST INTRO GOAL BACK PC LO METH Se Se GC RESU	ENDIX E: MATLAB CODE FOR ACTIVE GRAVITY COMPENSATOR  ENDIX: REFERENCES  RATURE REVIEW  PROCATING GAIT ORTHOSIS  WORDS  TRACT  RODUCTION  AL  KEROUND  AL  KEROUND  AL  KEROUND  AL  KEROUND  AL  KEROUND  AL  CHAPTER  COUNT  COUN	5759 RK NOT DEFINED6465656666666666
APPE APPE LITER RECIF KEYW ABST INTRO GOAI BACK PC LO METI Se GG RESU BO	ENDIX F: MATLAB CODE FOR ACTIVE GRAVITY COMPENSATOR  ENDIX: REFERENCES.  RATURE REVIEW ERROR! BOOKMAF  PROCATING GAIT ORTHOSIS ERROR! BOOKMAF  WORDS  TRACT  SODUCTION  AL  KEROUND  Araplegia  DOWER Limb Orthosis  THODS.  Bearch Methodology.  Belection Criteria  Bookmar  Bookmar  Brown Limb Orthosis  Control Criteria  Bookmar  Brown Limb Orthosis  Brown Limb Orthos	5759 RK NOT DEFINED6465656666666666
APPE APPE LITER RECIF KEYW ABST INTRO GOAI BACK PC LO METI See GC RESU BC CC	ENDIX F: MATLAB CODE FOR CURVILINEAR ACTUATOR  ENDIX: REFERENCES  RATURE REVIEW  PROCATING GAIT ORTHOSIS  ERROR! BOOKMAF  WORDS  TRACT  RODUCTION  AL  KKGROUND  Araplegia  Ower Limb Orthosis  HODS  Learch Methodology  election Criteria  Gathered Data  DUTS  assic terminologies  TOTAL COMPENSATOR  ERROR! BOOKMAF  ERRO	5759 RK NOT DEFINED646565666666666666
APPE APPE LITER RECIF KEYW ABST INTRO GOAI BACK PC LO METH Se GG RESU BC CC CC	ENDIX E: MATLAB CODE FOR ACTIVE GRAVITY COMPENSATOR  ENDIX: REFERENCES  RATURE REVIEW  PROCATING GAIT ORTHOSIS  ERROR! BOOKMAF  WORDS  TRACT  RODUCTION  AL  KKGROUND  Arraplegia  FOWER Limb Orthosis  FOWER LIMB ORTHOSIS	5759 RK NOT DEFINED6465656666666666666666
APPE APPE LITER RECIF KEYWABSTINTRO GOAI BACK PO LO METI Se GO RESU BC CC CC CC	ENDIX E: MATLAB CODE FOR ACTIVE GRAVITY COMPENSATOR  ENDIX: RATLAB CODE FOR CURVILINEAR ACTUATOR  ENDIX: REFERENCES  RATURE REVIEW  ERROR! BOOKMAF  PROCATING GAIT ORTHOSIS  ERROR! BOOKMAF  WORDS  TRACT  BODUCTION  BL  KGROUND  BL  BL  BL  BL  BL  BL  BL  BL  BL  B	
APPE APPE LITER RECIF KEYW ABST INTRO GOAL BACK PO LO METH See GO RESU BC CC	ENDIX E: MATLAB CODE FOR ACTIVE GRAVITY COMPENSATOR  ENDIX: REFERENCES  RATURE REVIEW  PROCATING GAIT ORTHOSIS  ERROR! BOOKMAF  WORDS  TRACT  RODUCTION  AL  KKGROUND  Arraplegia  FOWER Limb Orthosis  FOWER LIMB ORTHOSIS	

RGO Usage	81
Discussion	
CONCLUSION	
References	

## Introduction

Chapter 1

#### **UPPER LIMB LOSS**

A person's livelihood is hugely affected when he/she has a deformed or amputated limb(s). In the year 2005 in the US, it was estimated that 34.5% of the people with limb loss had upper limb loss and only 8% of people with limb loss had a major upper limb loss (i.e., excluding fingers) [1]. Trauma is the major cause of upper limb loss (68.6%-71.25%) [2, 3]. The upper limb amputation can be further classified according to the lesion level; partial-hand amputation (amputation of digits and/or metacarpals), wrist disarticulation, transradial amputation, elbow disarticulation, transhumeral amputation, shoulder disarticulation and forequarter amputation [4].

#### **UPPER LIMB PROSTHESIS**

There are various upper limb prostheses; depending upon the level of amputation, the patient is prescribed a prosthetic finger, hand or arm that would suit the patient's needs and rehabilitate some of the functions of the missing limb. This paper mainly focuses about transhumeral prosthesis.

#### TRANSHUMERAL PROSTHESIS

Transhumeral prosthesis, also known as above elbow prosthesis; it is prescribed to an amputee where his/her upper arm is amputated between the shoulder and elbow. Transhumeral prosthesis is used restore the functions of the missing elbow and hand. The basic components of the transhumeral prosthesis are the terminal device, the wrist unit, the elbow unit, the suspension unit and the control unit [4]. Upper limb prosthesis can be generally classified into three main types; passive/cosmetic, body-powered, external-powered.

The passive/cosmetic upper limb prosthesis doesn't have any active mechanical joints. They are mainly used to replace the missing limb part and restore body image. They can be used to hold objects with the use of static grasp. There are passive prosthetic arms whose joints could be manually rotated with the help of the abled arm.

The term "body-powered prosthesis" it is self-explanatory, that the prosthesis power is driven from the human body. Body-powered transhumeral prostheses have a functional elbow joint and a terminal device that is operated with the help of two Bowden cables and harness, Figure (1.1). One cable (Lock Cable LC) is used to unlock and lock the prosthetic elbow, in order to switch between the prosthetic elbow and terminal device. The second cable (Operating Cable OC) is used to operate the prosthetic elbow and the terminal device. The basic operating sequence of the system is as follows; in the unlocked state when the user applies a tension and pulls the OC by moving his/her body in a certain way, the prosthetic elbow flexes, and if the tension in the OC is released, the elbow extends back to its original position. Once the required angle of elbow flexion is achieved, a tension is applied and released on the LC, which in turn locks the prosthetic elbow. When the elbow is locked, if OC is pulled, the prehension device opens/closes for a voluntary opening/closing terminal device respectively; and when the tension is released, the prehension device closes/opens back to its original position. The LC requires roughly about 9 N of force and an excursion of 1.3 to cycle the elbow unit [4]. The combination of glenohumeral flexion and biscapular abduction is used to apply tension on the OC; an amputee could exert an average force of 222 N and excursion of 10 cm using this motion [5].

The external powered prosthesis uses actuator and external power source to operate the prosthetic arm. The current ones on the market only use servo motors and battery packs to operate the prostheses. There were, a few gas powered prostheses from Otto Bock, which are not in use anymore [6]. The most common source of a control signal is derived from EMG signal from the residual limb with the use of surface electrodes. The schematic of a basic two-site myoelectric control system is shown in Figure (1.2). One electrode is placed over Muscle A (Triceps) and other over Muscle B (Biceps). If the Electronic Motor Driver (EMD) gets a positive input, the elbow servo is driven and the prosthetic elbow is flexed, if the EMD gets a negative signal then the elbow is extended. When the elbow remains in the same position for a short period of time, then the control is automatically switched to operate the electric hand and the elbow is locked. A positive input to the EMD will open the hand and negative input would close the hand. In order to transfer the control back to the elbow, Muscles A and B is co-contracted quickly [4].

Introduction 3

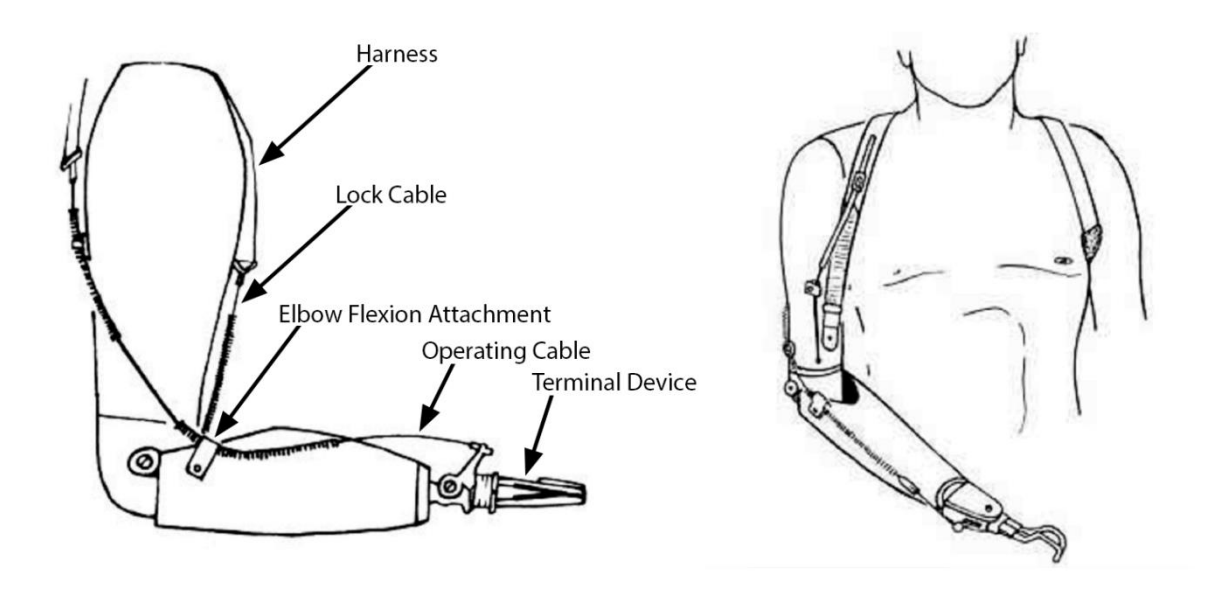


Figure 1.1: Body-Powered Transhumeral Prosthesis (adapted from [4]).

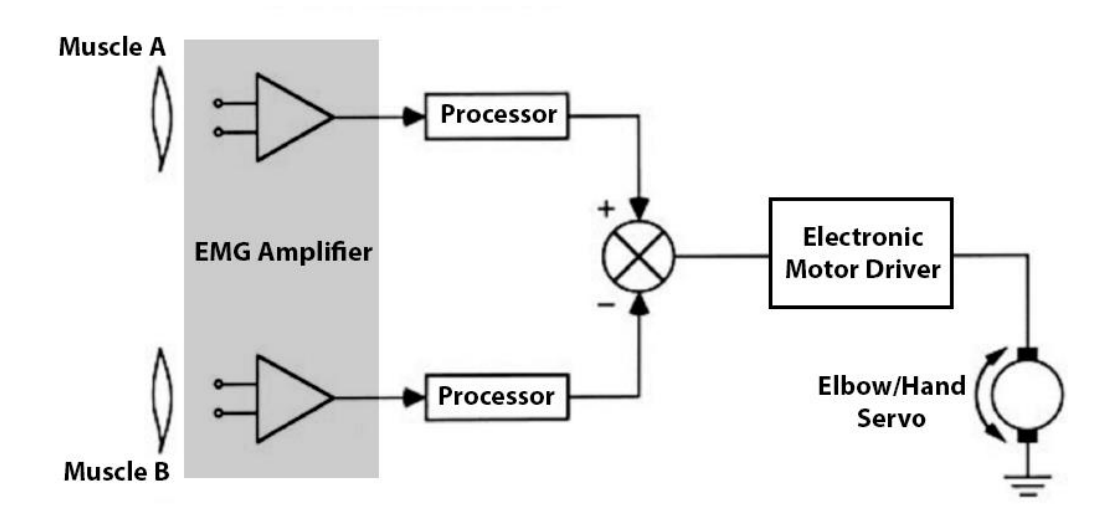


Figure 1.2: Schematic of a two-site myoelectric control system (adapted from [4]).

Apart from the three main types of upper limb prosthesis, there are two other types, boosted and hybrid prosthesis. Boosted transhumeral prosthesis uses a cable-harness system to give the input to a powered elbow. Hybrid transhumeral prosthesis is a myoelectric controlled powered elbow joint along with a body-powered end device or a body-powered elbow joint with a myoelectric end device [4].

#### **REJECTION RATES**

The upper limb amputee population is smaller than the lower limb amputee population [1, 2, 7, 8], but the rejection rate of upper limb prostheses (64%) are higher compared to lower limb prostheses (16%) [8]. When it comes to restoration of the missing limbs, replacing the functions of the human arm/hand with a prosthetic arm/hand is more complex than replacing the functions of the human leg/foot with a prosthetic leg/foot. The rejection rate of an above elbow prosthesis is higher compared to below elbow prosthesis [8-16]. The rejection rate of the above elbow prostheses range between 20%-60% [3, 9-16]. Rejection rates are not solely influenced on basis of functionality, comfort, reliability or price of the prosthesis; but other factors like: Was the prosthesis prescribed on time, did the patient take part in the prosthesis selection process, or the amount of support the amputee gets from his/her family and peers also has an effect on rejection/acceptance rate [17].

#### **USER'S CHOICE**

Prosthesis could be judged upon the following basic criteria; control, comfort, cosmesis, cost, and durability. For many users, a prosthetic arm should be able to perform similarly to that of their missing arm; a prosthetic arm should weigh less, such that the residual arm isn't strained in any fashion; the prosthetic arm should look beautiful; a prosthetic arm should be something that could be afforded by a working class family; a prosthetic should be able to last long without going through any major repair. Sadly, not even the state of the art prosthetic arm could meet all the expectations in all the criteria. It is tough to design and manufacture a prosthesis that would cater every single need of every individual, with the current technology. The end goal is to satisfy the prosthetic user's needs the best possible way.

Not every prosthetic user has the same set of priorities. Even though cosmetic arm lacks functionality, some patients prefer them for their high cosmetic value and light weight. A passive prosthesis weighs lighter when compared to body-powered or external powered prosthesis, due to fewer components. Non-working amputees prefer cosmetic hand prosthesis compared to body /external-powered ones [18].

Patients who prefer to have a prosthetic arm that has some functionality, moderately light in weight and less expensive might opt for a body-powered prosthesis. An additional advantage of body-powered prosthesis over the external-powered prosthesis is that the external-powered prosthetic users lack the proprioceptive feedback that the body-powered prosthetic users get from the tension in the harness and cable system. The lack of sensory feedback and heavy weight are some of the major reasons myoelectric prostheses are rejected [19, 20].

On the other hand, there are cases where the patient cannot produce sufficient tension on the cable to operate the body-powered arm. Some patients find discomfort with the harness in a body-powered system. The electric-powered prosthetic arm uses myoelectric signals to operate the prosthesis and it is suspended with a use of suction cups instead of a harness. Besides an external-powered transhumeral prosthesis has more number of degrees of freedom compared to a body-powered transhumeral prosthesis. If the patient perceives the weight and the cost of the prosthetic arm is reasonable and he/she can master to control the myoelectric arm with visual and indirect cues (sound or vibration from servo motors); the patient may opt for a myoelectric prosthetic arm [4, 17]. Various other feedback techniques like sensory substitution, modality matching, or direct nerve stimulation are being tested to improve the efficacy of the prosthetic feedback system; a more detailed review of these techniques could be found in [19, 20].

As a customer, there are various prosthetic options to choose from; Table 1.1 is the compilation of the technical details of some of the commercially available active above elbow units [21-24].

#### **USER'S CONCERN**

Patients were asked to list the various criteria that need to be focused for future prosthetic design according to their priority. Reduced weight of the prosthesis, took the most priority in all three type of upper limb prosthesis [25]. Compared to the load felt while wearing a prosthetic limb of the same weight of missing limb over the residual limb and the load distribution of a natural limb, some patients perceive the prosthetic limb to be heavier.

Brand	Model	Туре	Weight (g)	Live Lift (Nm)	Dead Lift (N)	Range (deg)	Lift Speed (deg/sec)
Hosmer	E-Two Elbow	Electric	540	3.25	111	5 - 135	100
Motion Control	Utah Arm 3+	Electric	904	13.25	216	15 - 150	112.5
LTI	Boston Digital Arm System	Electric	1000	13.5	NA	0 - 135	123
Otto Bock	DynamicArm	Electric	1000	15	230	15 - 145	270

Table 1.1: Technical details of commercial elbow units

Introduction 5

The natural arm's weight is 4.94% of the body weight (hand-0.61%, forearm-1.62% and upperarm-2.71%) [26]; the average human body weight is 62kg [27]. So the average weight of a human arm with an above elbow amputation is 3.585% of 62kg, i.e. under the assumption half of the upper arm is still intact; the average weight of the natural arm is approximately 2kg. In fact, the heaviest current state of the art external-powered transhumeral arm the Otto Bock Dynamic Arm weighs about 1kg [21]. There are other powered elbows that are lighter than Otto Bock's Dynamic Arm, but then they fall short when it comes to lifting capacity. Myoelectric prostheses use are more frequent for transradial loss and less frequent in transhumeral loss [16, 18]; more number of active joints leads to more components, meaning an increase in weight of the prosthesis. In addition to weight, there is also issue of cost. On 2011 the estimated initial cost of body-powered transhumeral prosthesis is \$50,000-\$75,000; on the other hand, body-powered transradial prosthesis is \$4000-\$8000, external-powered transradial prosthesis is \$25,000-\$50,000 [28].

#### FLUID ACTUATED TRANSHUMERAL PROSTHESIS

Due to the usage of DC motors, batteries and transmission drives, the current prosthetic limbs weigh heavier. The weight distribution problem can be faced from two fronts; designing a new suspension system, so that the load on the residual is well distributed or designing a lighter prosthetic arm with the use of light weight material, mini actuators, and other power sources. In this paper, we focus on the latter option.

The advantage of fluidic actuators over DC motors is that the fluidic actuators have a low mass-to-power ratio and low space requirements compared to DC motors; the disadvantage of the fluidic actuators is, these actuators may suffer from pressure leakages and noise problems due to improper design [29]. In the 60's and 70's there were several experimental and even a commercially available pneumatic elbow prosthesis, a brief review about these models could be found in [6]. Though the pneumatic actuators are comparatively lighter than the DC motors, the CO2 canisters that were used as the power supply can be heavy depending upon the amount of CO2 required for the system. In the last decade, there are a few research groups, who have come up with fluid powered transhumeral prosthesis which are still in experimental stages [30, 31]. Fite proposed an alternate way to produce high energy density gas utilizing monopropellant-powered gas generator [32]. A 70 mL, 180g tank of 70% liquid monopropellant hydrogen peroxide has the same amount of energy content a 350 mL, 900 g CO2 canister does [30].

#### PROBLEM DEFINITION

It is clear that the weight of the current above elbow prostheses is perceived heavy by the prosthetic user. The DC motors require additional transmission unit and battery packs to operate the system; unfortunately, this makes the system heavy. On the other hand, a lighter DC motor and transmission unit could be used, but this leads to low lifting capacity. Compared to DC motors, fluidic actuators have a low mass-to-power ratio. As an alternate to DC servo powered system; fluid actuated system could be used. Thereby making the system light yet have a good lifting capacity.

The fluidic systems could be further divided into two types, hydraulic and pneumatic. A pump or compressor is required to drive the hydraulic or pneumatic actuators respectively. A prosthetic user should have a power source that could be carried around and light in weight. CO<sub>2</sub> gas canisters or the chemo-fluidic approach proposed by [30, 32] would fulfill these criteria. Therefore, a pneumatic based system is opted, as the primary power source for this project.

#### **FORCE ANALYSIS**

The basic force analysis of an elbow joint is represented by a free body diagram in Figure 3.1. For simplicity purpose, the following are assumed: the plan of motion is fixed, the arm is made of two rigid body elements (upper arm and forearm), connected by a revolute joint (elbow joint) and the upper arm is stationary.

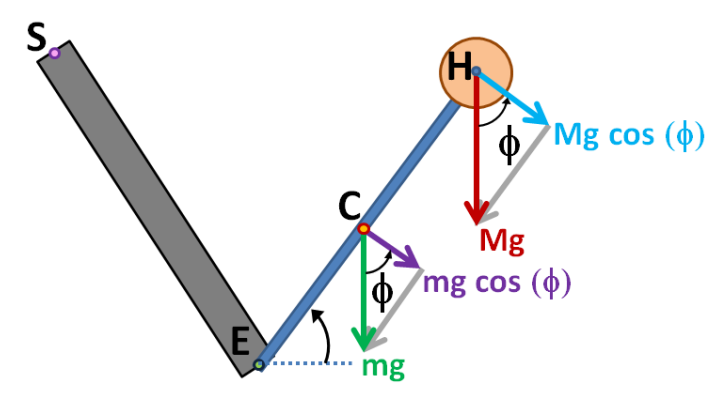


Figure 1.3: Free-body diagram of an elbow

Since the upper arm is assumed to be stationary, the overall system could be considered as a single link mechanism. When an object (external load) of mass, M, held at the hand, H, where the forearm makes an angle,  $\phi$ , with the horizontal axis and the acceleration due to gravity, g, is acting downwards; we know the (gravitational) torque,  $\tau_g$ , produced at the elbow joint, E, is equal to the product of the tangential force component,  $Mg \cos \phi$ , and the length of the forearm, h. Note the normal force component,  $Mg \sin \phi$ , is not considered to produce any torque.

$$\tau_a = Mg\cos\phi \ h \tag{1}$$

Equation (1) doesn't include the effects of the mass of the forearm, m, as part of the gravitational torque acting on the forearm. Assuming a point mass, m, is acting at the point, c, then the product of the tangential component of the weight the forearm, c, and the distance from the axis of rotation to the center of mass of the forearm, c, is added to (1).

$$\tau_{a} = Mg\cos\phi \ h + mg\cos\phi \ c \tag{2}$$

The gravitational torque is zero when the forearm is parallel to the vertical axis ( $\cos \phi = 0$ , for  $\phi = 90^{\circ}$ ); the maximum gravitational torque is experienced when the forearm is horizontal ( $\cos \phi = 1$ , for  $\phi = 0^{\circ}$ ).

$$\tau_{amax} = Mg \ h + mg \ c \tag{3}$$

#### SYSTEM REQUIREMENTS

The proposed elbow unit will be evaluated on the basis of the following parameters; live-lift capacity, dead-lift capacity, and weight. On comparing the commercially available elbow prostheses, the following demands were made as the basic requirement of the new elbow mechanism are made. The highest favorable value for each parameter was set as the optimistic target and the least favorable value as the minimalistic target. The average between the optimistic and minimalistic target values are kept as the realistic target. Table 1.2 contains the values of the optimistic, minimalistic and realistic targets specification for the elbow unit.

Table 1.2: New elbow mechanism's basic requirement

Live Lift		Dead Lift	Weight	
Scale		Nm	N	œ
	Minimalistic	3.25	111	1000
Target	Optimistic	15	230	540
	Realistic 9.125 (Min)		170.5 (Min)	770 (Max)
Rati	ionale	Should be able to flex without slipping when subjected to maximum live lift load	Should not break when subjected to high force	Should be light as possible

The proposed elbow unit should meet the following requirements; weight should be less than 770g, live-lift capacity should be more than 9.125 Nm, dead-lift capacity should be above 170.5 N.

Some spatial constraints were imposed on the proposed elbow unit; the elbow unit should fit inside the contour of the human arm. The following dimensions were assumed to define a human arm; a cylinder of size 85 mm diameter and 350 mm length is taken into consideration as a simple representation of the human arm, the wrist diameter of 50 mm, the palm to wrist length of 50 mm and the fore arm length 250 mm. The various parts of the elbow unit are designed depending upon the overall space left; so the spatial constraint for the each part would vary accordingly.

Additionally the prosthetic elbow should be able to flex 130 degrees. The supply pressure of the pneumatic system is set to 1.2 Mpa; since it is the optimum gas pressure to have for minimal gas consumption [33].

#### **GOAL**

The main objective of this project is to design a pneumatic powered elbow unit for an above elbow prosthesis that should satisfy the following objectives: should have a live lift capacity above 9.125 Nm, the dead lift capacity should be above 170.5 N, it should weigh less than 770 g, and finally, a range of motion about 130°.

#### REFERENCE

- 1. Ziegler-Graham, K., E.J. MacKenzie, P.L. Ephraim, T.G. Travison, and R. Brookmeyer, *Estimating the prevalence of limb loss in the United States: 2005 to 2050.* Archives of physical medicine and rehabilitation, 2008. **89**(3): p. 422-429.
- 2. Dillingham, T.R., L.E. Pezzin, and E.J. MacKenzie, *Limb amputation and limb deficiency: epidemiology and recent trends in the United States.* Southern medical journal, 2002. **95**(8): p. 875-883.
- 3. Datta, D., K. Selvarajah, and N. Davey, *Functional outcome of patients with proximal upper limb deficiency-acquired and congenital.* Clinical rehabilitation, 2004. **18**(2): p. 172-177.
- 4. Michael, J.W., J.H. Bowker, and A.A.o.O. Surgeons, *Atlas of amputations and limb deficiencies: surgical, prosthetic, and rehabilitation principles*. Vol. 2. 1992: American Academy of Orthopaedic Surgeons Rosemont, IL.978-0801602092
- 5. Weir, R.F. and J.W. Sensinger, *Design of artificial arms and hands for prosthetic applications*. 2003, McGraw Hill, New York. p. 32.1-32.61.
- 6. Plettenburg, D.H., *Pneumatically Powered Prosthesis: An Inventory*. 2002: Delft University of Technology.903700198X
- 7. Pezzin, L.E., T.R. Dillingham, E.J. MacKenzie, P. Ephraim, and P. Rossbach, *Use and satisfaction with prosthetic limb devices and related services*. Archives of physical medicine and rehabilitation, 2004. **85**(5): p. 723-729.
- 8. Raichle, K.A., M.A. Hanley, I. Molton, N.J. Kadel, K. Campbell, E. Phelps, D. Ehde, and D.G. Smith, *Prosthesis use in persons with lower-and upper-limb amputation*. Journal of rehabilitation research and development, 2008. **45**(7): p. 961.
- 9. Heger, H., S. Millstein, and G. Hunter, *Electrically powered prostheses for the adult with an upper limb amputation*. Journal of Bone & Joint Surgery, British Volume, 1985. **67**(2): p. 278-281.
- 10. Glynn, M., H. Galway, G. Hunter, and W. Sauter, *Management of the upper-limb-deficient child with a powered prosthetic device*. Clinical orthopaedics and related research, 1986. **209**: p. 202-205.
- 11. Millstein, S., H. Heger, and G. Hunter, *Prosthetic use in adult upper limb amputees: a comparison of the body powered and electrically powered prostheses.* Prosthetics and orthotics international, 1986. **10**(1): p. 27-34.
- 12. Sturup, J., H. Thyregod, J. Jensen, J. Retpen, G. Boberg, E. Rasmussen, and S. Jensen, *Traumatic amputation of the upper limb: the use of body-powered prostheses and employment consequences.*Prosthetics and orthotics international, 1988. **12**(1): p. 50-52.
- 13. Roeschlein, R. and E. Domholdt, *Factors related to successful upper extremity prosthetic use.* Prosthetics and orthotics international, 1989. **13**(1): p. 14-18.
- 14. Wright, T.W., A.D. Hagen, and M.B. Wood, *Prosthetic usage in major upper extremity amputations.* The Journal of hand surgery, 1995. **20**(4): p. 619-622.

- 15. Biddiss, E. and T. Chau, *Upper-limb prosthetics: critical factors in device abandonment*. American Journal of Physical Medicine & Rehabilitation, 2007. **86**(12): p. 977-987.
- 16. McFarland, L.V., S.L. Hubbard Winkler, A.W. Heinemann, M. Jones, and A. Esquenazi, *Unilateral upperlimb loss: satisfaction and prosthetic-device use in veterans and servicemembers from Vietnam and OIF/OEF conflicts.* J Rehabil Res Dev, 2010. **47**(4): p. 299-316.
- 17. Murray, C., Amputation, Prosthesis Use, and Phantom Limb Pain. 2010: Springer.0387874623
- 18. Kyberd, P.J. and W. Hill, *Survey of upper limb prosthesis users in Sweden, the United Kingdom and Canada.* Prosthetics and orthotics international, 2011. **35**(2): p. 234-241.
- 19. Antfolk, C., M. D'Alonzo, B. Rosén, G. Lundborg, F. Sebelius, and C. Cipriani, *Sensory feedback in upper limb prosthetics*. Expert review of medical devices, 2013. **10**(1): p. 45-54.
- 20. Schofield, J.S., K.R. Evans, J.P. Carey, and J.S. Hebert, *Applications of sensory feedback in motorized upper extremity prosthesis: a review.* Expert review of medical devices, 2014. **11**(5): p. 499-511.
- 21. *Elbow Prosthesis Otto bock*. Available from: <a href="http://www.ottobock.nl/media/local-media/prothesen/productinformatie/dynamicarm\_en.pdf">http://www.ottobock.nl/media/local-media/prothesen/productinformatie/dynamicarm\_en.pdf</a>.
- 22. Upper Limb Prosthesis Fillauer. Available from: <a href="http://fillauer.eu/prosthetics-upper">http://fillauer.eu/prosthetics-upper</a>.
- 23. Inc., L.T. *Prosthetic Elbows LTI*. Available from: http://www.liberatingtech.com/products/elbows/.
- 24. Utha Arm Motion Control. Available from: <a href="http://www.utaharm.com/files/">http://www.utaharm.com/files/</a>.
- 25. Biddiss, E., D. Beaton, and T. Chau, *Consumer design priorities for upper limb prosthetics*. Disability and Rehabilitation: Assistive Technology, 2007. **2**(6): p. 346-357.
- 26. De Leva, P., *Adjustments to Zatsiorsky-Seluyanov's segment inertia parameters.* Journal of biomechanics, 1996. **29**(9): p. 1223-1230.
- 27. Walpole, S.C., D. Prieto-Merino, P. Edwards, J. Cleland, G. Stevens, and I. Roberts, *The weight of nations: an estimation of adult human biomass.* BMC Public health, 2012. **12**(1): p. 439.
- 28. Resnik, L., M.R. Meucci, S. Lieberman-Klinger, C. Fantini, D.L. Kelty, R. Disla, and N. Sasson, *Advanced upper limb prosthetic devices: implications for upper limb prosthetic rehabilitation.* Archives of physical medicine and rehabilitation, 2012. **93**(4): p. 710-717.
- 29. Janocha, H., *Actuators: basics and applications*. 2013: Springer Science & Business Media.3662055872
- 30. Fite, K.B., T.J. Withrow, X. Shen, K.W. Wait, J.E. Mitchell, and M. Goldfarb, *A gas-actuated anthropomorphic prosthesis for transhumeral amputees.* Robotics, IEEE Transactions on, 2008. **24**(1): p. 159-169.
- 31. Foglia, M. and M. Valori. A high performance wire device for an elbow prosthesis. in Biomedical Robotics and Biomechatronics (BioRob), 2012 4th IEEE RAS & EMBS International Conference on. 2012. IEEE.
- 32. Fite, K.B., T.J. Withrow, K.W. Wait, and M. Goldfarb. *Liquid-fueled actuation for an anthropomorphic upper extremity prosthesis*. in *Engineering in Medicine and Biology Society, 2006. EMBS'06. 28th Annual International Conference of the IEEE*. 2006. IEEE.
- 33. Plettenburg, D.H., A sizzling hand prosthesis: On the design and development of a pneumatically powered hand prosthesis for children. 2002, TU Delft, Delft University of Technology.

Introduction 9

## Scientific Paper

Chapter 2

#### Novel Pneumatic Curvilinear Actuator for a Gas Powered Elbow Unit

Aravindan Sooryanarain

Delft Institute of Prosthetics and Orthotics, Department of Biomechanical Engineering

Delft University of Technology

Email: a.sooryanarain@student.tudelft.nl

#### **Abstract**

The objective of the study is to design a pneumatic actuator for an elbow unit as an alternative to DC servo motors that are used in the current market. As an exploratory concept, the curvilinear actuator was designed as part of a study which could be used to flex/extend a prosthetic elbow. In this paper, the design and testing of a new type of pneumatic servo that uses curvilinear translatory motion are presented. The prototype of the curvilinear actuator is 3D printed and tested. The results show the design curvilinear actuator can fit inside an elbow (sphere) of 36mm diameter has a lifting capacity of 2.9Nm. The prototype of the curvilinear actuator was 3D printed and the bench test results show the overall system efficiency varies from 26-72% depending upon the supply pressure.

Keywords: prosthesis, above elbow, transhumeral, curvilinear actuator, helical translation

#### I. INTRODUCTION

The overall rejection rate of above-elbow prosthesis varies from 20%-60% [1-9]. One of the major reasons for the users to reject the prosthesis is that the users perceive the prostheses to be heavy. When above elbow prosthetic users were asked to list the various criteria that need to be prioritized for future prosthetic design according to them, the weight of the above elbow prosthesis was their top priority [10]. The commercially available active elbow units use a DC servo motors to achieve elbow flexion/extension. The drawback of using DC motors is that they are often heavy if there is a high torque demand [11, 12]. Therefore, an alternative rotary actuator is required that can produce the required torques and the same time weighs lighter. Pneumatic actuators can be used in place of electrical motors to operate the system, as fluidic actuators have a low mass-to-power ratio and low space requirement [11, 12]. The overall objective of this paper is to design a pneumatic actuator as an alternative to a DC servo motor. This paper presents the basic working principle and the bench test results of the curvilinear actuator.

#### II. MATERIALS AND METHOD

#### a. Design criteria

As an exploratory study, the curvilinear actuator was designed, as for the design requirements of this study, the actuator should meet the following; it should be able to lift more than 500g acting at (@) 300mm (~1.5Nm). As per spatial constraints, the proposed lifting unit should fit inside the contour of a human elbow of 36mm diameter. Additionally, the range of motion was set to 130°. The supply pressure of the pneumatic system is set to 1.2Mpa; since it is the optimum gas pressure to have for minimal gas consumption [13].

Note: The reasons behind choosing this particular load condition are; the 500g was the assumed weight of a teacup filled with water and the 300mm is the average distance from the elbow to the hand.

#### b. Basic theory

The proposed pneumatic curvilinear actuator comprises of the following major elements: helical piston, hollow helical coil (helical cylinder), crank, central axle and output disc.

13

The basic principle behind the curvilinear actuator is that the helical piston traverses to and fro inside a hollow helical coil using a curvilinear translatory motion; the helical piston should be able to traverse along the helical path freely if the following conditions are satisfied:

- the pitch, coil diameter, and direction of rotation of the hollow helical coil should be the same as the helical piston
- the helical piston's and hollow helical coil's helical axes should coincide with each other
- the helical piston's cross-sectional diameter should be smaller than that of the inner diameter of the hollow cross-section

In simple term, the curvilinear actuator is a fluidic linear actuator twisted into a helix (Figure 2.1).

Note: Since the term linear actuator is commonly used in the field of actuators to refer an actuator that produces a straight line motion (rectilinear translation). Therefore, the term "linear" used in this paper in context with motion refers to rectilinear translation; even though the term curvilinear translation falls under the category of linear translation in terms of kinematics.

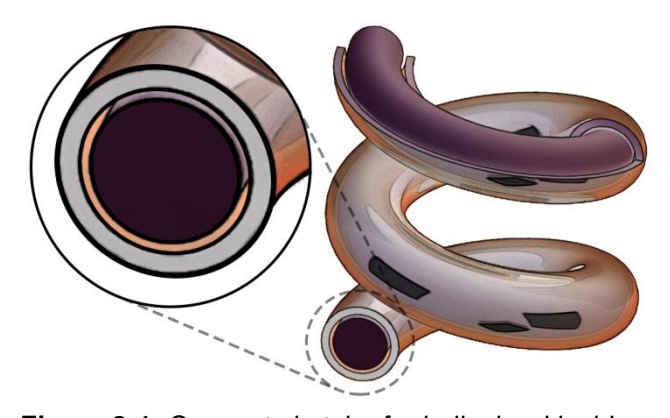


Figure 2.1: Concept sketch of a helical rod inside a hollow helical coil

The curvilinear translatory motion of the helical piston is used as the input to produce a rotary motion of the output disc and the crank is used to transfer the curvilinear translatory motion into rotary motion.

The output disc's axis of rotation and the central axis of the helix are in-line with elbow's axis of rotation. The output disc can only rotate about the elbow axis and its other degrees of freedom are restricted.

One end of the crank is attached to the outer end of the helical piston rod; therefore, the crank also makes a curvilinear translation along the helical path. In relation to the helical axis, the crank revolves around the helical axis as it translates along the helical axis.

The other end of the crank is passed through a slot on the output disc, forming a prismatic joint. So in relation to the output disc, the crank can only slide along the direction of the helical axis.

Assume the helical axis to be the z-axis and the plane of rotation to be the xy plane. The force applied to the helical piston,  $F_{HP}$ , can be found using the following equation:

$$F_{HP} = (p - p_a) A_{HP} \eta_{CA}$$
 (1)

Where:

 $F_{HP}$  = Input force p = Supply pressure  $p_a$  = Atmospheric pressure

 $A_{HP}$  = Cross-sectional area of piston head

 $\eta_{CA}$  = Overall actuator efficiency

 $F_{HP}$ , acts along the tangent of the helix; under the assumption that the helical piston head is perpendicular to the helix for any given instance.

 $F_{HP}$  makes an angle  $\lambda$  with the plane of rotation; where  $\lambda$  is the lead angle of the helix and the XY plane is the plane of rotation.

By splitting  $F_{HP}$  into its rectangular components,  $F_{HPZ}$ , is the force acting along the z axis and  $F_{HPR}$ , is the resultant force of  $F_{HPX}$  and  $F_{HPY}$ , acting on the plane of rotation (Figure 2.2).

Since  $F_{HP}$  makes a constant angle with the plane of rotation, for a constant input pressure, at any given instance,  $F_{HPZ}$  magnitude and direction remains constant throughout the curvilinear translation.

The magnitude of  $F_{HPR}$  is constant, but the angle it makes with the x and y axes changes as the helical piston translates through the hollow helical coil. Besides, the output disc and crank make a cylindrical joint,  $F_{HPZ}$  doesn't have any effect on the output disc, but  $F_{HPR}$  does. A helix without a translatory component is a circle. This implies  $F_{HPR}$  acts along the tangent of a circle, which in turn produces the output torque,  $\tau_{CA}$ .

$$\tau_{CA} = F_{HPR} R_H = F_{HP} \cos \lambda R_H \tag{2}$$

Where:

 $R_H$  = Radius of helix

 $\lambda$  = Lead angle of helix

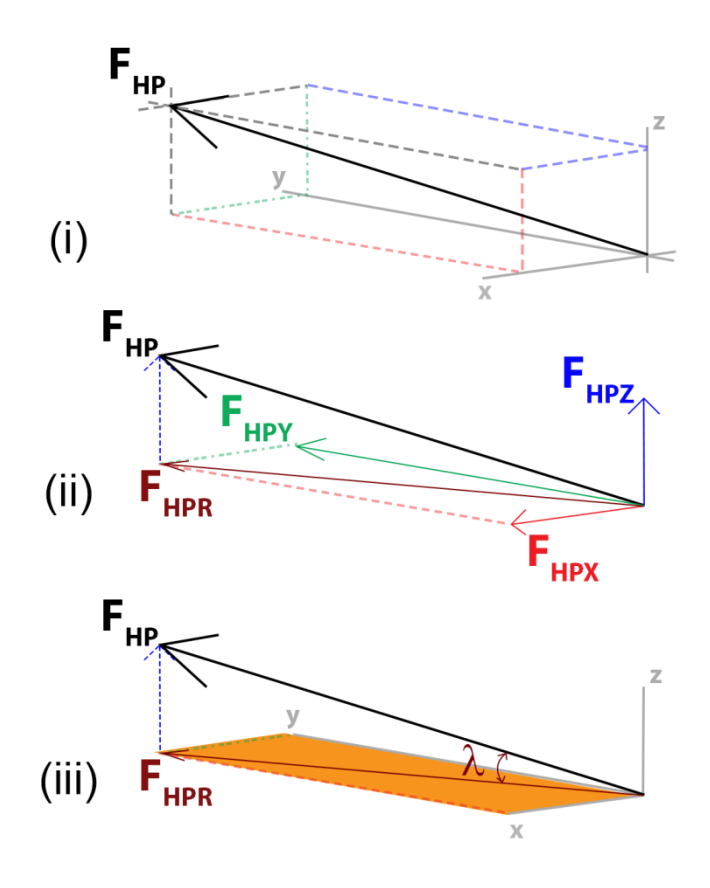


**Figure 2.2:** In (i)  $F_{HP}$  is represented in a 3D space. In (ii)  $F_{HPX}$ ,  $F_{HPY}$ , and  $F_{HPZ}$  are the rectangular components of  $F_{HP}$ ;  $F_{HPR}$  is the resultant force of  $F_{HPX}$  &  $F_{HPY}$ . In (ii)  $F_{HPR} = F_{HP} \cos \lambda$ .

Figure 2.3 represents the basic assembly of a single acting no return curvilinear actuator.

Using (1), the area and radius of the helical piston,  $A_{HP}$  and  $r_{HP}$  can be calculated for a given  $\tau_{CA}$ . The thickness of the hollow helical coil,  $t_{HP}$ , can be calculated when the hoop stress is equal to the tensile strength of the material used.

$$t_{HP} = \frac{p \, r_{HP}}{\sigma_{Mat}} \, FS \tag{3}$$

Where:

 $t_{HP}$  = Helical coil thickness  $r_{HP}$  = Radius of piston head

 $\sigma_{Mat}$  = Tensile strength of material used

FS = Factor of safety

We know for every complete rotation, the helix translates the distance of its pitch. As per the required angle of rotation,  $\theta$ , the stroke arc length,  $L_{CA}$ , of the curvilinear actuator can be calculated.

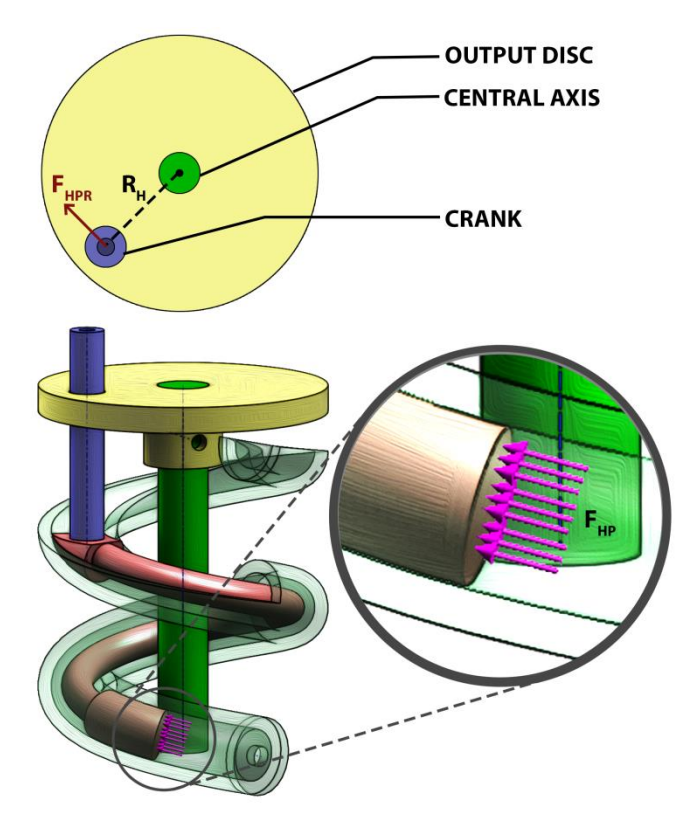


Figure 2.3: Basic assembly of a curvilinear actuator

From  $L_{CA}$  the volume of gas required to make one curvilinear stroke can be calculated.

$$L_{CA} = \sqrt{P_H^2 + (2\pi R_H)^2} \frac{\theta}{360}$$
 (4)

$$Vol_{CA} = \pi r_{HP}^2 L_{CA} \tag{5}$$

Where:

 $P_H$  = Pitch of helix  $Vol_{CA}$  = Stroke volume

The theoretical energy expenditure,  $E_{Th}$ , can be calculated using the following formula:

$$E_{Th} = \frac{\tau_{CA} \, \theta}{p \, Vol_{CA}} \tag{6}$$

The curvilinear actuator is required to satisfy the following design objectives; as mentioned before, in terms of load constrain the actuator should be able to produce a torque more than 1.5Nm, i.e. 500g at 300mm, a range of motion of 130° and in terms of spatial constraints it should fit within the space left in the elbow cup. The design is optimized to maximize the output torque using a MATLAB code.

Once the dimension of the best possible design is found, a 3D model of the curvilinear actuator is made in Solidworks, and the prototype is 3D printed.

#### c. Experimental setup

A bench test was run to test the experimental of the curvilinear efficiency actuator. The experimental setup consists of the following components; the curvilinear actuator, a custom made mounting rig, pressure regulating valve, solenoid valve (SMC VQZ115YR), two digital pressure (B+B Thermo-Technik DRTR-ED-10Vsensors RV10B) to measure the supply pressure before and after the solenoid valve, a rotary potentiometer to measure the angle, a data acquisition unit (NI USB-6211) to record all the data and a power supply.

#### d. Test Protocol

Only flexion experiments were done, the extension action of the actuator is not tested. The following protocol was used to test the curvilinear actuator; the overall efficiency of the curvilinear actuator was tested for various supply pressure when the actuator is loaded with a load of nearly 300g @ 300mm away from the axis of rotation conditions. The supply pressure was varied from 1bar to 6bar. For each pressure conditions five trials are taken. The mean of the five trials is calculated. Then the experimental data is used for data analysis.

#### e. Data Analysis

The experimental data is used to estimate the loss in efficiency due to friction. For a known value of pressure, we can calculate the theoretical output torque of the system using (2), under the assumption  $\eta_{CA}$  is be equal to one. From the angle achieved from experimental data we can calculate the gravitational torque,  $\tau_{q_0}$  created by the external load.

At equilibrium, the gravitational torque is equal to the actual output torque produced,  $\tau_{exp}$ .

$$\tau_{exp} = \tau_g + \tau_{\alpha} \tag{7}$$

Where:

 $\tau_{\infty}$  = Acceleration torque

The difference between the theoretical torque and the experimental torque acts as the indicator to frictional loss. The experimental energy expenditure,  $E_{Exp}$ , and the overall efficiency of the curvilinear actuator,  $\eta_{CA}$ , can be estimated using the following:

$$E_{exp} = \frac{\tau_{exp} \, \theta}{p \, Vol_{CA}} \tag{8}$$

$$\eta_{CA} = \frac{\tau_{exp}}{\tau_{CA}} = \frac{E_{exp}}{E_{Th}} \tag{9}$$

#### III. RESULTS

Table 2.1 contains the design specifications of the curvilinear actuator that can produce the maximum torque of 2.9Nm within the given space constraints. In theory, the designed curvilinear actuator can lift about 1kg; under the assumption that there is only frictional loss due to drag.

Table 2.1: Dimensions of the Curvilinear Actuator

Variable	Dimension	Max Torque
r <sub>HP</sub>	(mm)	7
$R_{H}$	(mm)	17
$t_{HP}$	(mm)	1.75
$ au_{CA}$	(Nm)	2.968
Lift Capacity	(Kg)	1.01

The designed curvilinear actuator consumes about 141mg of CO<sub>2</sub> to flex 130°. The 3D model of the complete assembly of the curvilinear actuator along with the exploded view is given in Figure 2.4.

As a proof of concept, the curvilinear actuator was 3D printed (Figure 2.5). When air pressure was supplied the helical piston was able to translate.

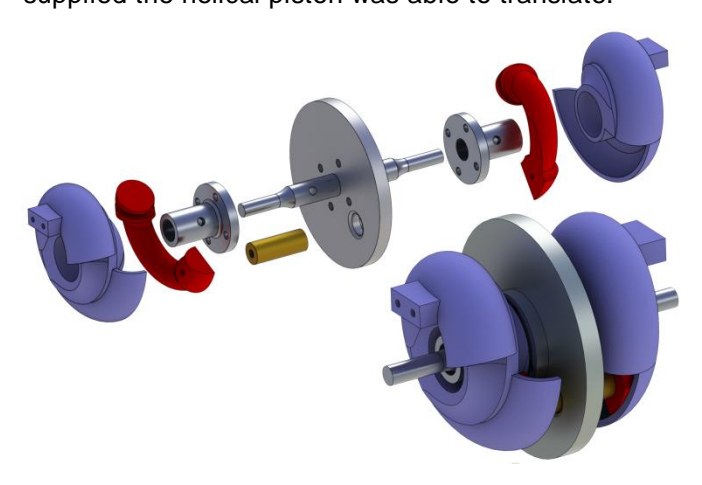


Figure 2.4: Curvilinear actuator



Figure 2.5: Curvilinear actuator

Table 2.2 shows the following results of the load test. Due to technical reasons, the experimental data for pressure @ 6bar was not added to the results and only 3 trials were done for pressure @ 5.5bar. The reason for this issue is discussed in the subsequent section.

Figure 2.6 shows the angle vs. time plot. Figure 2.7 shows the variation of  $E_{Exp}$ ,  $E_{Th}$ , and  $\eta_{CA}$  over time for different pressure conditions. Figure 2.8 shows the prototype of the curvilinear actuator on the test setup rig.

Table 2.2: Load Test Results

p [bar]	τ <sub>CA</sub> [Nmm]	$\theta_{exp}$ [deg]	τ <sub>exp</sub> [Nmm]	$\eta_{CA}$
1.14	154.12	2.8518	39.97	0.26
1.65	279.08	7.5994	107.74	0.39
2.10	388.71	11.8282	167.51	0.43
2.57	504.52	23.2862	323.93	0.64
3 .05	620.64	31.7542	431.57	0.69
3.58	749.85	41.2226	540.68	0.72
4.10	878.00	51.1990	639.66	0.73
4.59	997.80	67.1608	756.75	0.76
5.09	1118.85	83.1109	815.47	0.72
5.55	1230.10	110.8075	821.51	0.66

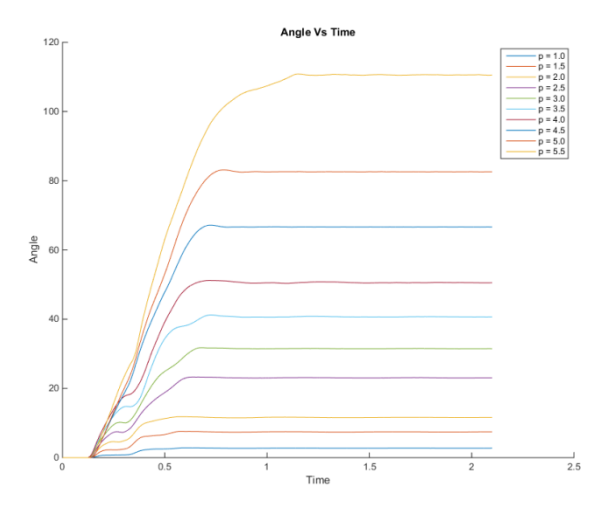
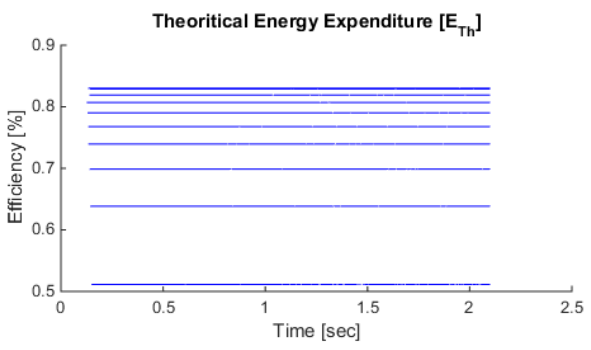
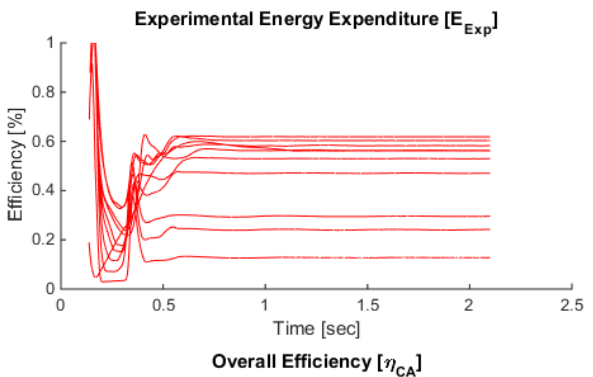


Figure 2.6: Angle vs. Time





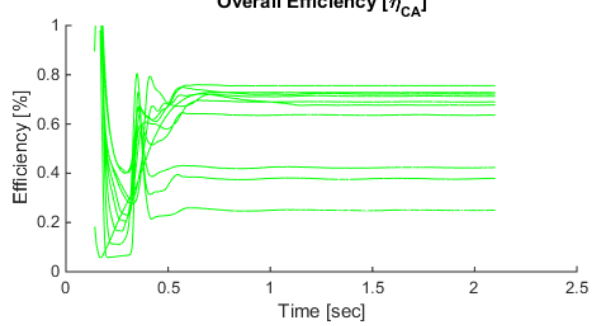


Figure 2.7: Efficiency plot



Figure 2.8: Test Setup

#### IV. DISCUSSION

There are quite some key issues that need to be addressed regarding the design of the final prototype of the curvilinear actuator.

First, the outer shape of the actuator where modified and more thickness was given to the cylinder walls. The 1<sup>st</sup> prototype was 3D printed exactly the same as in figure 2.4, but when a pilot test was run, the hollow helical cylinder broke at high pressure. So the thickness of the cylinder walls was increased (Figure 2.5).

Then there is a design error in the prototype compared to the theoretical concept, instead of making the head of the piston perpendicular to the helix, while designing in Solidworks, the piston head was made from a sweep where the cross-section of the circle to follow the helical path was placed on a plane parallel to the axis of rotation. This was only later realized after the final prototype was made, so, instead of making a completely new prototype, the change in angle of the piston head was compensated in the mathematical model.

Then as for the production process itself, there were some presence of some rugged patterns in on the helical cylinders. So, this might affect the overall friction loss in the system. Other production techniques need to be tried, instead of 3D printing the helical cylinder, maybe it can be made from CNC cut aluminum, which might help in reducing the frictional loss.

During the experimental phase, it was found for the load of ~850Nmm and a supply pressure above 5.5bar, the piston of the flexing side pops out of the cylinder a little bit and thus the actuator gets stuck (Figure 2.9). At times the O-rings also break as the forearm tries to get back to normal position. This is caused due to the impact, but overall it is due to a design flaw. While designing the piston and cylinder; both of them were made to sweep 130°. For tolerance purpose, the helical pistons diameter was reduced by 0.3mm. This makes the output disc to have a slight play in its range of motion. The helical cylinders helical arc length needs to be increased little bit, thereby the helical piston will stay inside the helical cylinders





Figure 2.9: Popped out Helical Piston

Then the design of the mounting the curvilinear actuator needs to be explored. While running the pilot tests, there was some wobbling along z axis, the distance between the two helical cylinders would expand and contract along the z axis. This might be due to a reaction force from curvilinear translation. As a quick fix to his problem additional support bushes were added along the central axis. The wobbling reduced significantly in the final prototype, but actuator's setup isn't completely free of wobbling. The exact cause of the problem needs to be found and then addressed

Then with the current design, the actuator's extension part was not included part of the experiment. This could also be tested in future.

For future work, more detailed mathematical models, using multibody dynamics and screw theory can be formulated. Then more experimental testing is also required, and the other production methods also need to be tried to improve the efficiency of the actuator. The curvilinear actuator needs to be implemented part of an elbow prosthesis. The current concept can also be used for another purpose, new curvilinear actuators can be designed, like ones that use hydraulic option, then instead of having two separate actuators to do flexion and extension, a single actuator with two-way actuation can be designed and tested. The range of motion can be increased, and all these changes to the concepts need to be designed and tested.

#### V. CONCLUSION

A new type of pneumatic actuator was designed to be used as an elbow unit. In theory, the actuator can lift up to 1kg. A prototype of the actuator was 3D printed and a simple bench test was conducted. The current prototype has an efficiency ranging from 26-72% depending upon the supply pressure. The bench test results indicate that the proposed curvilinear is a feasible concept that could be used to produce rotary motion.

#### VI. REFERENCE

1. Heger, H., S. Millstein, and G. Hunter, Electrically powered prostheses for the adult with an upper limb amputation. Journal of Bone & Joint Surgery, British Volume, 1985. 67(2): p. 278-281.

- 2. Glynn, M., H. Galway, G. Hunter, and W. Sauter, *Management of the upper-limb-deficient child with a powered prosthetic device*. Clinical orthopaedics and related research, 1986. **209**: p. 202-205.
- 3. Millstein, S., H. Heger, and G. Hunter, Prosthetic use in adult upper limb amputees: a comparison of the body powered and electrically powered prostheses. Prosthetics and orthotics international, 1986. **10**(1): p. 27-34.
- 4. Sturup, J., H. Thyregod, J. Jensen, J. Retpen, G. Boberg, E. Rasmussen, and S. Jensen, Traumatic amputation of the upper limb: the use of body-powered prostheses and employment consequences. Prosthetics and orthotics international, 1988. 12(1): p. 50-52.
- 5. Roeschlein, R. and E. Domholdt, Factors related to successful upper extremity prosthetic use. Prosthetics and orthotics international, 1989. **13**(1): p. 14-18.
- 6. Wright, T.W., A.D. Hagen, and M.B. Wood, Prosthetic usage in major upper extremity amputations. The Journal of hand surgery, 1995. **20**(4): p. 619-622.
- 7. Datta, D., K. Selvarajah, and N. Davey, Functional outcome of patients with proximal upper limb deficiency-acquired and congenital. Clinical rehabilitation, 2004. **18**(2): p. 172-177.
- 8. Biddiss, E. and T. Chau, *Upper-limb* prosthetics: critical factors in device abandonment. American Journal of Physical Medicine & Rehabilitation, 2007. **86**(12): p. 977-987.
- 9. McFarland, L.V., S.L. Hubbard Winkler, A.W. Heinemann, M. Jones, and A. Esquenazi, Unilateral upper-limb loss: satisfaction and prosthetic-device use in veterans and servicemembers from Vietnam and OIF/OEF conflicts. J Rehabil Res Dev, 2010. **47**(4): p. 299-316.
- Biddiss, E., D. Beaton, and T. Chau, Consumer design priorities for upper limb prosthetics.
   Disability and Rehabilitation: Assistive Technology, 2007. 2(6): p. 346-357.

19

- 11. Fite, K.B., T.J. Withrow, X. Shen, K.W. Wait, J.E. Mitchell, and M. Goldfarb, *A gasactuated anthropomorphic prosthesis for transhumeral amputees*. Robotics, IEEE Transactions on, 2008. **24**(1): p. 159-169.
- 12. Janocha, H., *Actuators: basics and applications*. 2013: Springer Science & Business Media.3662055872
- 13. Plettenburg, D.H., A sizzling hand prosthesis: On the design and development of a pneumatically powered hand prosthesis for children. 2002, TU Delft, Delft University of Technology.

# Design Paper

Chapter 3

# Design of a Pneumatic Active Gravity Compensation Mechanism for a Gas Powered Above Elbow Prosthesis

Aravindan Sooryanarain

Delft Institute of Prosthetics and Orthotics, Department of Biomechanical Engineering
Delft University of Technology

Email: a.sooryanarain@student.tudelft.nl

#### **Abstract**

The commercially available powered above-elbow prostheses are perceived heavy by a prosthetic user and are also very expensive. The main reason is because these elbow units use electro-mechanical actuators. The goal of this paper is to design a pneumatic powered active gravity compensation mechanism to reduce the overall actuation torque required to operate an elbow unit. The proposed active gravity compensator uses the concept of spring-mass static balancer, who's configuration can be adjusted actively using a pneumatic multiplex actuator. The mechanism also conceptualizes a locking mechanism that is used to lock the overall mechanism while its configuration is changed according to the load acting on it. The designed gravity compensation mechanism can be used to compensate a maximum torque about 15Nm and the estimated weight of the gravity compensator is about 275g. For future work, both the gravity compensation and the locking mechanism needs to be prototyped and tested.

Keywords: prosthesis, above elbow, transhumeral, active gravity compensator

#### I. INTRODUCTION

Losing an upper limb would affect a person's livelihood immensely. There are a wide variety of prosthetic options that could replace the missing limb. The overall acceptance rate of the below-elbow limb prosthesis is higher compared to above-elbow limb prosthesis [1-4]; especially the acceptance rate of the above-elbow prosthesis range from 40%-80% [1, 2, 4-10]. The use of myoelectric prosthesis is more frequent in below-elbow prosthesis and less frequent in aboveelbow prosthesis [4, 11]. The above-elbow prosthesis has more active joints compared to the below-elbow prosthesis; the additional components would lead to more weight and cost. One of the major reason for upper limb prosthetic rejection is that the prosthetic users perceive the prostheses to be heavy; the weight of a prosthesis takes the top most priority when the users were asked to list their set of design considerations for future prosthetic design [12]. The external powered prostheses that are available in today's market only use an electro-mechanical system to operate. The drawback of using DC motors is that they are often heavy if there is a high torque demand [13, 14]. Therefore, the prosthetic elbow unit requires an alternate system that can produce high torques and the same time weighs lighter. Pneumatic actuators can be used in place of electrical motors to operate the system, as fluidic actuators have a low mass-to-power ratio and low space requirement [13, 14].

There are some of the pneumatic powered elbow units that are only in concept phase in literature [13, 15]. As part of a larger study, to explore the possibilities of designing a pneumatic powered-elbow unit; this paper only focuses on a small section it. Another way of reducing the overall torque of the system is by using a gravity compensator. There is a lot of literature regarding gravity compensators [16-21], but in the topic of elbow prosthesis, there isn't much.

The overall objective of this paper is to design an active gravity compensator for the elbow unit, in order to reduce the torque demand of the overall system.

23

Design Paper

Once the basic design goals are defined, this paper summarizes the following: The basic principle of static balancing, the short comings of a regular gravity compensator, design of an active gravity compensator, pneumatic multiplex actuator's theory. Finally, the results of the study are concluded along with some discussion for future works.

#### II. MATERIALS AND METHOD

#### a. Design criteria

The proposed gravity compensator is evaluated on the basis of its torque capacity and weight. The commercial active elbow units have either a low torque with less weight or a higher torque with heavier weight; Table 3.1 has the details about the weight and torque produced by the commercial active elbow units [22-24].

After taking the technical specifications of the commercially available active elbow units into account the proposed gravity compensator is designed with the intension to achieve the highest possible torque with the lowest possible weight. So, the gravity compensator should be able to compensate more than 15 Nm and weigh less than 540g.

Some spatial constraints were imposed on the proposed elbow unit; the elbow unit should fit inside the contour of the human arm. The following dimensions were assumed to define a human arm; a cylinder of size 85 mm diameter and 350 mm length is taken into consideration as a simple representation of the human arm, the wrist diameter of 50 mm, the palm to wrist length of 50 mm and the fore arm length 250 mm. The various parts of the elbow unit are designed depending upon the overall space left; so the spatial constraint for the each part would vary accordingly.

The supply pressure of the pneumatic system is set to 1.2 Mpa; since it is the optimum gas pressure to have for minimal gas consumption [25].

Table 3.1: Commercial elbow units

Model	Weight (g)	Torque (Nm)
E-Two Elbow	540	3.25
Utah Arm 3+	904	13.25
Boston Digital Arm System	1000	13.5
Dynamic Arm	1000	15

### b. Design approach

A force oriented design approach is used for this study; load capacity and spatial constrains were given more priority compared to weight and other functional constrains during the preliminary design phase. The parts are primarily designed with the intention to fit into a given volume of space and fulfill the set load constrains the best possible way. Finally, the weight of the proposed design is estimated and if the estimated weight of the proposed system is above the set limit, then the design can be reiterated.

The gravity compensator should be able to balance a gravitational torque of:

$$\tau_a = (Mg \ h + mg \ c) \cos \phi \tag{1}$$

Where:

 $\tau_a$  = Gravitational torque

M = External mass

m = Mass of forearm

*h* = Length of the forearm

c = Forearm's center of mass

 $\phi$  = Angle with horizontal axis

g = Acceleration due to gravity

Considering the basic load requirement, the following values are assigned to variables:  $\boldsymbol{h}$  is 300 mm,  $\boldsymbol{c}$  is 135 mm,  $\boldsymbol{M}$  is 5 kg,  $\boldsymbol{m}$  is 1 kg and  $\boldsymbol{g}$  is 9.81 m/s<sup>2</sup>; therefore, the gravity compensation mechanism is designed to compensate a maximum torque ( $cos\phi = 1$ ) of 16.04 Nm. Likewise, the locking mechanism should be able to withstand  $\boldsymbol{\tau_{g}}$ .

In terms of spatial constraints, first, the gravity compensation mechanism is designed to fit within the contour of a human arm; the locking mechanism is designed to fit within the available space inside the outer shell.

All the 3D models are designed with the use of Solidworks and some of the important design parameters are calculated using MATLAB.

### c. Basic principle of static balancing

The basic principle behind statically balanced mechanism is that, the gravitational torque is counteracted by the torque produced by the gravity compensator with the use of a counterweight or spring. In a spring-to-mass static balancer (Figure 3.1), the sum of the moment created by the spring force,  $M_{SF}$  about elbow joint E and the gravitational torque is zero in a statically balanced system [16].

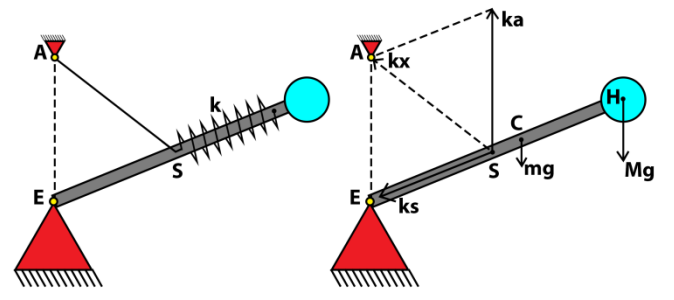


Figure 3.1: Spring-to-mass Gravity compensators

$$M_{SF} + \tau_a = 0 \tag{2}$$

For a zero free-length spring with a spring constant,  $\mathbf{k}$ , we can calculate  $\mathbf{M}_{SF}$  using the following equation:

$$M_{FS} = k \ a \cos \phi \ s \tag{3}$$

Where  $k \ a \cos \phi$ , is the tangential component of the spring force, and the distance from the axis of rotation to the point **S** on the forearm, **s**. Substituting (1) and (3) in (2); the negative sign is added to (1) to denote the moment is acting in the opposite direction.

$$k \ a \cos \phi \ s - Mg \cos \phi \ h - mg \cos \phi \ c = 0$$
 (4)

$$k a s = Mg h + mg c (5)$$

For a given set of load and spatial constraints, the spring constant can be determined.

$$k = \frac{\tau_{gmax}}{a.s} \tag{6}$$

This implies for a given wire diameter, d, coil diameter, D; the number of active turns, n, and the pitch,  $P_s$ , of a helical spring with the required k value can be designed using the following formulae [26].

$$k = \frac{G d^4}{8 n D^3} \tag{7}$$

Where:

G = Modulus of rigidity

## d. Short comings of static balancing

The purpose of using the gravity compensation mechanism to reduce the overall effort required to change the system's position. One of the biggest catch with regular gravity compensators is that they need a stable base and they are designed to compensate a constant external load.

In reality there are few more issues the gravity compensator needs to tackle if it is implemented for an elbow-prosthesis: the upper arm is not going to be always in-line with the vertical axis, the mass of the external object is not going to be constant and the plan of motion could also rotate. This implies in order to maintain the overall moment of the system at zero; the moment created due to spring force should vary accordingly.

When the upper arm is not in-line with the vertical axis, this means the anchor point is also moved away from the vertical axis. This, in turn, affects the overall system dynamics. This problem is overcome by integrating a four-bar mechanism for the upper-arm, which will ensure the anchor point is in-line with the vertical axis.

The in-plane external load component varies either due to change in the actual mass of the external load itself or due to the change in direction of the gravitational force with respect to the plane of motion. There are some good examples in literature about gravity compensator that can adjust its spring stiffness for varying load conditions, and some even achieve them in an energy free fashion [16, 18, 20, 21].

There are some limitations to these mechanisms; either we have to spend energy to change the systems configuration, or these mechanisms can be configured at an energy-free fashion at a particular angle in order for the spring to be fully relaxed.

Considering these above mentioned systems and their limitations, to be used for an elbow-prosthesis; even though there is an energy free approach, it wouldn't be apt to lower the prosthetic arm every time the external load changes. So, in this study the gravity compensator is adjusted with the help of a pneumatic actuator.

Instead of spending excess energy for lifting the elbow every single cycle, the active gravity compensator can reduce the load acting on the elbow joint over multiple cycles, but this depends upon how frequent the in-plane load changes per cycle.

### e. Active Gravity compensation mechanism

In this study, the moment created by the spring force is varied by altering the distance  ${\bf s}$ . Therefore,

Design Paper 25

the active gravity compensator has a pneumatic multiplex cylinder added along with the spring, which is used for varying the distance **s**.

The basic schematic of the active gravity compensator is given in Figure 3.2. The pulley  $P_s$  represents point S. The red lines represent the Bowden cable that runs across the system. The slider is connected with the actuator and it can move a maximum distance s along the forearm. The pulleys  $P_s$ ,  $P_1$ ,  $P_2$ , and  $P_3$  will also traverse the same distance s. Due to the particular arrangement of the pulleys the sliding end of the spring will traverse from 0 to 2s, depending on the angle.

As for the pneumatic multiplex actuator, it should produce more force than the spring force, the output stroke length should be equal to spring deflection required to compensate the external load and it should fit within the available space.

$$F_{MC} > 2ks$$

$$s_{MC} = \frac{Mgh}{ka} = \frac{Mgh}{\tau_{gmax}} s$$
 (8)

Where:

 $F_{MC}$  = Actuation Force of multiplex cylinder  $s_{MC}$  = Stroke length of multiplex cylinder

### e.i. Pneumatic multiplex cylinder

The multiplex cylinder was inspired from the concept of duplex cylinders; the only difference is this consists of N pneumatic cylinders stacked in series. Since there are N cylinders, the actuation force of a single cylinder segment,  $F_{SC}$ , is reduced to the following:

$$F_{SC} = \frac{F_{MC}}{N} \tag{9}$$

From  $F_{SC}$ , the area and the radius of the piston,  $A_{SC}$  and  $r_{SC}$ , are calculated.

#### **Top View**

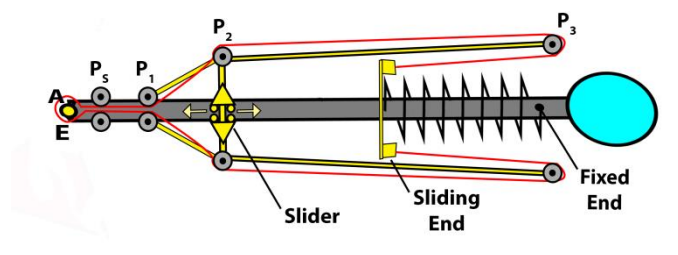


Figure 3.2: Gravity compensator schematic diagram

The stroke length of the  $i^{th}$  cylinder is calculated using the following formula:

$$s_{Ci} = \frac{s_{MC}}{N} i \tag{10}$$

Where:

'i' is a positive integer, varying from 5 to N

The basic schematic of the multiplex cylinder is given in Figure 3.3

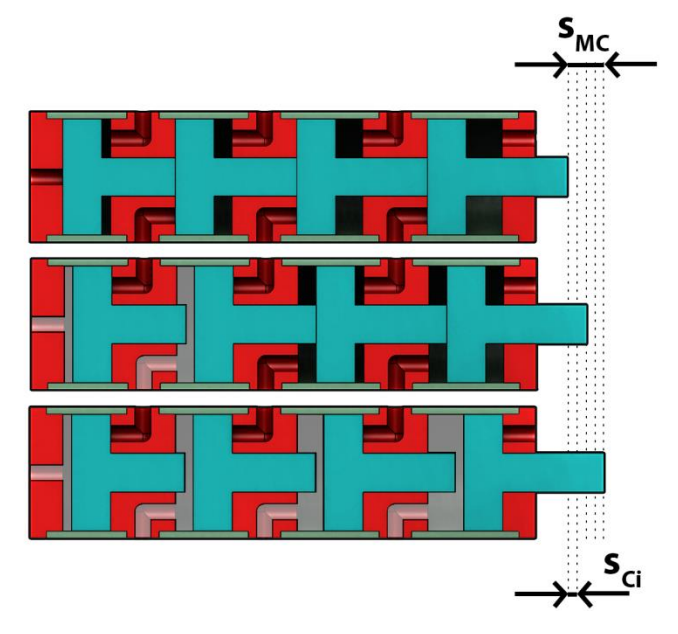


Figure 3.3: Multiplex cylinder

#### e.ii. Design optimization

The maximum load capacity of the gravity compensation mechanism is set 16.04 Nm, i.e. 5kg of external load acting at a distance of 300mm, plus a 1kg of presumptive forearm weight acting at a distance of 135mm. A Matlab code was written in order to compute the optimum values of the design variables. Out of the multiple possible configurations, the optimum configuration is found. For this study the following criteria were taken into to consideration, weight, space occupied and energy expenditure of the overall system. Therefore the following variables were used for the optimization process.

$$OV = \frac{EF}{SF \ EW} \tag{11}$$

$$EF = \frac{\frac{1}{2}k x^2}{p \ vol_{air}} \tag{12}$$

$$SF = L_{MC} D \tag{13}$$

$$EW = w_S + w_{MC} \tag{14}$$

Where:

OV = Optimization Variable

EF = EfficiencySF = Spatial factorEW = Estimated Weight

 $L_{MC}$  = Overall length of multiplex cylinder

 $w_S$  = Weight of spring

 $w_{MC}$  = Weight of multiplex cylinder  $vol_{air}$  = Volume of air consumed

For each dataset the  $\emph{OV}$  value is calculated and the dataset with the highest  $\emph{OV}$  value is the most optimum design.

The dimensions of the variable of the gravity compensation mechanism were optimized according to the properties of set of stock springs. The following website [27] was used as the reference set of stock springs. In order to minimize the search results from the website, the following boundary conditions were set: Max  $\bf d$  =6.5mm, Max  $\bf D$  =50mm, Min  $\bf k$  =430N/mm and Max  $\bf L_f$  =160mm.

Finally, once the optimum values of the various variables are determined, depending upon the variation in the values of M and  $\Delta$ , the mapping of how the different stages of the multiplex cylinder needs to be actuated could be done.

#### f. Locking mechanism

As the curvilinear actuator (discussed on the previous paper) has an output disc, a disc brake mechanism is opted as the locking mechanism.

The locking mechanism has two major parts, the brake shoes and the fluidic actuator. Figure 3.7 represents the basic schematics of the disc brake.

The braking mechanism should be able to compensate the torque produced by the external load. The braking torque,  $\tau_b$ , and the normal contact force,  $N_b$ , is calculated from the following formula [28].

$$\tau_b = \frac{2 \pi n_f \mu p_{bmax} (r_{bo}^3 - r_{bi}^3)}{3} \frac{\beta}{2\pi}$$
 (15)

$$\tau_h = M g h \tag{16}$$

$$N_b = p_{bmax} \pi (r_{bo}^2 - r_{bi}^2) \frac{\beta}{2\pi}$$
 (17)

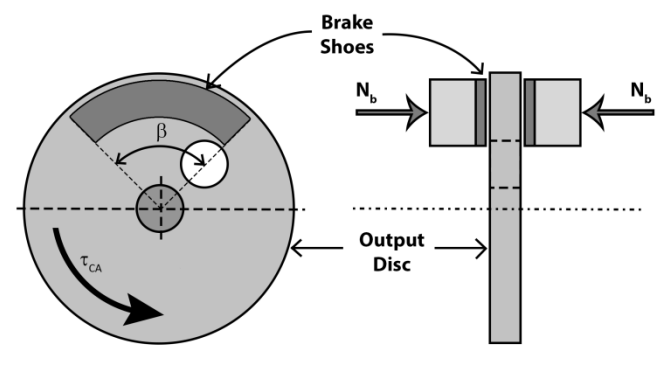


Figure 3.4: Disc brake

Where:

 $n_f$  = Number of frictional interfaces

 $\mu$  = Coefficient of friction

 $p_{bmax}$  = Maximum allowable pressure  $r_{bo}$  = Outer radius of brake shoes  $r_{bi}$  = Inner radius of brake shoes  $\beta$  = Angle subtended by brake shoes

The dimensions of the brake shoe and the actuator force are dependent on the dimensions of the output disc and available space left.

Some of the assumptions that were made are; the design will be based on the of uniform pressure assumption. The brake shoes will be made from a non-asbestos lining material, where the  $\mu$  value is 0.63 and  $p_{bmax}$  is 1.03 MPa [28]. The value of  $n_f$  is assumed to be equal to 2.  $\beta$  can be found by substituting (34) into (33). From  $\beta$ ,  $N_b$ , can be found. Once the value of  $N_b$  is known the dimensions of the fluidic actuator can be determined.

#### III. RESULTS

#### a. Gravity compensation mechanism

As for the online search, 130 stock springs satisfied the base boundary conditions. Out of the 130 only 4 stock springs where able to satisfy the spatial and load constraints of the complete gravity compensator assembly.

Figure 3.8 represents the 3D scatter plot of the optimization parameters (SF, WF, EF) and the radar chart of dimensions of few important design variables (a,  $s_{MC}$ , d, D,  $r_{SC}$ , N).

#### Spatial Factor vs Estimated Weight vs Efficiency Constraints Satisfied Most optimal Datapoint 0.8 0.6 0.4 0.2 600 500 6000 5500 400 5000 4500 300 EW 4000

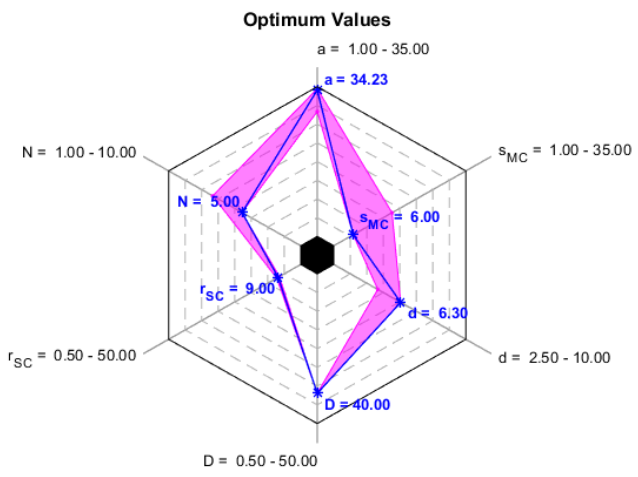


Figure 3.5: Dataset of Gravity compensation mechanism

Table 3.2 has the details about the possible range for the various variables and the value of each variable at the most optimum point, i.e. highest OV value.

Table 3.2: Dimensions of a Gravity Compensator

Variable	Dimension	Range	Optimum
а	(mm)	29.34 – 34.52	34.23
S	(mm)	6.54 – 17.44	6.54
d	(mm)	5 – 6.3	6.3
D	(mm)	40	40
n		3.5 - 8.5	3.5
$r_{SC}$	(mm)	8.5 – 9.5	9
$L_MC$	(mm)	99-140	99
S <sub>MC</sub>	(mm)	6-16	6
N		5-7	5
EW	(g)	235-548	300
EF	(%)	78.5 – 91.92	89.29
OV	(10 <sup>-11</sup> )	2.33 – 14.58	14.58

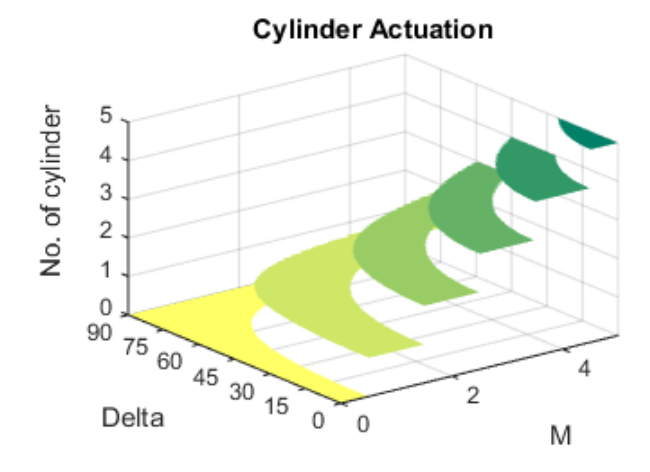
The final model of the gravity compensator has few additional components that is used for the sliding action of point **S** and also hold the spring and multiplex actuator in their respective places. The 3D rendering of the complete gravity compensator assembly is given in Figure 3.6.

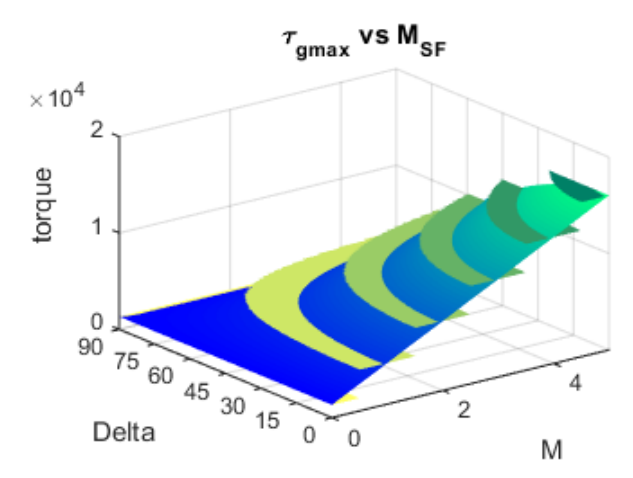
The mapping of the multiplex actuator designed for the most optimal data-point (market spring) is shown Figure 3.7. The shoulder abduction is assumed to vary only between 0-90.

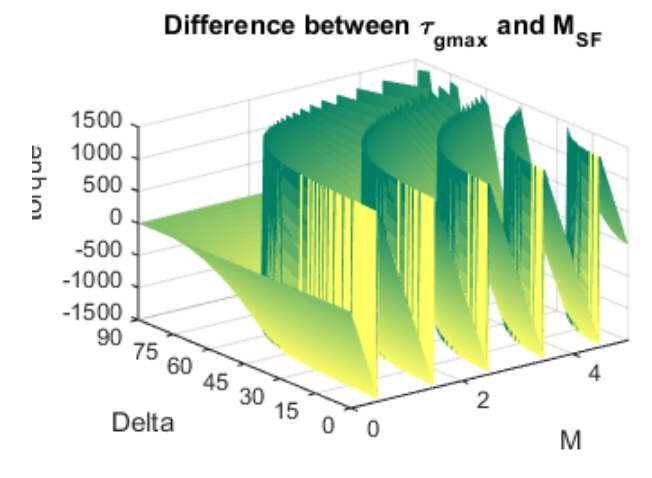
The multiplex cylinder consumes about 113mg of  $CO_2$  (at 20°C), when all five stages are extended. The multiplex actuator alone weighs about 42g, the overall weight of the complete assembly is estimated to be 275g, (computed from Solidworks). A Dyneema or a Bowden cable can be used to connect spring with the anchor point.



Figure 3.6: Gravity compensation mechanism







**Figure 3.7:** Cylinder actuation mapping of the multiplex cylinder

#### b. Braking Mechanism

The value  $r_{bo}$  and  $r_{bi}$  was set to 33mm and 22mm respectively, after taking the dimensions of the output disc of the curvilinear actuator into consideration.

In order to meet the required braking capacity  $(\tau_b)$ ,  $\beta$  was set to be 80°  $(\beta > 77^\circ)$  and  $N_b$  is about 418.73N. To actuate the brake shoes, five small hydraulic actuators are attached to it to produce the required force. The diameter of the hydraulic piston was assumed to be 5.5mm and a supply pressure of 3.55 MPa. Figure 3.8 represents the simple 3D model of the brake shoes along with the output disc.

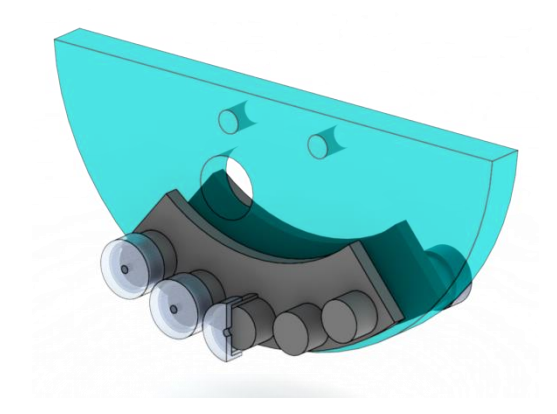


Figure 3.8: Braking mechanism

#### IV. DISCUSSION

The major focus of this study was the active gravity compensation mechanism. The gravity compensation mechanism and locking mechanism were only conceptualized in theory and 3D models.

In theory the gravity compensation mechanism should be able to compensate a maximum external load of 5kg; but, this needs to be tested in practice. One of the challenge one might face while building the gravity compensation mechanism is, clamping the dyneema ropes. If the ropes are not clamped properly then the gravity compensator might be off by some value, and this might create an imbalance.

Another point of concern with the gravity compensator is the nodes at which the multiplex actuator shifts stages. There is a drastic change in the overall moment of the system at theses nodes. Therefore the shifting of stages can only happen when the arm (output disc) is in a locked state.

In this paper only the preliminary design phase of the gravity compensator was discussed. A detailed feedback and control loop, along with the additional sensors, servo valves and regulatory valves needs to be designed. Additionally, the current design of the gravity compensator only takes the out of plane rotation into account. The current design doesn't incorporate a compensation mechanism for upper arm flexion and extension. In the future design this problem can be overcome by adding a passive four-bar mechanism.

#### V. DESIGN SUMMARY

The design of an active gravity compensation mechanism, along with the design of a multiplex actuator and locking mechanism was conceptualized for pneumatic elbow unit. The gravity compensation mechanism can compensate up to 5kg of external mass and presumptive 1kg of self-load of the prosthesis. The complete assembly of the active gravity compensator estimated weight is about 275g and the multiplex actuator's weight is estimated to be 42g. The gravity compensator's consumes about 113mg of CO2 and has a theoretical efficiency of 89%. The braking mechanism is designed to produce a braking torque of 15Nmm. For future work the active gravity compensator must be prototyped and tested in order to check if the proposed system is practically feasible or not.

#### VI. REFERENCE

- 1. Wright, T.W., A.D. Hagen, and M.B. Wood, Prosthetic usage in major upper extremity amputations. The Journal of hand surgery, 1995. **20**(4): p. 619-622.
- 2. Biddiss, E. and T. Chau, *Upper-limb* prosthetics: critical factors in device abandonment. American Journal of Physical Medicine & Rehabilitation, 2007. **86**(12): p. 977-987.
- 3. Raichle, K.A., M.A. Hanley, I. Molton, N.J. Kadel, K. Campbell, E. Phelps, D. Ehde, and D.G. Smith, *Prosthesis use in persons with lower-and upper-limb amputation*. Journal of rehabilitation research and development, 2008. **45**(7): p. 961.
- 4. McFarland, L.V., S.L. Hubbard Winkler, A.W. Heinemann, M. Jones, and A. Esquenazi, Unilateral upper-limb loss: satisfaction and prosthetic-device use in veterans and servicemembers from Vietnam and OIF/OEF conflicts. J Rehabil Res Dev, 2010. **47**(4): p. 299-316.
- 5. Heger, H., S. Millstein, and G. Hunter, Electrically powered prostheses for the adult

- with an upper limb amputation. Journal of Bone & Joint Surgery, British Volume, 1985. **67**(2): p. 278-281.
- 6. Glynn, M., H. Galway, G. Hunter, and W. Sauter, *Management of the upper-limb-deficient child with a powered prosthetic device*. Clinical orthopaedics and related research, 1986. **209**: p. 202-205.
- 7. Millstein, S., H. Heger, and G. Hunter, Prosthetic use in adult upper limb amputees: a comparison of the body powered and electrically powered prostheses. Prosthetics and orthotics international, 1986. **10**(1): p. 27-34.
- 8. Sturup, J., H. Thyregod, J. Jensen, J. Retpen, G. Boberg, E. Rasmussen, and S. Jensen, *Traumatic amputation of the upper limb: the use of body-powered prostheses and employment consequences.* Prosthetics and orthotics international, 1988. **12**(1): p. 50-52.
- 9. Roeschlein, R. and E. Domholdt, Factors related to successful upper extremity prosthetic use. Prosthetics and orthotics international, 1989. **13**(1): p. 14-18.
- 10. Datta, D., K. Selvarajah, and N. Davey, Functional outcome of patients with proximal upper limb deficiency-acquired and congenital. Clinical rehabilitation, 2004.

  18(2): p. 172-177.
- 11. Kyberd, P.J. and W. Hill, Survey of upper limb prosthesis users in Sweden, the United Kingdom and Canada. Prosthetics and orthotics international, 2011. **35**(2): p. 234-241.
- 12. Biddiss, E., D. Beaton, and T. Chau, *Consumer design priorities for upper limb prosthetics*.

  Disability and Rehabilitation: Assistive
  Technology, 2007. **2**(6): p. 346-357.
- 13. Fite, K.B., T.J. Withrow, X. Shen, K.W. Wait, J.E. Mitchell, and M. Goldfarb, *A gasactuated anthropomorphic prosthesis for transhumeral amputees*. Robotics, IEEE Transactions on, 2008. **24**(1): p. 159-169.
- 14. Janocha, H., Actuators: basics and applications. 2013: Springer Science & Business Media.3662055872

- 15. Foglia, M. and M. Valori. A high performance wire device for an elbow prosthesis. in Biomedical Robotics and Biomechatronics (BioRob), 2012 4th IEEE RAS & EMBS International Conference on. 2012. IEEE.
- 16. Herder, J.L., *Energy-free Systems. Theory,* conception and design of statically. Vol. 2. 2001.9037001920
- 17. Vrijlandt, N. and J. Herder, Seating unit for supporting a body or part of a body. 2002, Google Patents.
- 18. Van Dorsser, W.D., R. Barents, B.M. Wisse, and J.L. Herder, *Gravity-balanced arm support with energy-free adjustment*. Journal of medical devices, 2007. **1**(2): p. 151-158.
- 19. Wisse, B.M., W.D. Van Dorsser, R. Barents, and J.L. Herder. *Energy-free adjustment of gravity equilibrators using the virtual spring concept*. in 2007 IEEE 10th International Conference on Rehabilitation Robotics. 2007. IEEE.
- 20. Van Dorsser, W., R. Barents, B. Wisse, M. Schenk, and J. Herder, Energy-free adjustment of gravity equilibrators by adjusting the spring stiffness. Proceedings of the Institution of Mechanical Engineers, Part C: Journal of Mechanical Engineering Science, 2008. 222(9): p. 1839-1846.
- 21. Barents, R., M. Schenk, W.D. van Dorsser, B.M. Wisse, and J.L. Herder, *Spring-to-spring*

- balancing as energy-free adjustment method in gravity equilibrators. Journal of Mechanical Design, 2011. **133**(6): p. 061010.
- 22. Elbow Prosthesis Otto bock. Available from: http://www.ottobock.nl/media/localmedia/prothesen/productinformatie/dynami carm\_en.pdf.
- 23. *Utha Arm Motion Control*. Available from: http://www.utaharm.com/files/.
- 24. *Upper Limb Prosthesis Fillauer*. Available from: http://fillauer.eu/prosthetics-upper.
- 25. Plettenburg, D.H., A sizzling hand prosthesis: On the design and development of a pneumatically powered hand prosthesis for children. 2002, TU Delft, Delft University of Technology.
- 26. Committee, S.S., *Spring Design Manual*. 1996: Society of Automotive Engineers.156091680X
- 27. Tevema industrial springs. Available from: <a href="http://www.tevema-industrial-springs.com/index">http://www.tevema-industrial-springs.com/index</a> en.html.
- 28. Collins, J.A., H.R. Busby, and G.H. Staab,
  Mechanical design of machine elements and
  machines: a failure prevention perspective.
  2010: John Wiley & Sons.0470413034

Design Paper 31

# Appendix

Chapter 4

## Appendix A: Design Process of a Pneumatic Elbow Unit

The elbow unit was designed to meet a set of base line requirements as a whole, but the different parts of the elbow unit have their own set of individual targets to achieve. The parts were primarily designed with the intention to fit into a given volume of space and fulfill the set load constrains the best possible way.

The load constraints set for the various parts of the elbow unit are as follows:

- As the base structural element, the outer shell should withstand a load (dead-lift) of 230N.
- The gravity compensation mechanism should be able to compensate a maximum torque (live-lift) of 16.04 Nm, i.e. external mass **M** is 5kg @ **h** is 300mm and forearm mass **m** is 1kg @ **c** is 135mm.
- The locking mechanism should be able to withstand 16.04Nm load.
- The lifting mechanism should be able to lift a minimum of 500g acting at a distance of 300mm.
- Additionally the prosthetic elbow should be able to flex 130°.
- The supply pressure of the pneumatic system is set to 1.2Mpa;

The spatial constraints that were set on the proposed elbow unit:

- The elbow unit should fit inside the contour of the human arm.
- A simple representation of the human forearm was assumed the following dimensions:
  - o a cylinder of size 85mm diameter and 350mm length
  - a wrist diameter of 50mm
  - a palm to wrist length of 50mm
  - o a forearm length 250mm

First, the outer shell is designed to fit within the contour of a human arm; then the gravity compensation mechanism, lifting mechanism and locking mechanism are designed to fit within the available space inside the outer shell.

All the 3D models are designed with the use of Solidworks and some of the important design parameters were calculated using MATLAB

Appendix 35

# Appendix B: Outer Shell

The outer shell should be able to withstand a load 69Nm i.e. 230N @ 300mm. The outer shell is further divided into three elements: upper-arm link, elbow cup and forearm; Figure B.1 represent the concept (Photoshop) sketch of the outer shell. The bending moment of few crucial sections of the outer shell is calculated to determine the thickness of the shell at these sections and the outer shell is designed accordingly.

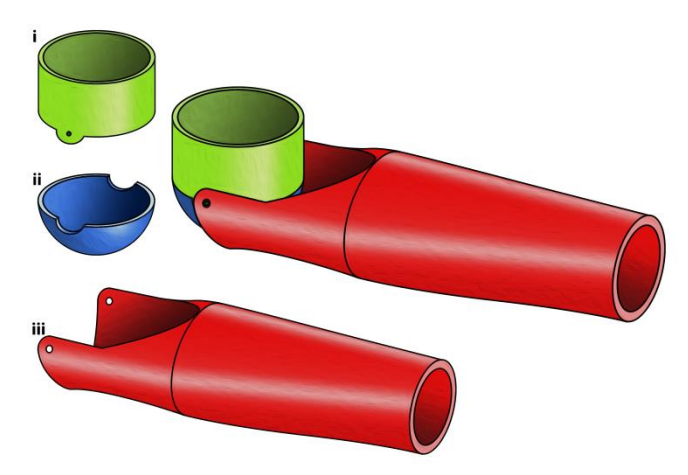


Figure B.1 Concept sketch of the outer shell; i) Upper-arm link, ii) Elbow cup, iii) Forearm

The various parts of final 3D model of the outer shell in the exploded view along with few other important dimensions are shown in Figure B.2. In the final assembly, instead of connecting the forearm shell directly with the elbow axle, a connecting strip was added.

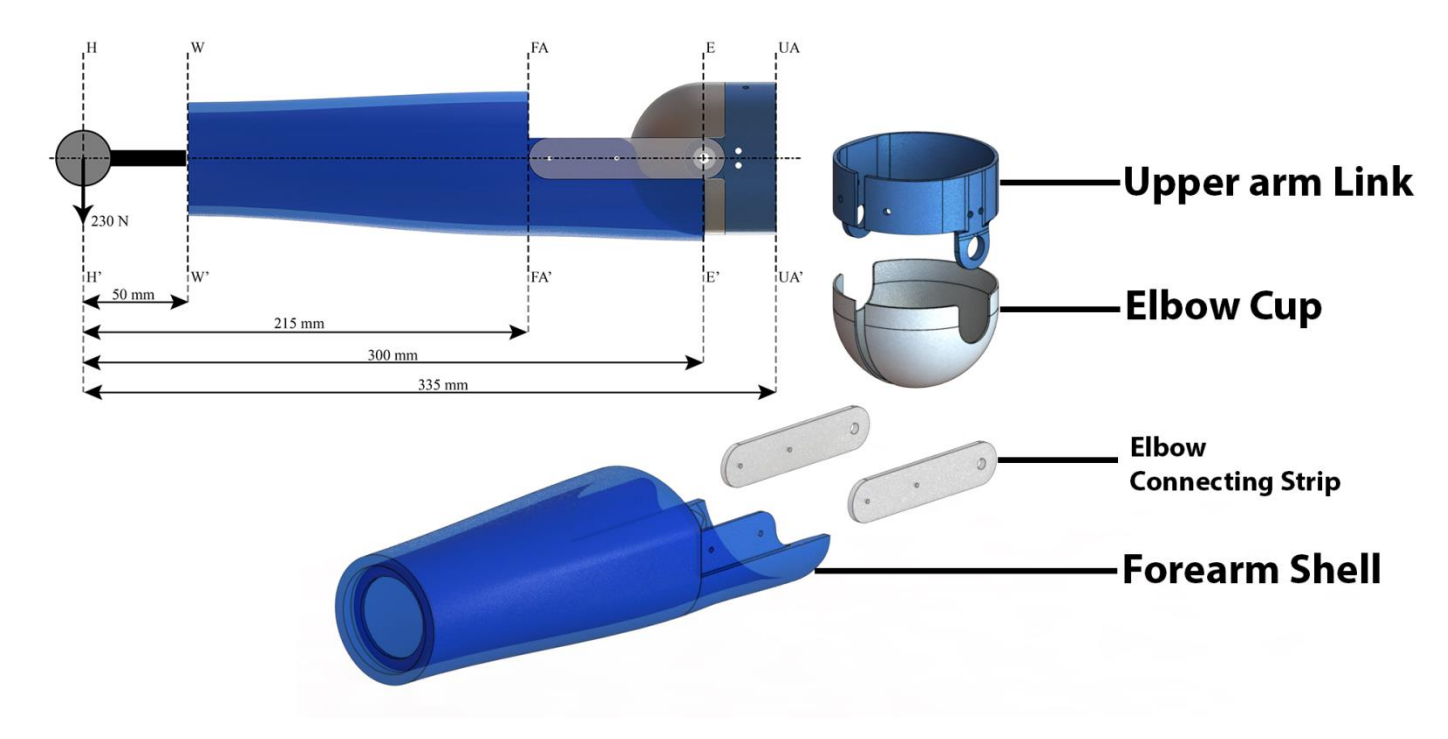


Figure B.2 Outer shell

As the basis structural element the crushing stress of the central axle was calculated to find out what type of bearing and what the minimum diameter of the central axis needs to be. An Aluminum alloy 6061 T6, was considered to be used for the central axis rod, whose tensile strength is 241N/mm^2.

Therefore:

$$Dia = \frac{Load}{\sigma_c * Thickness * n} FS$$

$$Dia_{Central\ Axle} \ge \frac{230\ N}{241 * 3 * 2} \ 8 \ge 1.3mm$$
(1)

Where:

FS = Factor of safety n = No. of sites

But the minimum inner diameter (ID) for a ball bearing is 5mm. So the central axle's diameter was also set to 5mm. As for the ball bearing, its ID is 5mm, outer diameter (OD) is 13mm and thickness of 3mm.

The strip's thickness was assumed to be 3mm and it was made out of aluminum alloy 6061 T6. The width of the strip was calculated from the bending moment, for design purpose it was rounded up to 20mm.

For simplicity purpose, cross-sections of the wrist WW', forearm FAFA' and upper arm UAUA' were considered to be hollow circles in order to find the thickness. The following formula was used to find the bending stress and thickness of the cross-section. The outer shell is made from 3D printing, and the material strength was assumed to be 48N/mm^2. The upper-arm link was considered to be made out of aluminum alloy 6061 T6

$$\frac{M}{Z} \le Tensile Strength of material \tag{2}$$

$$Z = \frac{\pi}{32} \left( \frac{OD^4 - ID^4}{OD} \right) \tag{3}$$

Where:

M = Bending momentZ = Sectional modulus

The bending moment, ID, and OD for the following cross-sections are listed on Table B.1. The dimensions of an ID or OD were assumed in relation to the preexisting designs.

Table B.1: Stress due to bending moment

Cross-section	Bending Moment (Nm)	ID (mm)	OD (mm)	Required Min Thickness (mm)
Wrist (W-W')	11.50	50	NA	0.024
Forearm (FA-FA')	49.45	NA	65	0.63
Upper Arm (UA-UA')	77.05	NA	74	0.47

# Appendix C: Gravity Compensator Design

The major design challenges faced while incorporating basic static balancing for elbow prosthesis:

• Variation in the in-plane load component.

The in-plane external load component varies either due to change in the actual mass of the external load itself (Figure C.1) or due to the change in direction of the gravitational force with respect to the plane of motion (Figure C.2). This problem can be overcame by adjusting the values of the variables k, a, or s to vary the moment created by the spring force. In this study, the distance s is altered to the match change in payload.

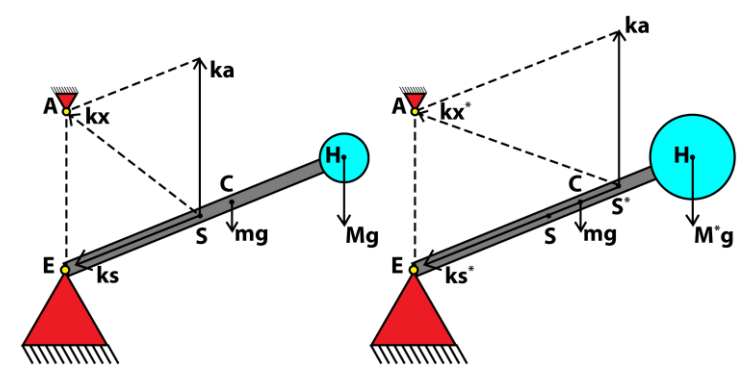


Figure C.1 Change in actual mass

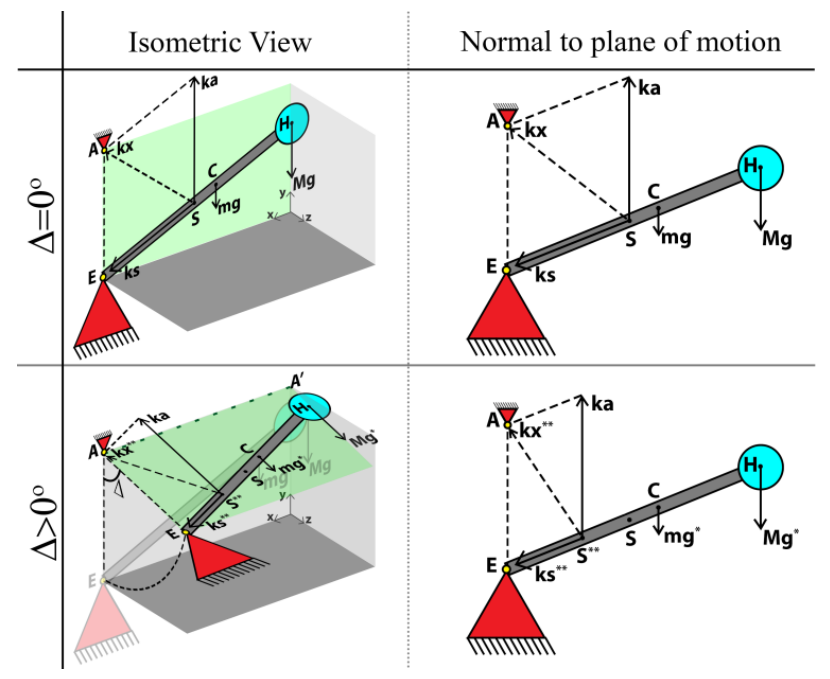


Figure C.2 Change in direction of gravity with respect to the plane of motion

We know s is proportional to M. If the mass of the external load increases to  $M^*$ , then the distance s is also increased to  $s^*$  in a linear fashion. When the plane of motion rotates about the axis AA', and makes an angle  $\Delta$ , then the distance s is varied in form of a cosine function, since

$$g^* = g \cos \Delta \tag{1}$$

There are quite a number of solutions given in literature regarding adjustable gravity compensator [1-4], the gravity compensation mechanism is adjusted either by spending energy or the mechanism can be adjusted at a certain angle in an energy-free fashion. The active gravity compensator has a pneumatic multiplex cylinder added along with the spring, which is used for varying the distance s.

Overall design requirement for the gravity compensator:

• The maximum load capacity of 16.04Nm, i.e. 5kg external load @ 300mm, plus a 1kg forearm weight @ 135mm.

#### a. Spring Design

For a given wire diameter, d, coil diameter, D; the number of active turns, n, and the pitch,  $P_s$ , of a helical spring with the required k value can be designed using the following formulae [5].

$$n = \frac{G d^4}{8 k D^3} \tag{2}$$

$$P_S = \frac{L_f - 2d}{n} \tag{3}$$

$$L_f = (n+2)d + 1.15x (4)$$

$$x = 2s \tag{5}$$

Where:

G = Modulus of rigidity

 $L_f$  = Free length

x = Maximum spring deflection

The calculated stress,  $\sigma_s$ , of the spring at the maximum deflection should be less than the tensile strength of the selected material for the given wire diameter [5].

$$\sigma_S = \frac{8 k \times D}{G d^3} K_w \tag{6}$$

$$K_w = \frac{4C - 1}{4C - 4} + \frac{0.615}{C} \tag{7}$$

$$C = \frac{D}{d} \tag{8}$$

Where:

 $K_w$  = Wahl's stress correction factor

C = Spring index

#### b. Pneumatic multiplex cylinder Design

Design requirements of the multiplex cylinder are:

- Pneumatic multiplex actuator should produce more force than the spring force
- The output stroke length should be equal to spring deflection required to compensate the external load.
- Should fit within the available space.

This implies

$$F_{MC} > 2ks$$

$$s_{MC} = \frac{Mgh}{ka} = \frac{Mgh}{\tau_{amax}} s \tag{9}$$

$$F_{SC} = \frac{F_{MC}}{N} \tag{10}$$

$$A_{SC} = \frac{F_{SC}}{(p - p_a) \, \eta_{MC}} \tag{11}$$

$$r_{SC} = \sqrt{\frac{A_{SC}}{\pi}} \tag{12}$$

Where:

 $F_{MC}$  = Actuation Force of multiplex cylinder  $s_{MC}$  = Stroke length of multiplex cylinder  $F_{SC}$  = Force of a single cylinder segment

N = No. of segments

 $A_{SC}$  = Cross-sectional area of piston head

 $\begin{array}{ll} p & = \text{Supply pressure} \\ p_a & = \text{Atmospheric pressure} \\ \eta_{MC} & = \text{Actuator efficiency} \\ r_{SC} & = \text{Radius of piston head} \end{array}$ 

The cylinder thickness of the multiplex cylinders,  $t_{MC}$ , can be calculated when the hoop stress is equal to the tensile strength of the material used,  $\sigma_{Mat}$ . **FS** is the factor of safety

$$t_{MC} = \frac{p \, r_{SC}}{\sigma_{Mat}} \, FS \tag{13}$$

The stroke length of the *i*<sup>th</sup> cylinder is calculated using the following formula:

$$s_{Ci} = \frac{s_{MC}}{N} i \tag{14}$$

Where:

'i' is a positive integer, varying from 5 to N

#### c. Design optimization algorithm

The logic behind the optimization algorithm is a set of following independent ( $\boldsymbol{a}$ ,  $\boldsymbol{s}_{MC}$ ,  $\boldsymbol{d}$ ,  $\boldsymbol{D}$ ,  $\boldsymbol{r}$ ,  $\boldsymbol{N}$ ), the rest of the other design variables were computed using the formulae given above. The independent variables were allowed to vary (mostly) from 1 to their corresponding spatial limitation. Then the rest of load and spatial constraints were checked. If all conditions were satisfied, then a dataset containing all the values of the dependent and independent variables were appended one after the other.

The spring is made from music wire, therefore, the standard wire diameter and tensile strength of a music wire,  $TS_s$  were used [5].

The distance a, and the output stroke length  $s_{MC}$ , are assumed to vary up to the maximum space left in the elbow. The value of distance s and k can be found using (12) and (1). The coil spring is designed to meet the required k value for various, standard wire diameter and coil diameter configurations.

The coil diameter is varied up to the maximum wrist space left. Likewise, for the multiplex actuator, the piston radius made to vary within the rest of the available space and the number of segments the multiplex cylinder is also varied. The other design parameters are computed accordingly. If the calculated values satisfy the load and spatial constraints, they are stored in a dataset. The basic algorithm used to calculate the dimensions of the spring and the pneumatic multiplex cylinder is depicted in Figure C.3.

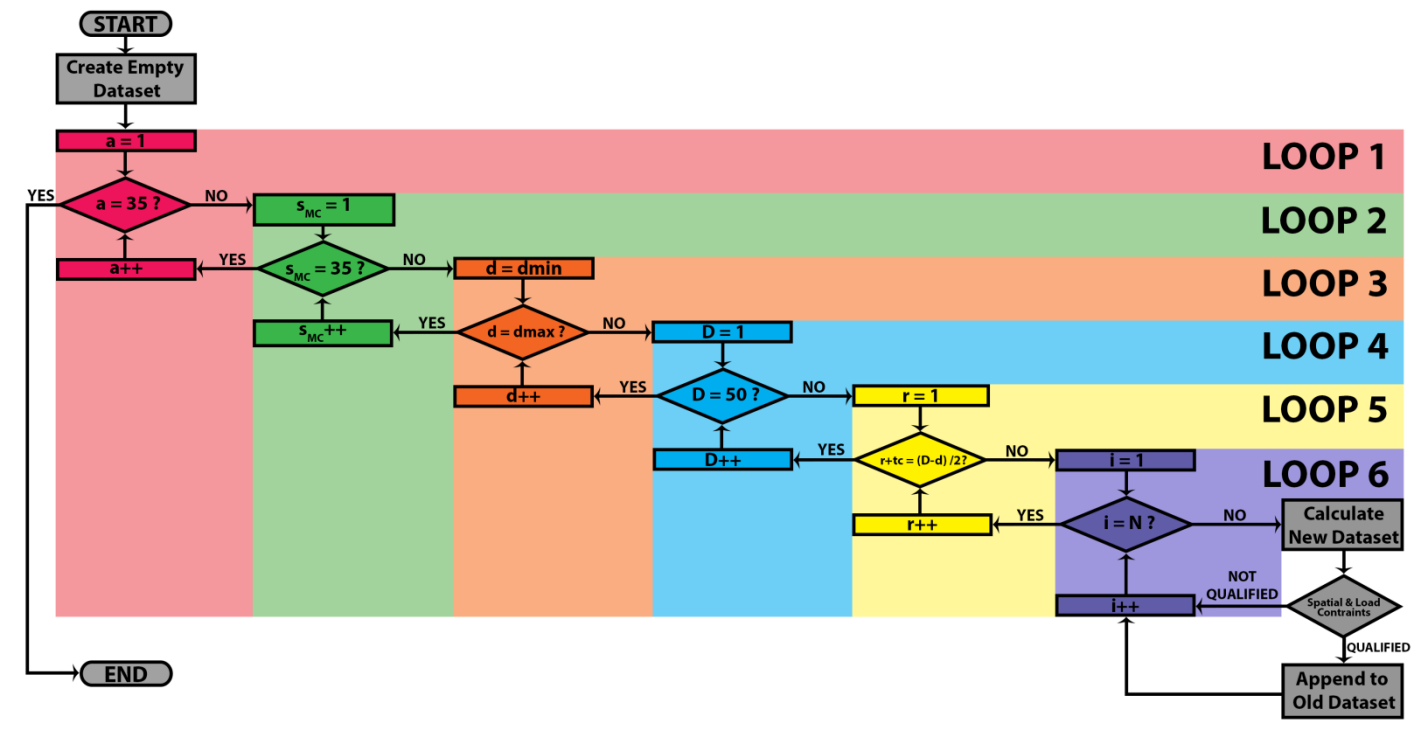


Figure C.3 Basic algorithm flow-chart

Out of the multiple possible configurations, the optimum configuration is found by taking the following criteria were taken into to consideration, weight, space occupied and energy expenditure of the overall system. Therefore the following variables were used for the optimization process.

$$OV = \frac{EF}{SF \ EW} \tag{15}$$

$$EF = \frac{\frac{1}{2}k x^2}{p \ vol_{air}} \tag{16}$$

$$SF = L_{MC} D (17)$$

$$EW = W_S + W_{MC} \tag{18}$$

Where:

OV = Optimization Variable

EF = EfficiencySF = Spatial factorEW = Estimated Weight

 $L_{MC}$  = Overall length of multiplex cylinder

 $w_{\rm S}$  = Weight of spring

 $w_{MC}$  = Weight of multiplex cylinder  $vol_{air}$  = Volume of air consumed

For each dataset the *OV* value is calculated and the dataset with the highest *OV* value is the most optimum design. The optimization code uses a basic brute force method of optimizing. For future work, the optimization code can be improved by using discreet optimization techniques.

Finally, once the optimum values of the various variables are determined, depending upon the variation in the values of M and  $\Delta$ , the mapping of how the different stages of the multiplex cylinder needs to be actuated is done. The Matlab code for the optimization algorithm is given in Appendix E.

41

Table C.1 has the details about the possible range for the various variables and the value of each variable at the most optimum point. Figure C.5 represents the 3D scatter plot of the optimization parameters (SF, WF, EF) and the radar chart of dimensions of the independent variables (a,  $s_{MC}$ , d, D,  $r_{SC}$ , N). Figure C.5 represents a multivariant graph that shows how the data-points are distributed.

Table C.1: Gravity Compensator with custom spring

Variable	Dimension	Range	Optimum
а	(mm)	27.72 – 34.99	32.75
S	(mm)	5.45 – 18.53	5.45
d	(mm)	6 - 6.5	6
D	(mm)	39.5 – 42.5	41.5
n		1.75 – 10.25	2
$L_f$	(mm)	33.52 – 121.65	35.8
$P_{S}$	(mm)	10.3 – 12.3	11.9
$r_{sc}$	(mm)	8.5-10	9
$L_MC$	(mm)	95-144	95
S <sub>MC</sub>	(mm)	5-17	5
N		5-7	5
EW	(g)	206-609	206
EF	(%)	56 – 93.5	93.34
OV	(10 <sup>-7</sup> )	2.17 – 11.47	11.47

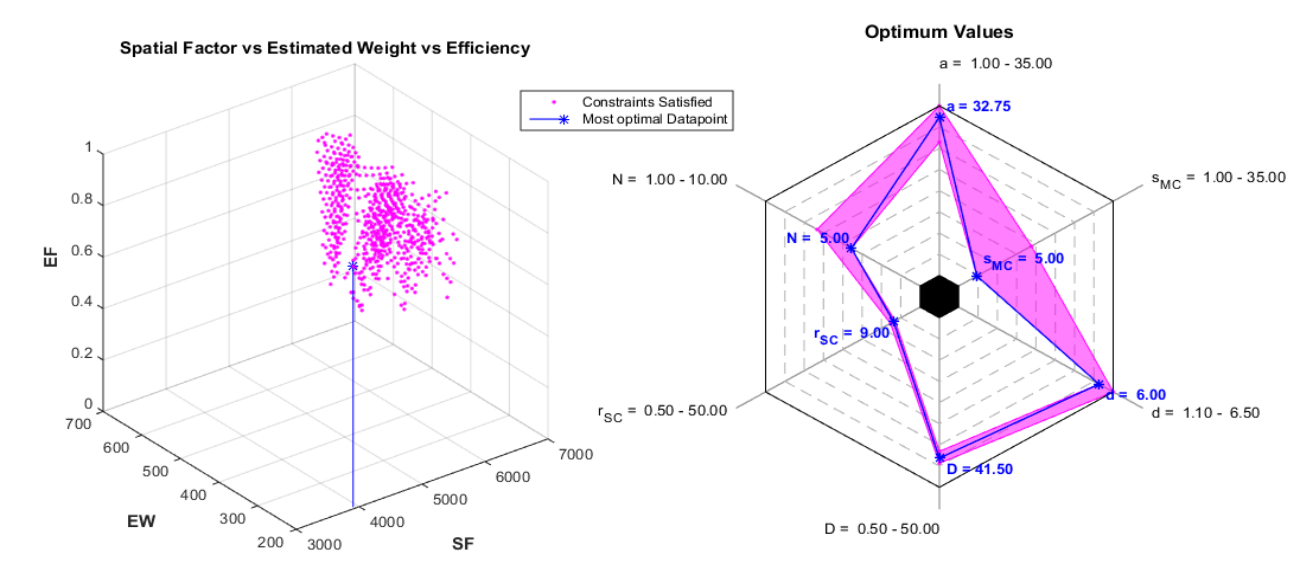


Figure C.4 Dataset of gravity compensation mechanism with custom made springs

In the above algorithm the gravity compensation mechanism is optimized according to a custom made spring. Stock springs are less expensive than custom made springs. So instead of designing a spring to meet a specific k value; the value of distance a is adjusted to compensate for the k value of the stock spring. Then dimensions of the other variables of the gravity compensation mechanism are computed accordingly. The results of the optimization of the gravity compensator using a market spring data are already presented in the design paper. The 3D model of the complete assembly of the active gravity compensation mechanism is given in Figure C.6. The exploded view of the active gravity compensator is given in Figure C.7 and Figure C.8 contains the exploded view of the multiplex actuator sub-assembly.

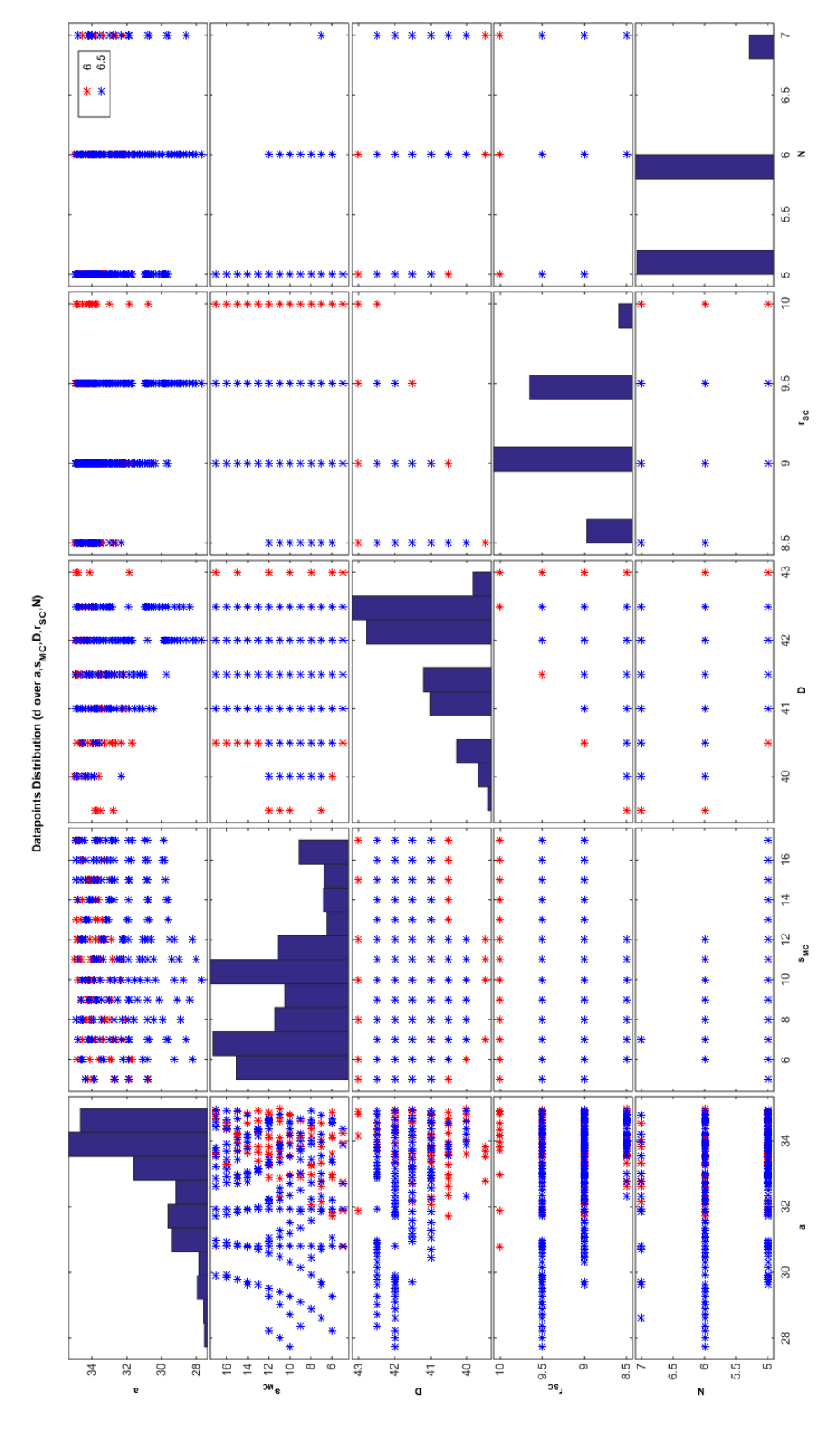


Figure C.5 Datapoints distribution of the all the possible configuration for a gravity compensator

43

Appendix

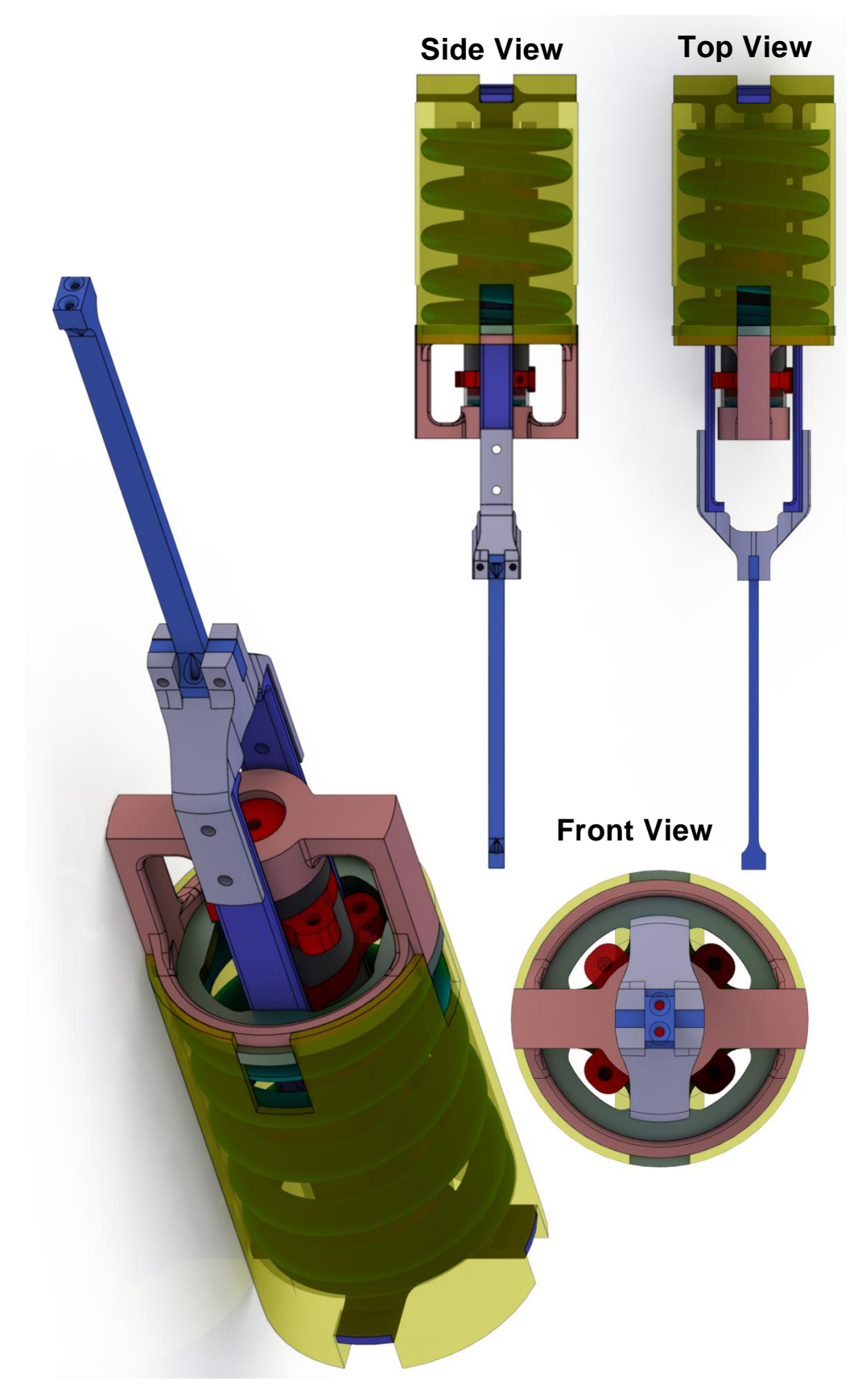


Figure C.6 Complete assembly of the gravity compensator

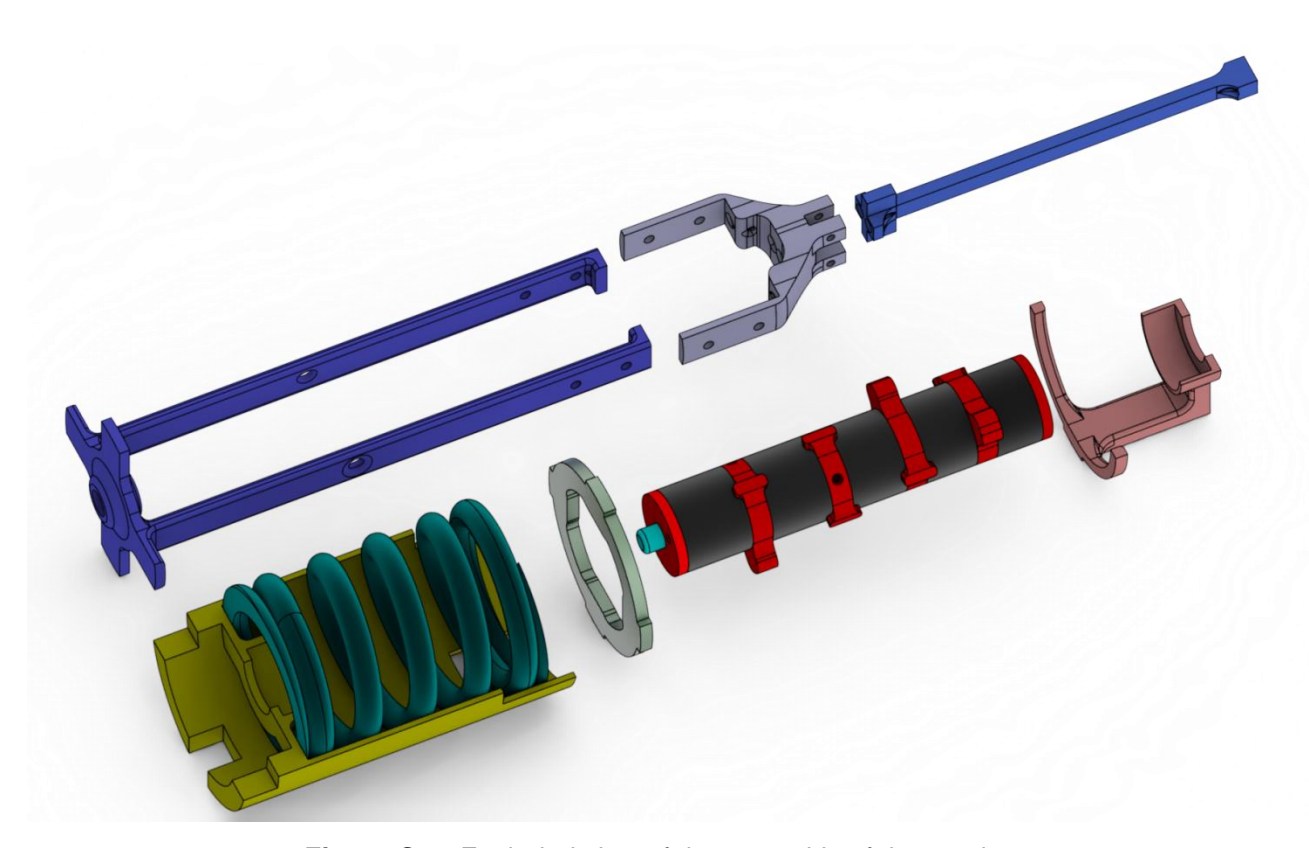


Figure C.7 Exploded view of the assembly of the gravity compensator

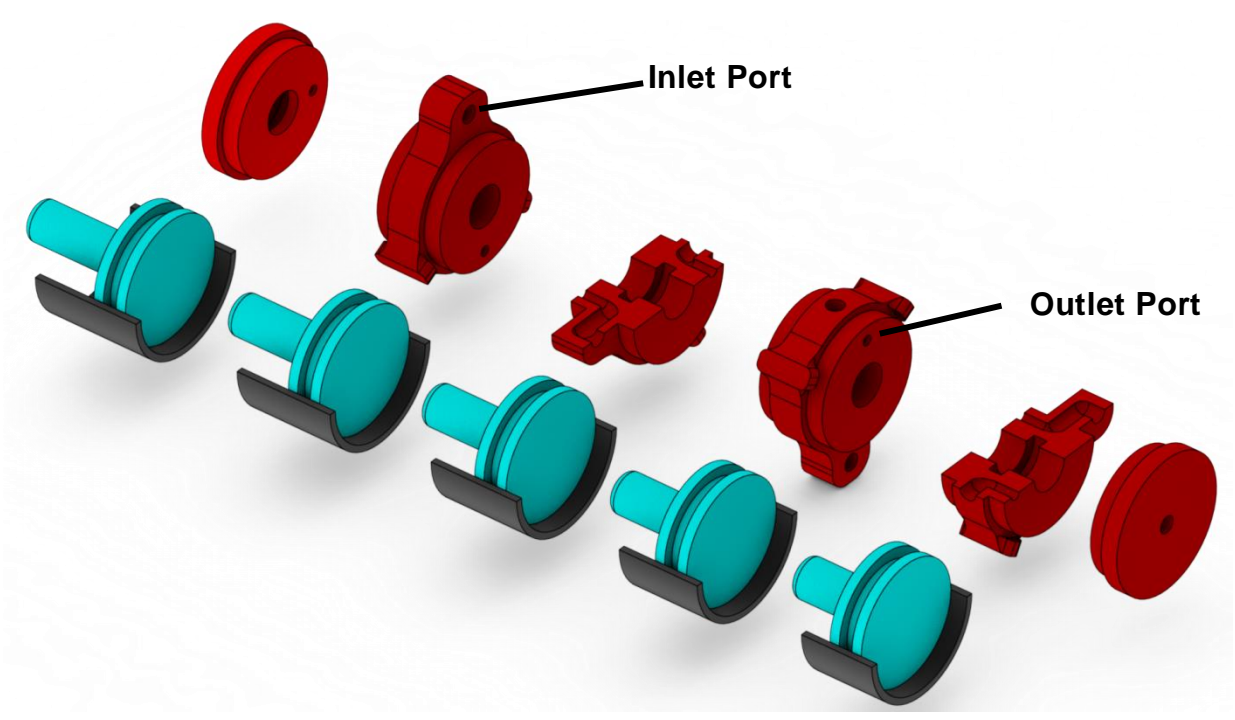


Figure C.8 Exploded view of multiplex actuator

The small protrusion seen on the cylinder caps used between two cylinder segments are made in order to connect a 3mm fitting

45

# Appendix D: Curvilinear Actuator Design and Testing

The curvilinear actuator study was done purely done as an exploratory research. The main reason behind designing this actuator was, there was no literature found regarding the topic of curvilinear actuation, and some curiosity. The curvilinear actuator's was inspired by the actions of a kid sliding down thorough a helical tube in water theme parks. At the beginning the idea was to come out with multiple concepts for a lifting mechanism.

Some of the examples of the mechanisms that came up during the brainstorming phase were:

- Simple revolute joint
- · Cable and pulley
- Rack and pinion
- Slider and crank
- Four bar mechanism
- Parallel mechanism

As for selecting what actuators can be used to actuate these mechanisms, the following were considered:

- 2 Linear cylinders (one-way no-return) acting as antagonistic pairs
- A single linear cylinder with 2-way action
- McKibben muscles
- Vane motors
- Radial motors
- Swash plate motor
- Curvilinear Actuator

Since the basic theory is already given in the scientific paper. In this section only the design algorithm and testing protocol is explained.

#### a. Design algorithm

The basic concept of the design algorithm is similar to the one used for the gravity compensation mechanism, The following variables were considered as the independent variable that control the loops; ( $r_{P-HP}$  and  $R_H$ ). The rest of the other variables were calculated using these formulae

$$F_{HP} = (p - p_a) A_{HP} \eta_{CA} \tag{1}$$

Where:

 $F_{HP}$  = Input force p = Supply pressure

 $p_a$  = Atmospheric pressure

 $A_{HP}$  = Cross-sectional area of piston head

 $\eta_{CA}$  = Overall actuator efficiency

$$\tau_{CA} = F_{HP} \cos \lambda \ R_H \tag{2}$$

Where:

 $\tau_{CA}$  = Output Torque

 $R_H$  = Radius of helix

 $\lambda$  = Lead angle of helix

Due to the design error, the Output torque was changed to the following equation:

$$\tau_{CA} = F_{HP} \cos \lambda \, \cos \lambda \, R_H \tag{3}$$

$$L_{CA} = \sqrt{P_H^2 + (2\pi R_H)^2} \frac{\theta}{360} \tag{4}$$

$$Vol_{CA} = A_{HP} L_{CA} (5)$$

$$E_{Th} = \frac{\tau_{CA} \, \theta}{p \, Vol_{CA}} \tag{10}$$

Where:

 $L_{CA}$  = Stroke arc length

 $P_H$  = Pitch of helix

 $R_H$  = Radius of helix

 $\theta$  = Angle of rotation

 $Vol_{CA}$  = Stroke volume

 $E_{Th}$  = Theoretical energy expenditure.

The Matlab code for the design algorithm is given in Appendix F. After the code was run, the design with the highest output torque was modeled in Solidworks. Figure D.1 shows the distribution of the all data-points that satisfied the spatial and load constraints.

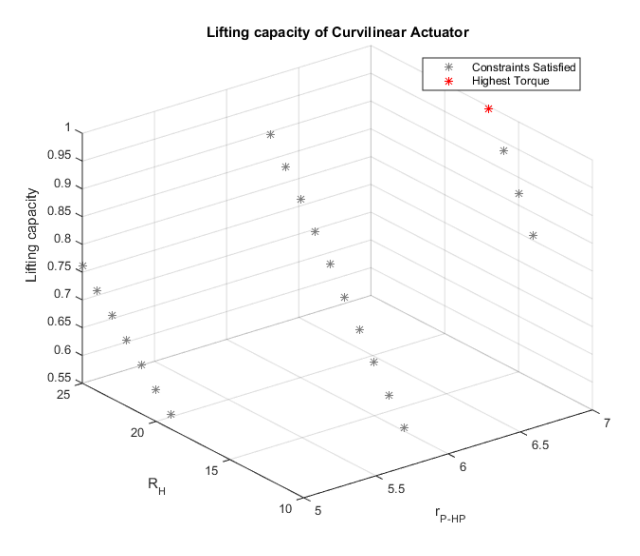


Figure D.1 r<sub>P-HP</sub> vs R<sub>H</sub> vs Lifting capacity

### b. Experimental Protocol

The procedure for a single trial is conducted in the following manner:

- 1. The required pressure is set by turning the pressure regulatory valve
- 2. The potentiometer is set to zero when the arm is facing vertically down.
- 3. Run the LabVIEW code.
- 4. Data from the pressure sensors and potentiometer starts to record
- 5. After a delay of 1/10<sup>th</sup> of a second the solenoid valve is opened
- 6. Then the data for the next 2 seconds is recorded.
- 7. Once the program stops, the forearm (metal strip) is set back to its original position manually.
- 8. Repeat step 1 to 7 for five trials each for one pressure setting.
- 9. Once all five trails are over, change the pressure setting by turning the pressure regulatory valve.
- 10. Repeat steps 1 to 9 for pressure conditions vary from 1bar to 6bar at an increment phase of 0.5bar.

The Figure D.2 shows the overall experimental setup

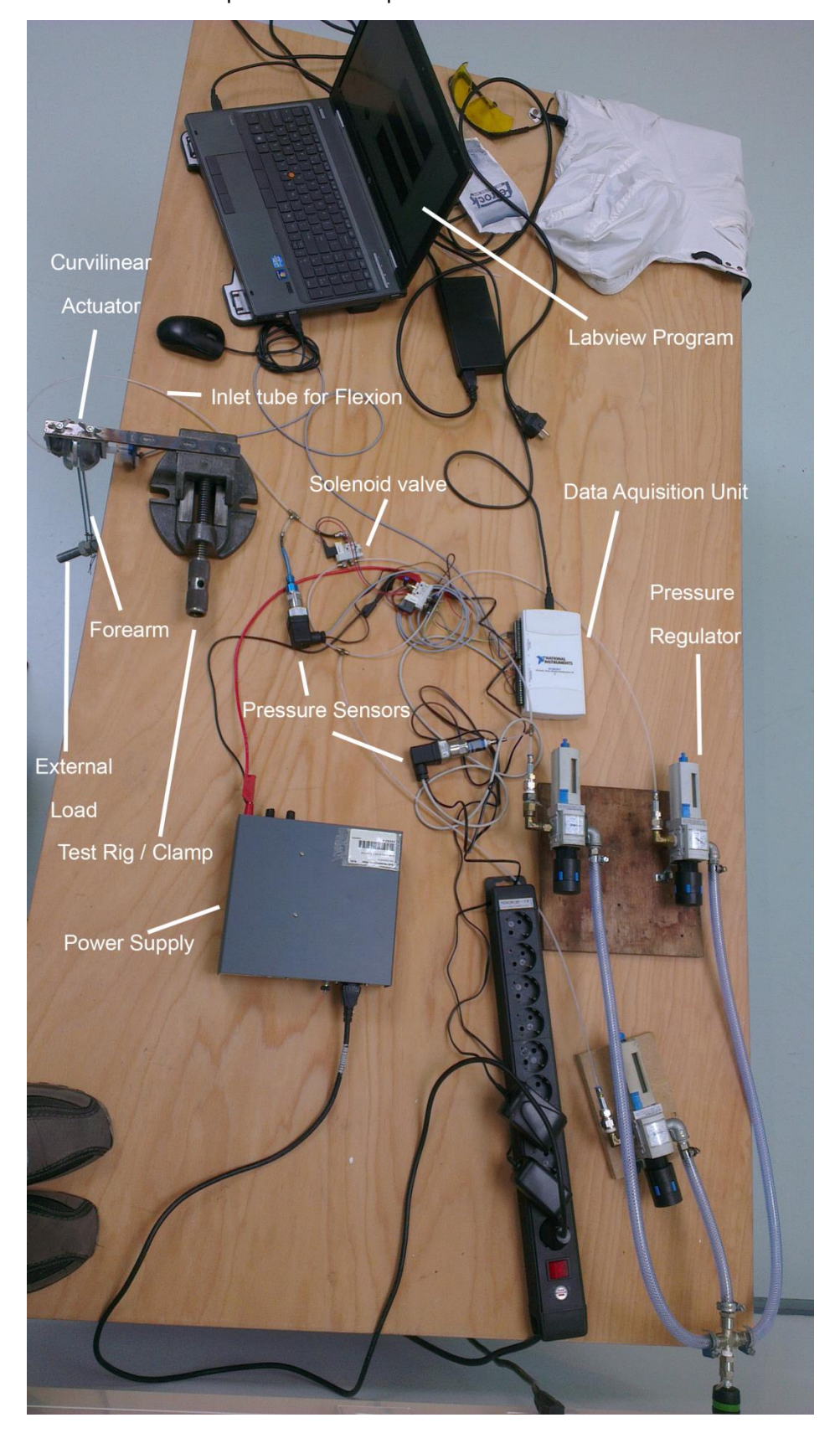


Figure D.2 Experimental setup

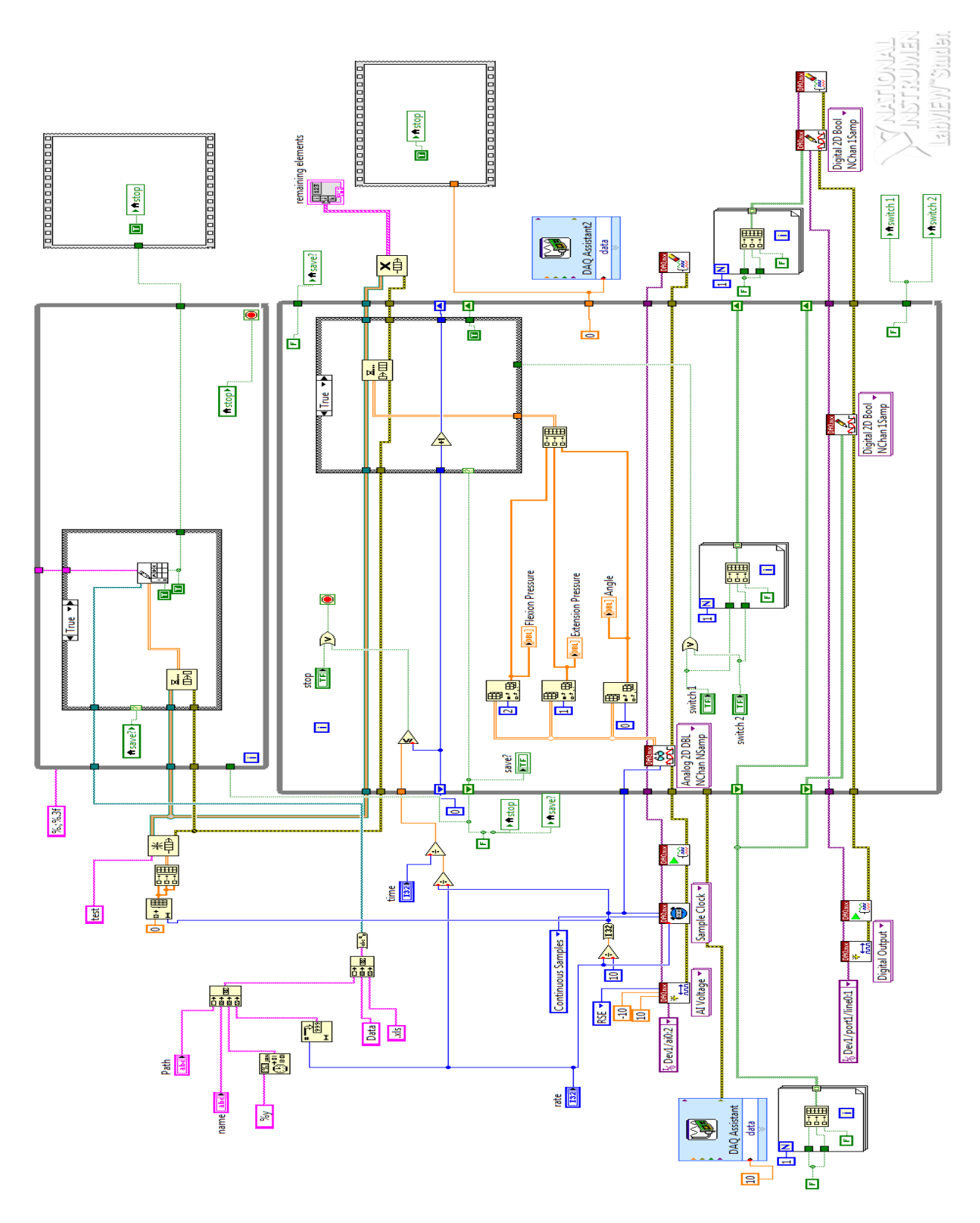


Figure D.3 LabVIEW block diagram

## Appendix E: Matlab code for Active Gravity Compensator

```
clc
clear all
```

#### **Global Constants**

```
%mass of forearm [kg]
m=1;
g=9.81;
                                                                              %acc. due to gravity [m/sec^2]
h=300;
                                                                              %length of forearm [mm]
c=300*0.45;
                                                                              %center of gravity [mm]
                                                                              %max external load [kg]
M=5;
p=1.2;
                                                                               %working pressure [MPa]
                                                                               %Modulus of rigidity [N/mm^2]
G=79.3*(10^3);
rho_MW=7.85;
                                                                              %density of music wire[g/cm^3]
rho_AL=2.7;
                                                                              %density of Aluminium alloy 6061
T6[g/cm^3]
rho_PL=1.18;
                                                                              %density of 3D printed
plastic[g/cm^3]
rho_PTFE=2.3;
                                                                              %density of PTFE plastic[g/cm^3]
rho_CO2=0.0234;
                                                                              %density of CO2 @ 20C; 1.2MPa
[g/cm^3]
                                                                              %amount of CO2 in gas can [g]
gasCan=16;
                                                                              %std dia and tensile strength of
mp=[1.1,2120;
spring wire SAE J178 [music wire]
    1.2,2100;
    1.4,2050;
    1.6,2000;
    1.8,1980;
    2,1950;
    2.2,1900;
    2.5,1850;
    2.8,1820;
    3,1800;
    3.5,1750;
    4,1700;
    4.5,1680;
    5,1650;
    5.5,1620;
    6,1600;
    6.5,1530];
```

#### We know #kas = Tgmax

```
T_gmax=m*g*c+M*g*h; %Gravitational torque [Nmm]

d=mp(:,1); %spring wire dia [mm]

s_mat=0.40*mp(:,2); %allowable uncorrected tensile
```

```
strength [N/mm^2]
                                                                              %empty dataset
ledt=[];
elbowR=36;
wristR=50;
alim=elbowR-1;
s_MClim=elbowR-1;
dlim=max(d);
Dlim=wristR;
r_SClim=wristR;
Nlim=10;
ilim=size(d);
Lim=[alim;s_MClim;dlim;Dlim;r_SClim;Nlim];
for a=1:50
                                                                            %anchor point distance loop [mm]
    for s_MC=1:s_MClim;
                                                                              %stroke length of multiplex
cylinder loop [mm]
        s=s_MC*T_gmax/(M*g*h);
                                                                              %spring forearm point [mm]
                                                                              %max spring delfection [mm]
        x=s*2;
        k=(T_gmax)/(a*s);
                                                                              %spring constant required [N/mm]
        for i=1:ilim(1)
                                                                              %wire dia loop [mm]
            for D=0.5:0.5:Dlim
                                                                              %coil dia loop [mm]
                % spatial constraint
                if D>=d(i) && D+d(i)<=Dlim-1</pre>
                                                                              %number of coil turns
                    n=(G*d(i)^4)/(8*k*D^3);
                    fos=1.15;
                                                                              %factor of safety
                    L_f=(n+2)*d(i)+(fos*x);
                                                                              %free length of spring [mm]
                    P_S=(L_f-2*d(i))/(n);
                                                                              %pitch [mm]
                                                                              %spring index
                    C=D/d(i):
                    wsf=((4*C-1)/(4*C-4))+(0.615/C);
                                                                              %wahl's stress correction factor
                    S_{cal}=(8*k*fos*x*D/(pi*(d(i)^3)))*wsf;
                                                                              %calculated stress [N/mm^2]
                    vol_S=(n+2)*d(i)*pi*((D+d(i))^2-(D-d(i))^2)/4;
                                                                              %volume of spring [mm^3]
                    m_S=rho_MW*vol_S*10^-3;
                                                                              %mass of spring [g]
                    %rounded values for manufacturing reason
                    %the above calculated values of n and pitch are
                    %rounded of to one decimal point
                                                                                      %adjusted number of coil
                    nNew=round(n/0.25)*0.25;
turns
                    if nNew>n
                        nNew=nNew-0.25;
                    end
                    kNew=(G*d(i)^4)/(8*nNew*D^3);
                                                                              %adjusted spring constant [N/mm]
                    aNew=(T_gmax)/(kNew*s);
                                                                              %adjusted anchor point distance
[N/mm]
                      aNew=round(aNew,1);
```

```
P_SNew=round(P_S,1);
                                                                             %adjusted pitch [mm]
                    L_fNew=P_SNew*nNew+2*d(i);
                                                                             %adjusted free length [mm]
                    fosNew=(L_fNew-(nNew+2)*d(i))/x;
                                                                             %adjusted factor of safety
                    S_{calNew}=(8*kNew*fosNew*x*D/(pi*(d(i)^3)))*wsf;
                                                                             %adjusted calculated stress
[N/mm^2]
                    vol_SNew=(nNew+2)*d(i)*pi*((D+d(i))^2-(D-d(i))^2)/4;
                                                                             %adjusted volume of spring
[mm^3]
                    m_SNew=rho_MW*vol_SNew*10^-3;
                                                                             %adjusted mass of spring [g]
                    % If the spring's calculated stress doesn't exceed the
                    % tensile strength of the material, then the design is satisfactory.
                    % Load and spatial contraints for the spring
                      if S_cal<=S_mat(i) && L_f<=160
                    %adjusted settings
                    if S_calNew<=S_mat(i) && L_fNew<=160 && fosNew>1 && aNew<=alim
                    % Linear Actuator to push the max load produced by spring force
                        for r_sc=0.5:0.5:r_sclim
                                                                             %radius of Pneumatic piston loop
[mm]
                            for N=5:Nlim
                                                                             %number of multiplex cylinder
segments
                                  F_req=k*x/N;
                                                                          %force required to be produced by a
single segment [N]
                                                                             %adjusted force required to be
                                F_req=kNew*x/N;
produced by a single segment [N]
                                A_SC=pi*r_SC^2;
                                                                             %area of Pneumatic piston[mm^2]
                                1p_sc=5;
                                                                             %length of Pnuematic piston head
[mm]
                                FS=10;
                                                                             %factor of safety
                                t_MC=FS*p*r_SC/241;
                                                                             %thickness of cylinder [mm]
                                if t_MC<1</pre>
                                    t_MC=1;
                                end
                                r_PR=r_SC/2;
                                                                             %piston rod radius [mm]
                                if r_PR>3.5
                                    r_{PR=3.5};
                                end
                                A_PR=pi*r_PR^2;
                                                                             %area of piston rod [mm^2]
                                F_SC=p*A_SC-(N-1)*0.101*(A_SC-A_PR);
                                                                             %force created by a Pnematic
piston [N]
                                s_SC=s_MC/N;
                                                                             %stroke lenght of single segment
of mutiplex actuator [mm]
                                                                             %cylinder lenght of single
                                L_SC=s_SC+lp_SC;
segment of mutiplex actuator [mm]
```

```
vol_SC=pi*((r_SC+t_MC)^2-r_SC^2)*L_SC; %volume of single cylinder
 segment [mm^3]
                                                                                                         L_MC=((N+1)*N*0.5*s_SC)+s_MC+N*(10+lp_SC); %overall length of the multiplex
actuator [mm]
                                                                                                         %rough estimate of total weight of the multiplex cylinder [q]
                                                                                                         m_MC=(vol_SC*(N+1)*N*0.5)*rho_AL*10^-3 ...
                                                                                                                                                                                                                                                                                                                                         %weight
of AL cylinders
                                                                                                                      +((N*5*pi*((r_SC+t_MC)^2)-A_PR)+(N*5*A_SC))*rho_PL*10^-3...
                                                                                                                                                                                                                                                                                                                                         %weight
od 3D printed cyl covers
                                                                                                                      +(N*1p_SC*A_SC)*rho_PTFE*10^-3 ...
                                                                                                                                                                                                                                                                                                                                         %weight
of piston heads
                                                                                                                      +((((N+1)*N*0.5*s_SC)*A_SC)+(N*10)*A_PR)*rho_PTFE*10^-3;
                                                                                                                                                                                                                                                                                                                                         %weigth
of piston rods
                                                                                                         %volume of air consumed [mm^3]
                                                                                                         vol_air=(A_SC*s_MC) ...
                                                                                                                                                                                                                                                                                                                                         %overall
stroke volume
                                                                                                                      +((N+0.5)*N*0.5*(A_SC-A_PR)*s_SC) ...
                                                                                                                                                                                                                                                                                                                                         %space
left in between cyl and piston rod
                                                                                                                       -((N+0.5)*N*0.5*(A_SC-A_PR)*s_SC)*(0.101)/(p+0.101);
                                                                                                                                                                                                                                                                                                                                         %minus
the atm air filled in the in between space
                                                                                                          CO2_consump=rho_CO2*vol_air*10^-3;
                                                                                                                                                                                                                                                         %amount of CO2 consumed [g]
                                                                                                                                                                                                                                                          %spatial factor
                                                                                                          SF=L_MC*D;
                                                                                                         E_in=p*vol_air;
                                                                                                                                                                                                                                                         %energy inputed
%
                                                                                                                PE_S=(k*(2*s_MC)^2)/2;
                                                                                                                                                                                                                                                                %spring's potential energy
                                                                                                                                                                                                                                                                %efficiency
%
                                                                                                                EF=PE_S/E_in;
%
                                                                                                               WF=m_S+m_MC;
                                                                                                                                                                                                                                                                %weight factor
                                                                                                               OV=EF/(WF*SF);
                                                                                                                                                                                                                                                                %optimization variable
%
                                                                                                         PE SNew=(kNew*(2*s MC)^2)/2:
                                                                                                                                                                                                                                                         %adjusted spring's potential
energy
                                                                                                         EF_New=PE_SNew/E_in;
                                                                                                                                                                                                                                                         %adjusted efficiency
                                                                                                                                                                                                                                                         %adjusted weight factor
                                                                                                          WF_New=m_SNew+m_MC;
                                                                                                          OV_New=EF_New/(WF_New*SF);
                                                                                                                                                                                                                                                         %adjusted optimization variable
                                                                                                         % Load and spatial contraints for the spring
                                                                                                               if (L_MC+15)<160 \&\& (r_SC+t_MC+6)<(D-d(i)-2)/2 \&\& F_SC*0.9>=F_req \&\& F_SC*0.9>=F_req &\& F_SC*0.9>=F_req && F_SC*0.9>=F_req &&
s_SC>=1 \&\& WF<770
                                                                                                         if (L_MC+15)<160 && (r_SC+t_MC+6)<(D-d(i)-2)/2 && F_SC*0.9>=F_req && s_SC>=1
&& WF_New<770 %adjusted constraints
 \\ \text{quali=[aNew,s,d(i),D,nNew,L\_fNew,P\_SNew,kNew,F\_SC,OV\_New,r\_SC,L\_MC,N,s\_MC,10001,S\_mat(i),S\_calNew,SF,WF\_New,R_SC,D\_MC,N,S\_MC,R_SMC,R_SMC,R_SMC,R_SMC,R_SMC,R_SMC,R_SMC,R_SMC,R_SMC,R_SMC,R_SMC,R_SMC,R_SMC,R_SMC,R_SMC,R_SMC,R_SMC,R_SMC,R_SMC,R_SMC,R_SMC,R_SMC,R_SMC,R_SMC,R_SMC,R_SMC,R_SMC,R_SMC,R_SMC,R_SMC,R_SMC,R_SMC,R_SMC,R_SMC,R_SMC,R_SMC,R_SMC,R_SMC,R_SMC,R_SMC,R_SMC,R_SMC,R_SMC,R_SMC,R_SMC,R_SMC,R_SMC,R_SMC,R_SMC,R_SMC,R_SMC,R_SMC,R_SMC,R_SMC,R_SMC,R_SMC,R_SMC,R_SMC,R_SMC,R_SMC,R_SMC,R_SMC,R_SMC,R_SMC,R_SMC,R_SMC,R_SMC,R_SMC,R_SMC,R_SMC,R_SMC,R_SMC,R_SMC,R_SMC,R_SMC,R_SMC,R_SMC,R_SMC,R_SMC,R_SMC,R_SMC,R_SMC,R_SMC,R_SMC,R_SMC,R_SMC,R_SMC,R_SMC,R_SMC,R_SMC,R_SMC,R_SMC,R_SMC,R_SMC,R_SMC,R_SMC,R_SMC,R_SMC,R_SMC,R_SMC,R_SMC,R_SMC,R_SMC,R_SMC,R_SMC,R_SMC,R_SMC,R_SMC,R_SMC,R_SMC,R_SMC,R_SMC,R_SMC,R_SMC,R_SMC,R_SMC,R_SMC,R_SMC,R_SMC,R_SMC,R_SMC,R_SMC,R_SMC,R_SMC,R_SMC,R_SMC,R_SMC,R_SMC,R_SMC,R_SMC,R_SMC,R_SMC,R_SMC,R_SMC,R_SMC,R_SMC,R_SMC,R_SMC,R_SMC,R_SMC,R_SMC,R_SMC,R_SMC,R_SMC,R_SMC,R_SMC,R_SMC,R_SMC,R_SMC,R_SMC,R_SMC,R_SMC,R_SMC,R_SMC,R_SMC,R_SMC,R_SMC,R_SMC,R_SMC,R_SMC,R_SMC,R_SMC,R_SMC,R_SMC,R_SMC,R_SMC,R_SMC,R_SMC,R_SMC,R_SMC,R_SMC,R_SMC,R_SMC,R_SMC,R_SMC,R_SMC,R_SMC,R_SMC,R_SMC,R_SMC,R_SMC,R_SMC,R_SMC,R_SMC,R_SMC,R_SMC,R_SMC,R_SMC,R_SMC,R_SMC,R_SMC,R_SMC,R_SMC,R_SMC,R_SMC,R_SMC,R_SMC,R_SMC,R_SMC,R_SMC,R_SMC,R_SMC,R_SMC,R_SMC,R_SMC,R_SMC,R_SMC,R_SMC,R_SMC,R_SMC,R_SMC,R_SMC,R_SMC,R_SMC,R_SMC,R_SMC,R_SMC,R_SMC,R_SMC,R_SMC,R_SMC,R_SMC,R_SMC,R_SMC,R_SMC,R_SMC,R_SMC,R_SMC,R_SMC,R_SMC,R_SMC,R_SMC,R_SMC,R_SMC,R_SMC,R_SMC,R_SMC,R_SMC,R_SMC,R_SMC,R_SMC,R_SMC,R_SMC,R_SMC,R_SMC,R_SMC,R_SMC,R_SMC,R_SMC,R_SMC,R_SMC,R_SMC,R_SMC,R_SMC,R_SMC,R_SMC,R_SMC,R_SMC,R_SMC,R_SMC,R_SMC,R_SMC,R_SMC,R_SMC,R_SMC,R_SMC,R_SMC,R_SMC,R_SMC,R_SMC,R_SMC,R_SMC,R_SMC,R_SMC,R_SMC,R_SMC,R_SMC,R_SMC,R_SMC,R_SMC,R_SMC,R_SMC,R_SMC,R_SMC,R_SMC,R_SMC,R_SMC,R_SMC,R_SMC,R_SMC,R_SMC,R_SMC,R_SMC,R_SMC,R_SMC,R_SMC,R_SMC,R_SMC,R_SMC,R_SMC,R_SMC,R_SMC,R_SMC,R_SMC,R_SMC,R_SMC,R_SMC,R_SMC,R_SMC,R_SMC,R_SMC,R_SMC,R_SMC,R_SMC,R_SMC,R_SMC,R_SMC,R_SMC,R_SMC,
E_in,10001,L_SC,t_MC,lp_SC,s_SC,m_S,m_MC,CO2_consump,gasCan/CO2_consump,EF_New];
                                                                                                                       ledt=[ledt;quali];
                                                                                                          end
                                                                                            end
                                                                              end
                                                                  end
                                                     end
```

Appendix

53

```
end
end
end

if size(ledt)>0

[lowerend,posmini]=min(ledt);
  [upperend,posmaxi]=max(ledt);
  optimum=ledt(posmaxi(10),:);

Res=[lowerend' upperend' optimum'];

finR=array2table(Res);
writetable(finR,'Custom_Spring.xls');
```

#### **PLOTING RESULTS**

```
graphData=[[1;1;min(d);0.5;0.5;1],[Res(1,:);Res(14,:);Res(3:4,:);Res(11,:);Res(13,:)],Lim];
    mulvar=[ledt(:,1) ledt(:,14) ledt(:,4) ledt(:,11) ledt(:,13)];
    varNames={'a';'s_M_C';'D';'r_S_C';'N'};
    figure(1)
    subplot(1,2,1)
    plot3(ledt(:,18),ledt(:,19),ledt(:,30),'m.')
    title('Spatial Factor vs Estimated Weight vs Efficiency');
    xlabel('SF','fontweight','bold');
    ylabel('EW','fontweight','bold');
    zlabel('EF','fontweight','bold');
    grid on
    hold on
    stem3(optimum(18),optimum(19),optimum(30),'b*')
    legend({'Constraints Satisfied';'Most optimal Datapoint'},'Location','northeast');
    hold off
    subplot(1,2,2)
    radarPlot(graphData)
    figure(2)
    gplotmatrix(mulvar,[],ledt(:,3),['r' 'b'],['*' '*'],[],'on');
    text([.1 .3 .50 .70 .9], repmat(-.035,1,5), varNames, 'FontSize',8,'fontweight','bold');
    text(repmat(-.02,1,5), [.90 .70 .5 .3 .1], varNames, 'FontSize',8, 'Rotation',90,'fontweight','bold');
    ha = axes('Position',[0 0 1 1],'Xlim',[0 1],'Ylim',[0
1], 'Box', 'off', 'visible', 'off', 'Units', 'normalized', 'clipping', 'off');
    text(0.5, 1,'\bf Datapoints Distribution (d over
a,s\_M\_C,D,r\_S\_C,N)','HorizontalAlignment','center','VerticalAlignment', 'top')
```

#### **GRAVCOMP MAPPING**

```
F_SChp=9.81*M/(optimum(13)); %half point force of a single cylinder
```

```
[mass,delta]=meshgrid(0:0.01:M,0:90);
g_p=9.81*cosd(delta);
mass_p=mass.*g_p;
cyl=round((1/F_SChp)*mass_p);
ds=cyl*optimum(25)+ones(91,501)*(m*g*c/(optimum(8)*optimum(1)));
T_S=optimum(8)*optimum(1)*ds;
cy10=(cy1==0);
cyl0=ones(91,501).*cyl0;
cy10(cy10==0)=NaN;
T_S0=T_S.*cy10;
cy10=cy1.*cy10;
cyl1=(cyl==1);
T_S1=T_S.*cyl1;
cyl1=cyl.*cyl1;
cyl1(cyl1==0)=NaN;
T_S1(T_S1==0)=NaN;
cy12=(cy1==2);
T_S2=T_S.*cy12;
cy12=cy1.*cy12;
cy12(cy12==0)=NaN;
T_S2(T_S2==0)=NaN;
cy13=(cy1==3);
T_S3=T_S.*cyl3;
cy13=cy1.*cy13;
cy13(cy13==0)=NaN;
T_S3(T_S3==0)=NaN;
cyl4=(cyl==4);
T_S4=T_S.*cy14;
cy14=cy1.*cy14;
cy14(cy14==0)=NaN;
T_S4(T_S4==0)=NaN;
cy15=(cy1==5);
T_S5=T_S.*cy15;
cyl5=cyl.*cyl5;
cy15(cy15==0)=NaN;
T_S5(T_S5==0)=NaN;
T_ext=mass_p*300;
T_arm = m*g*c*ones(91,501);
dT=T_S-(T_ext)-T_arm;
figure(3)
subplot(3,1,1);
surf(mass,delta,cyl0,'linestyle','none')
surf(mass,delta,cyl1,'linestyle','none')
hold on
surf(mass,delta,cyl2,'linestyle','none')
```

Appendix 55

```
hold on
surf(mass,delta,cyl3,'linestyle','none')
surf(mass,delta,cyl4,'linestyle','none')
hold on
surf(mass,delta,cyl5,'linestyle','none')
hold off
title('Cylinder Actuation');
xlabel('M');
ylabel('\delta');
zlabel('No. of cylinder');
grid on
colormap(flipud(summer));
freezeColors
subplot(3,1,2)
surf(mass,delta,T_ext+T_arm,'linestyle','none')
hold on
colormap('winter');
freezeColors
surf(mass,delta,T_S0,'linestyle','none')
hold on
surf(mass,delta,T_S1,'linestyle','none')
surf(mass,delta,T_S2,'linestyle','none')
hold on
surf(mass,delta,T_S3,'linestyle','none')
hold on
surf(mass,delta,T_S4,'linestyle','none')
hold on
surf(mass,delta,T_S5,'linestyle','none')
hold off
colormap(flipud(summer));
title('\tau_g_m_a_x vs M_S_F');
xlabel('M');
ylabel('\delta');
zlabel('torque');
grid on
hold off
freezeColors
subplot(3,1,3)
surf(mass,delta,dT,'linestyle','none')
title('Difference between \tau_g_m_a_x and M_S_F');
xlabel('M');
ylabel('\delta');
zlabel('torque');
grid on
colormap(flipud(summer));
```

end

## Appendix F: Matlab code for Curvilinear Actuator

```
clc
clear all
```

#### **Global Constants**

```
g=9.81;
                                                                              %acc. due to gravity [m/sec^2]
1=300;
                                                                              %length of forearm [mm]
                                                                              %working pressure [MPa]
p=1.2;
W = .5;
                                                                              %max external load [kg]
                                                                              %factor of safety
FS=10;
rho_CO2=0.0234;
                                                                              %density of CO2 @ 20C; 1.2MPa
[g/cm^3]
gasCan=16;
                                                                              %amount of CO2 in gas can [g]
Tmax = W*g*1;
                                                                              %maximum torque that could be
experienced
rom=130;
r_HPlim=36;
Tcol=[];
for r_HP=1:r_HPlim
                                                                              %radius of helical piston loop
[mm]
    pF=(p*pi*r_HP^2)-((0.101*pi*(r_HP^2)/2));
                                                                              %piston force
    1p=p*pi*r_HP/(2*48);
                                                                              %length of piston head [mm]
    if 1p<5
        1p=5;
    tc=FS*p*r_HP/48;
                                                                              %thickness of cylinder [mm]
    if tc<1
        tc=1;
    end
                                                                              %radius of helix loop [mm]
    for R_H=1:36
                                                                              %required tangential force [N]
        F_req=Tmax/R_H;
                                                                              %outer radius [mm]
        oR=R_H+r_HP+tc;
                                                                              %inner radius [mm]
        iR=R_H-r_HP-tc;
        arclp=360*(lp)/(2*3.14*R_H);
                                                                              %arc length of piston head [deg]
        cpdia=F_req/(2*48);
                                                                              %crank diameter [mm]
                                                                              %pitch of the helix [mm]
        P_H=2*(r_HP+tc)+0.05;
                                                                              %helix angle [deg]
        lamda=atand(P_H/(2*pi*R_H));
        tau_CA_T=pF*cosd(lamda)*R_H;
                                                                              %output torque (theoritical)
```

```
[Nmm]
        lift_T=tau_CA_T/(g*1);
                                                                             %lifting capacity (theoritical)
[kg]
                                                                             %output torque (with design
        tau_CA_WDE=tau_CA_T*cosd(lamda);
error) [Nmm]
        lift_WDE=tau_CA_WDE/(g*1);
                                                                             %lifting capacity (with design
error) [kg]
        L_CA=sqrt(P_H^2 + (2*pi*R_H)^2)*rom/360;
                                                                             %overall stroke arc length [mm]
        vol_CA=L_CA*pi*(r_HP^2);
                                                                             %storke volume [mm^3]
                                                                             %amount of CO2 consumed [g]
        CO2_consump=rho_CO2*vo1_CA*10^-3;
        en=p*vol_CA*130/rom;
                                                                             %energy spent for make 90 deg
lift [Nmm]
        effi_T=(tau_CA_T*130*pi)/(180*en);
                                                                             %actuator efficiency
(theoritical) [%]
        effi_WDE=(tau_CA_WDE*130*pi)/(180*en);
                                                                             %actuator efficiency (with
design error) [%]
        Dsg_err=(effi_T-effi_WDE)*100/effi_T;
                                                                             %design error percentage [%}
        %spatial constraints parameters
        totT=P_H+3;
        mdiag=sqrt(totT^2+R_H^2);
        ang=atand(totT/R_H);
        %checking spatial and load constraints
        if pF*cosd(lamda)*0.9>F_req && R_H>tc+r_HP && R_H+tc+r_HP<=36 && mdiag<=36 && totT*R_H<0.25*pi*36^2
&& r_{HP}>2 && totT<=36 && R_{H+}(r_{HP+tc})*cosd(ang)<=36*cosd(ang) && iR>5
col=[r_HP,R_H,P_H,tc,lp,oR,iR,arclp,cpdia,lamda,pF,tau_CA_T,lift_T,lift_WDE,L_CA,vol_CA,en,effi_T,effi_WDE,D
sg_err,CO2_consump,gasCan/CO2_consump];
            Tcol=[Tcol;col];
        end
    end
end
plot3(Tcol(:,1),Tcol(:,2),Tcol(:,14),'*','color',[0.5 0.5 0.5]);
title('Lifting capacity of Curvilinear Actuator');
xlabel('r_P_-H_P');
ylabel('R_H');
zlabel('Lifting capacity');
grid on
hold on
[upperend, posmaxi] = max(Tcol);
maxT=Tcol(posmaxi(14),:);
plot3(maxT(1),maxT(2),maxT(14),'r*');
% opt=Tcol(posmaxi(18),:);
% plot3(opt(1),opt(2),opt(14),'b*');
legend({'Constraints Satisfied';'Highest Torque';'Most optimal Datapoint'},'Location','northeast');
hold off
```

## Appendix: References

- 1. Herder, J.L., *Energy-free Systems. Theory, conception and design of statically*. Vol. 2. 2001.9037001920
- 2. Vrijlandt, N. and J. Herder, Seating unit for supporting a body or part of a body. 2002, Google Patents.
- 3. Van Dorsser, W., R. Barents, B. Wisse, M. Schenk, and J. Herder, *Energy-free adjustment of gravity equilibrators by adjusting the spring stiffness*. Proceedings of the Institution of Mechanical Engineers, Part C: Journal of Mechanical Engineering Science, 2008. **222**(9): p. 1839-1846.
- 4. Barents, R., M. Schenk, W.D. van Dorsser, B.M. Wisse, and J.L. Herder, *Spring-to-spring balancing as energy-free adjustment method in gravity equilibrators*. Journal of Mechanical Design, 2011. **133**(6): p. 061010.

5. Committee, S.S., Spring Design Manual. 1996: Society of Automotive Engineers. 156091680X

•

Appendix 59

# Literature Review

Chapter 5

# Reciprocating Gait Orthosis



A.Sooryanarain, 4252241
Supervisor:Dick Plettenburg & Gerwin Smit

#### **KEYWORDS**

RGO Reciprocating Gait Orthosis AFO Ankle Foot Orthosis KAFO Knee Ankle Foot Orthosis KO Knee Orthosis  KO Knee Orthosis  HKAFO Hip Knee Ankle Foot Orthosis  WHCH Whelchair  HGO Hip Guidance Orthosis  ARGO Advanced Reciprocating Gait Orthosis  IRGO Isocentric Reciprocating Gait Orthosis  WO Walkabout Orthosis  PW ParaWalker  DA-AFO Dorsiflexion Assist Ankle Foot Orthosis  FES Functional Electrical Stimulation  SCO Stance Control Orthosis  TLSO Thoracolumbosacral Orthosis  PGO Powered Gait Orthosis  PCI Physical Cost Index  VO2 Cost Oxygen Cost  HR Heart Rate  ADL Activities of Daily Life  SB Spina Bifida  SCI Spinal cord injury  CP Cerebral Palsy  MD Muscular Dystrophy	RETWORDS	·
KAFO Knee Ankle Foot Orthosis  KO Knee Orthosis  HKAFO Hip Knee Ankle Foot Orthosis  WHCH Wheelchair  HGO Hip Guidance Orthosis  ARGO Advanced Reciprocating Gait Orthosis  IRGO Isocentric Reciprocating Gait Orthosis  WO Walkabout Orthosis  PW ParaWalker  DA-AFO Dorsiflexion Assist Ankle Foot Orthosis  FES Functional Electrical Stimulation  SCO Stance Control Orthosis  HNP Hybrid-NeuroProsthesis  TLSO Thoracolumbosacral Orthosis  PCI Physical Cost Index  VO2 Cost Oxygen Cost  HR Heart Rate  ADL Activities of Daily Life  SB Spina Bifida  SCI Spinal cord injury  CP Cerebral Palsy	RGO	Reciprocating Gait Orthosis
KO Knee Orthosis  HKAFO Hip Knee Ankle Foot Orthosis  WHCH Wheelchair  HGO Hip Guidance Orthosis  ARGO Advanced Reciprocating Gait Orthosis  IRGO Isocentric Reciprocating Gait Orthosis  WO Walkabout Orthosis  PW ParaWalker  DA-AFO Dorsiflexion Assist Ankle Foot Orthosis  FES Functional Electrical Stimulation  SCO Stance Control Orthosis  HNP Hybrid-NeuroProsthesis  TLSO Thoracolumbosacral Orthosis  PGO Powered Gait Orthosis  PCI Physical Cost Index  VO2 Cost Oxygen Cost  HR Heart Rate  ADL Activities of Daily Life  SB Spina Bifida  SCI Spinal cord injury  CP Cerebral Palsy	AFO	Ankle Foot Orthosis
HKAFO Hip Knee Ankle Foot Orthosis  WHCH Wheelchair  HGO Hip Guidance Orthosis  ARGO Advanced Reciprocating Gait Orthosis  IRGO Isocentric Reciprocating Gait Orthosis  WO Walkabout Orthosis  PW ParaWalker  DA-AFO Dorsiflexion Assist Ankle Foot Orthosis  FES Functional Electrical Stimulation  SCO Stance Control Orthosis  HNP Hybrid-NeuroProsthesis  TLSO Thoracolumbosacral Orthosis  PGO Powered Gait Orthosis  PCI Physical Cost Index  VO2 Cost Oxygen Cost  HR Heart Rate  ADL Activities of Daily Life  SB Spina Bifida  SCI Spinal cord injury  CP Cerebral Palsy	KAFO	Knee Ankle Foot Orthosis
WHCH Wheelchair  HGO Hip Guidance Orthosis  ARGO Advanced Reciprocating Gait Orthosis  IRGO Isocentric Reciprocating Gait Orthosis  WO Walkabout Orthosis  PW ParaWalker  DA-AFO Dorsiflexion Assist Ankle Foot Orthosis  FES Functional Electrical Stimulation  SCO Stance Control Orthosis  HNP Hybrid-NeuroProsthesis  TLSO Thoracolumbosacral Orthosis  PGO Powered Gait Orthosis  PCI Physical Cost Index  VO2 Cost Oxygen Cost  HR Heart Rate  ADL Activities of Daily Life  SB Spina Bifida  SCI Spinal cord injury  CP Cerebral Palsy	КО	Knee Orthosis
HGO Hip Guidance Orthosis  ARGO Advanced Reciprocating Gait Orthosis  IRGO Isocentric Reciprocating Gait Orthosis  WO Walkabout Orthosis  PW ParaWalker  DA-AFO Dorsiflexion Assist Ankle Foot Orthosis  FES Functional Electrical Stimulation  SCO Stance Control Orthosis  HNP Hybrid-NeuroProsthesis  TLSO Thoracolumbosacral Orthosis  PGO Powered Gait Orthosis  PCI Physical Cost Index  VO2 Cost Oxygen Cost  HR Heart Rate  ADL Activities of Daily Life  SB Spina Bifida  SCI Spinal cord injury  CP Cerebral Palsy	HKAFO	Hip Knee Ankle Foot Orthosis
ARGO Advanced Reciprocating Gait Orthosis IRGO Isocentric Reciprocating Gait Orthosis WO Walkabout Orthosis PW ParaWalker DA-AFO Dorsiflexion Assist Ankle Foot Orthosis FES Functional Electrical Stimulation SCO Stance Control Orthosis HNP Hybrid-NeuroProsthesis TLSO Thoracolumbosacral Orthosis PGO Powered Gait Orthosis PCI Physical Cost Index VO2 Cost Oxygen Cost HR Heart Rate ADL Activities of Daily Life SB Spina Bifida SCI Spinal cord injury CP Cerebral Palsy	WHCH	Wheelchair
IRGO Isocentric Reciprocating Gait Orthosis  WO Walkabout Orthosis  PW ParaWalker  DA-AFO Dorsiflexion Assist Ankle Foot Orthosis  FES Functional Electrical Stimulation  SCO Stance Control Orthosis  HNP Hybrid-NeuroProsthesis  TLSO Thoracolumbosacral Orthosis  PGO Powered Gait Orthosis  PCI Physical Cost Index  VO <sub>2</sub> Cost Oxygen Cost  HR Heart Rate  ADL Activities of Daily Life  SB Spina Bifida  SCI Spinal cord injury  CP Cerebral Palsy	HGO	Hip Guidance Orthosis
WO Walkabout Orthosis  PW ParaWalker  DA-AFO Dorsiflexion Assist Ankle Foot Orthosis  FES Functional Electrical Stimulation  SCO Stance Control Orthosis  HNP Hybrid-NeuroProsthesis  TLSO Thoracolumbosacral Orthosis  PGO Powered Gait Orthosis  PCI Physical Cost Index  VO <sub>2</sub> Cost Oxygen Cost  HR Heart Rate  ADL Activities of Daily Life  SB Spina Bifida  SCI Spinal cord injury  CP Cerebral Palsy	ARGO	Advanced Reciprocating Gait Orthosis
PW ParaWalker  DA-AFO Dorsiflexion Assist Ankle Foot Orthosis  FES Functional Electrical Stimulation  SCO Stance Control Orthosis  HNP Hybrid-NeuroProsthesis  TLSO Thoracolumbosacral Orthosis  PGO Powered Gait Orthosis  PCI Physical Cost Index  VO2 Cost Oxygen Cost  HR Heart Rate  ADL Activities of Daily Life  SB Spina Bifida  SCI Spinal cord injury  CP Cerebral Palsy	IRGO	Isocentric Reciprocating Gait Orthosis
DA-AFO Dorsiflexion Assist Ankle Foot Orthosis FES Functional Electrical Stimulation SCO Stance Control Orthosis HNP Hybrid-NeuroProsthesis TLSO Thoracolumbosacral Orthosis PGO Powered Gait Orthosis PCI Physical Cost Index VO2 Cost Oxygen Cost HR Heart Rate ADL Activities of Daily Life SB Spina Bifida SCI Spinal cord injury CP Cerebral Palsy	WO	Walkabout Orthosis
FES Functional Electrical Stimulation  SCO Stance Control Orthosis  HNP Hybrid-NeuroProsthesis  TLSO Thoracolumbosacral Orthosis  PGO Powered Gait Orthosis  PCI Physical Cost Index  VO <sub>2</sub> Cost Oxygen Cost  HR Heart Rate  ADL Activities of Daily Life  SB Spina Bifida  SCI Spinal cord injury  CP Cerebral Palsy	PW	ParaWalker
SCO Stance Control Orthosis  HNP Hybrid-NeuroProsthesis  TLSO Thoracolumbosacral Orthosis  PGO Powered Gait Orthosis  PCI Physical Cost Index  VO2 Cost Oxygen Cost  HR Heart Rate  ADL Activities of Daily Life  SB Spina Bifida  SCI Spinal cord injury  CP Cerebral Palsy	DA-AFO	Dorsiflexion Assist Ankle Foot Orthosis
HNP Hybrid-NeuroProsthesis  TLSO Thoracolumbosacral Orthosis  PGO Powered Gait Orthosis  PCI Physical Cost Index  VO2 Cost Oxygen Cost  HR Heart Rate  ADL Activities of Daily Life  SB Spina Bifida  SCI Spinal cord injury  CP Cerebral Palsy	FES	Functional Electrical Stimulation
TLSO Thoracolumbosacral Orthosis  PGO Powered Gait Orthosis  PCI Physical Cost Index  VO2 Cost Oxygen Cost  HR Heart Rate  ADL Activities of Daily Life  SB Spina Bifida  SCI Spinal cord injury  CP Cerebral Palsy	SCO	Stance Control Orthosis
PGO Powered Gait Orthosis  PCI Physical Cost Index  VO₂ Cost Oxygen Cost  HR Heart Rate  ADL Activities of Daily Life  SB Spina Bifida  SCI Spinal cord injury  CP Cerebral Palsy	HNP	Hybrid-NeuroProsthesis
PCI Physical Cost Index  VO <sub>2</sub> Cost Oxygen Cost  HR Heart Rate  ADL Activities of Daily Life  SB Spina Bifida  SCI Spinal cord injury  CP Cerebral Palsy	TLSO	Thoracolumbosacral Orthosis
VO2 CostOxygen CostHRHeart RateADLActivities of Daily LifeSBSpina BifidaSCISpinal cord injuryCPCerebral Palsy	PGO	Powered Gait Orthosis
HR Heart Rate ADL Activities of Daily Life SB Spina Bifida SCI Spinal cord injury CP Cerebral Palsy	PCI	Physical Cost Index
ADL Activities of Daily Life  SB Spina Bifida  SCI Spinal cord injury  CP Cerebral Palsy	VO <sub>2</sub> Cost	Oxygen Cost
SB Spina Bifida SCI Spinal cord injury CP Cerebral Palsy	HR	Heart Rate
SCI Spinal cord injury CP Cerebral Palsy	ADL	Activities of Daily Life
CP Cerebral Palsy	SB	1 .
·	SCI	
MD Muscular Dystrophy	СР	Cerebral Palsy
	MD	Muscular Dystrophy

## Reciprocating Gait Orthosis

#### **ABSTRACT**

The aim of this review is to shed some light over the rejection rates and energy cost of the Reciprocating Gait Orthosis (RGO). The previous literature works were accessed through internet databases like Scopus and PubMed. The keyword 'Reciprocating Gait Orthosis' was used for the search. The review elucidates a brief introduction to the field of orthosis and mainly focuses in terms RGOs, their performance characteristics, rejection rates, and other correlations. Around 115 articles were found on the internet (Scopus+PubMed), based on reading their abstract, 54 articles were selected. Most of the articles were about gait parameters or energy cost of a RGO compared to another mode of ambulation and there were a few articles regarding rejection rates. From all these articles, one could clearly conclude that the RGO is slower and requires a lot of energy compared to a wheelchair, but while comparing the RGO with other orthoses, there is no clear conclusion which one is better. The RGO is still prescribed to the patients because it has other therapeutic benefits like psychological moral boost, improved bone density, lesser pressure sores, etc. Likewise the patients also find RGOs as more of therapeutic device and not something for daily use.

#### **INTRODUCTION**

There are multiple ways to make a paraplegic patient ambulate, ranging from wheelchairs to various types of orthosis. The prime focus of this article is about RGOs, an orthotic system that enables the individual to ambulate with a reciprocal gait pattern that initiates hip flexion with weight shifting and trunk extension to the contra lateral side. The dynamic coupling between the two hip joints provides simultaneous mechanical hip flexion and contra lateral hip extension stability. This control at the hip provides increased stability and enables the individual to stand with greater ease than with a bilateral KAFO system. The hip joints on an RGO can also be disengaged and a traditional swing-through gait pattern can be used [1]. The RGO requires good upper extremity strength to safely utilize the system[2]. There are different types of RGOs; they vary in terms of the production company, mechanism-used, appearance, functionality and so on. The RGO might be advantageous over the wheelchair in terms of therapeutic reasons [3], but this doesn't mean the patients continue to use the RGO in long run. There is huge rejection rate of RGO in long term use [4, 5]. Paraplegic patients prefer wheelchairs over RGOs. The major reason being one has to spend too much of effort to ambulate with a RGO compared to a wheelchair [6-8]. A lot of researches have been made in the past years to deal with this issue about energy cost. Researchers have come up with various ideas like including a FES (Functional Electrical Stimulation) system with a RGO or by augmenting the RGO with actuators to reduce the energy cost. The RGO aids the patient to walk, this in return gives them a moral boost, but the toll taken in terms of energy cost is too high [1], thereby it doesn't help to promote the RGO as a device for activities of daily life (ADL).

#### **GOAL**

The objective of this paper is to give a review about the performance characteristics and rejection rate of a RGO. This review contains the summary of various researches that have been done on RGOs and the other modes of ambulation it is compared with, in order to give some pointers how we should proceed the future research.

#### **BACKGROUND**

#### **Paraplegia**

The spinal cord one of the major part of the human body one would have to deal with when coming across paraplegic patients. In simple words the spinal cord is like the neural highway of the human body that connects the brain with the most of the other body parts. The condition of the patient depends upon the lesion level on the spine and its severity [2]. Figure 1 represents the structure of the spinal cord.

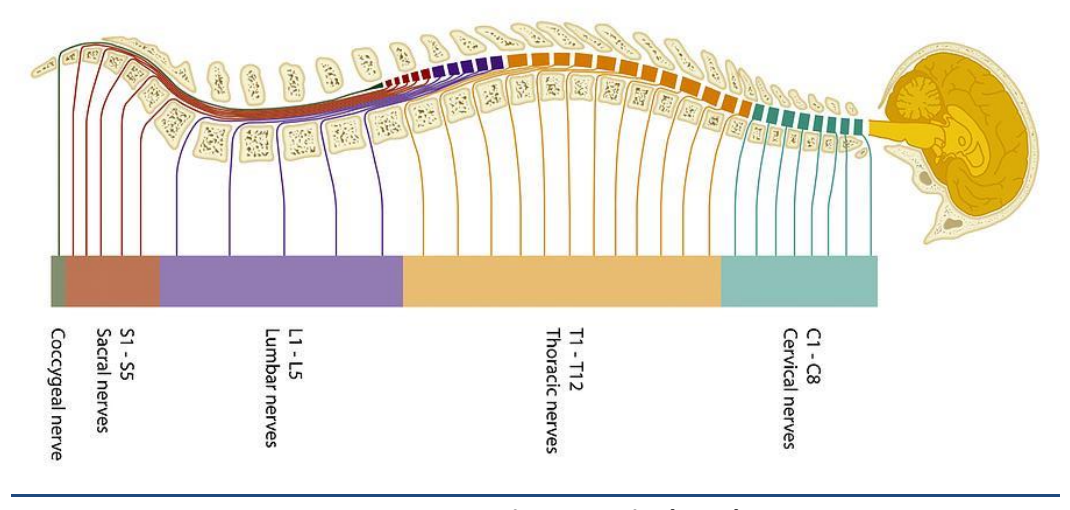


**Figure 1 Spinal Cord** 

The paraplegic patients would have impairment in the motor and/or sensory skills of their thoracic, lumbar or sacral region. The severity of the impairment is denoted in terms of American Spinal Injury Association (ASIA) Impairment Scale [9]. So if a person is having problems in his/her Lumbar-2 (L2) and falls under the category of ASIA B, then that person doesn't have any motor function from their hip and the parts below that. The RGO users are often the victim of the following types of paraplegia; Spinal Cord Injury [2], Spina Bifida [10], Cerebral Palsy [11] and Muscular Dystrophy [12].

#### **Lower Limb Orthosis**

A lower limb orthoses is a device that provides support for the lower limbs by distributing pressure or realigning the joints while standing, walking or running [1]. There are many types of lower limb orthoses namely, Ankle Foot Orthosis, Knee Ankle Foot Orthosis, Knee Orthosis, Hip Knee Ankle Foot Orthosis, Reciprocating Gait Orthosis, Powered Gait Orthosis.

An ankle-foot orthosis (AFO) is an orthosis that braces the ankle and foot together, so that the ankle does not move with respect to the lower leg. AFOs can be used to support weak limbs, or to realign a limb with contracted muscles to its normal position. They are prescribed by doctors for drop foot, arthritis or fracture [1].

A knee-ankle-foot orthosis (KAFO) is an orthosis that supports the knee, ankle and foot. The KAFO can be used in order to stop, limit, or assist the motion of the foot, ankle or knee in any or all of the 3 planes of motion. A KAFO could be used in conditions like paralysis, arthritis, fracture, etc [1].

A knee orthosis (KO) is a brace that is used to support or align the knee. It encumbers above and below the knee joint. A KO can aid a knee to have a stable flexion or extension and also reduce the pain in case of injury [1].

A hip-knee-ankle-foot orthosis (HKAFO) is used to support the lower body starting from the hip along with the lower limbs. The HKAFO is a bi-lateral KAFO with additional corset to support the hip.

The Reciprocal Gait Orthosis (RGO) provides stability at the hip, knee, and ankle for an individual with bilateral lower extremity weakness. The primary motivation for the RGO's development was to harness the power of working hip flexors for ambulation and prevent torso jack-knifing. It allows for hands-free standing without immobilization of the hips. The RGO orthoses shows a great deal of promise from a functional standpoint. There are different types of RGOs available, the three major ones discussed in literature are; the Louisiana State University- Reciprocating Gait Orthosis (LSU-RGO) (Douglas et al., 1983) (Figure 5a), the Advanced Reciprocating Gait Orthosis (ARGO) [13] (Figure 5b) and the Isocentric Reciprocating Gait Orthosis (IRGO) [14] (Figure 5c). The RGO have their hip hinges reciprocally coupled through a mechanical link. The LSU-RGO is commonly referred as the RGO has it's hip joints coupled by two bowden cables, the ARGO couples the left and the right hip joints via a single bowden cable and the IRGO was designed to incorporate the reciprocal coupling by means of isocentric rod, levers and ball bearings [15]. There are other reciprocal walking devices with de-coupled hip joints, namely; the Parawalker (PW) [16], the Hip Guidance Orthosis (HGO) [17] and the Walkabout Orthosis (WO) [18].

The powered gait orthosis (PGO) are mechanical lower limb orthosis which are driven with the help of a electrical or hydraulic or pneumatic actuator [19]. There are various types of models in PGO, which will not be discussed in this paper since it is beyond the scope of research of this paper.



Figure 5a) Louisiana State University- Reciprocating Gait Orthosis; 5b) Advanced Reciprocating Gait Orthosis; 5c) Isocentric Reciprocating Gait Orthosis;

#### **METHODS**

#### **Search Methodology**

The literature for this review was accessed from internet database like Scopus and PubMed. The following keywords were used Reciprocating Gait Orthosis or Reciprocating Gait Orthoses or Reciprocal Gait Orthosis or Reciprocal Gait Orthoses. The articles dated from 1980's till current date, were considered. In Scopus the search returned 171 articles and in PubMed 117 results were found. There were 61 "Full text" available in Scopus and 95 in PubMed. Out of the 156 "Full texts", there were 41 recurring articles in the "Full text" data collection. The final 115 articles abstract were further scrutinized to match the "Selection criteria". Few more articles/books from Scholar Google and Google Patents were also included in the review for extra reference.

#### **Selection Criteria**

The main schema of the search was to comprise all the articles related to RGOs on i) Energy efficiency; ii) Performance comparison with other orthotic devices like HKAFOs, HGOs, or PGOs; iii) Technological add-ons like FES, feedback systems; iv) Rejection rates; v) Reviews. Articles written in English were only taken into account and ones that had available full text were only included in the review. Studies which used only healthy subjects as test subjects were excluded. Case-studies in which the lesion level of the all test subjects was above the thoracic region were excluded. Trials that were conducted to study the energy expenditure exclusively for sit-ups were also excluded.

#### **Gathered Data**

Out of the 115 articles collectively found in both the database Scopus and PubMed (excluding the repeated articles). 84 articles had accessible "Full text", from which 54 were selected for the review after taking the selection criteria in to account. Most of the articles were comparative studies, both controlled studies and uncontrolled. The literature also contained few exclusive studies which only elucidated about one particular type of orthosis. The miscellaneous articles comprises of correlational research articles and introductory articles about new RGO design. There were five review articles. The Figure 6 represents how the articles were distributed.

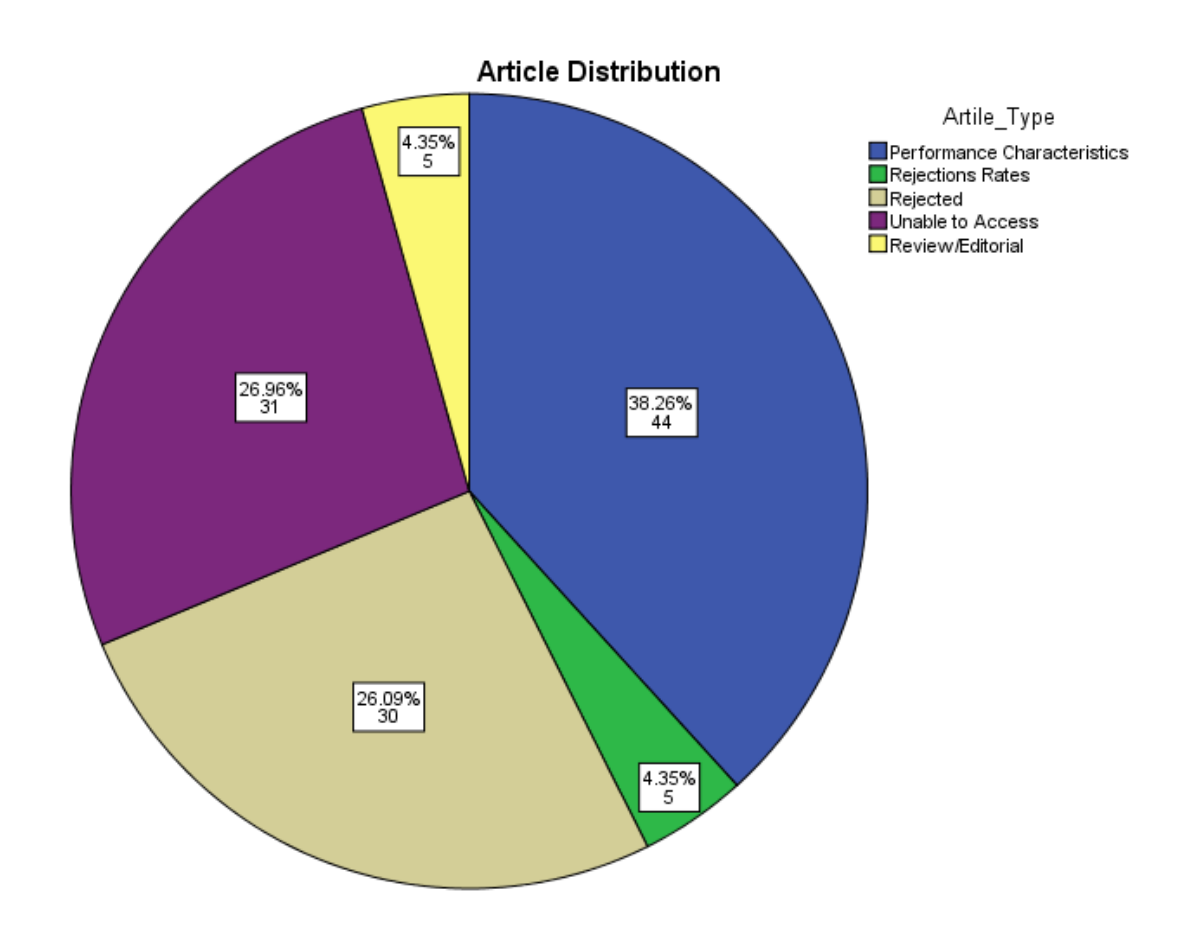


Figure 6 Distribution of article

#### RESULTS

The following are the summary of the articles related to reciprocating gait orthosis. The following are the major topic of interest, rejection rates and performance characteristics. The performance characteristics are further classified in terms of energy cost and gait parameters. 33 out of 49 studies were comparative studies. In the comparative studies the RGOs were compared against other means of ambulation like wheelchair (WHCH), non-reciprocal gait orthosis (NRGO), other reciprocal orthosis, hybrid RGO systems or normal able-bodied person. 11 more additional references were added to this article.

#### **Basic terminologies**

#### Energy cost of a RGO

The energy expenditure of a subject is measured in multiple ways, the most common ones are either Oxygen cost ( $VO_2$  cost, ( $O_2$ ) ml/kg m) or Walking Energy Cost (WEC, J/kg m) or Physical Cost Index (PCI, beats/m).

 $VO_2 = (O_2 \ Uptake \ during \ Walking - O_2 \ Uptake \ during \ Resting)[ml/kg \ min]$ 

$$VO_2Cost = \frac{VO_2[ml/kg \ min]}{Walking \ Velocity \ [m/min]}$$

 $WEC = k * VO_2 cost [J/kg m]$ 

Where, k = 20.9, viz. under the assumption of 1ml of  $O_2$  consumption yields 20.9J.

HR = (Walking Heart Rate - Resting Heart Rate)[beats/min]

$$PCI = \frac{HR [beats/min]}{Walking Velocity [m/min]}$$

#### Gait parameters of a RGO

The basic three gait parameters are cadence, stride length and velocity. There are other parameters that are measured like adduction/abduction/flexion/extension of the hip and knee joint motion, crutch forces, centre of gravity (COG), and centre of pressure (COP).

#### Comparison between RGO and Wheelchair/Normal Gait

Even though there is competition between various types of orthotic gait systems, the wheelchair (WHCH) has been the arch rival of them all. In most of the rejection rate studies it is mentioned the RGO should not be considered as a alternative to WHCH and the patient prefer the WHCH locomotion for long run [5, 20-22]. Due to increasing body weight and size, the metabolic demands for walking upright with an RGO is high compared to WHCH ambulation, patients prefer the WHCH [23].

Three articles contained information pertaining to RGO vs. WHCH comparison. The wheelchair is nearly 7 to 10 times energy efficient than a RGO [6, 7, 24], but it is the velocity that has the significant difference between RGO and wheelchair locomotion. The wheelchair is 5 to 10 times faster than the RGO [6, 24]. There was no significant difference found in terms of VO2 [6, 24]. On the other hand for the same cardiac load and VO2 cost, the RGO helps to have an increased actual reach space for performing daily activities. Since the RGO allows the subjects to stand and work, this could further reduce the demand to adopt the work environment for paraplegic people [24]. During rest state, the HR and VO2 of the RGO (standing) is higher than WHCH (sitting), this might be due to isometric contraction the upper limb and trunk muscles in order to balance [24]. There is also psychological influence too; the RGO does improve the subject's psychological moral [5]. At the same time the subjects tend to choose the WHCH over the RGO because of peer pressure [23].

Likewise there were studies which compared the RGO user's energy expenditure against a normal person [7, 8, 24, 25]. It was found that walking speed of a normal person is nearly 3 to 7 times faster than the RGO users [7, 8, 24, 25]. The RGO users most comfortable speed can't even match the slow speed of a normal person [8, 25]. The energy efficiency during locomotion of the able-bodied person is 5 to 25 times of a RGO user [7, 8, 25].

The basic layouts of these studies tend to use a closed system approach, where they try to study the difference between system 1 and 2. On the other hand, this whole setup could be considered from an open system approach, where  $VO_2$  or HR or COP as the input (stimulus) which goes through a black box (human+RGO) and the velocity achieved as the output (response). In the open system approach, the human and environment are dynamically coupled with each other. So a person using a RGO is in a completely different umwelten compared to a one using a wheelchair or an able-bodied person [26]. In short WHCH are better mode of locomotion compared to RGO, if just one is going to take the energy expenditure into account. Is that enough? No, RGOs does have their own benefits. The researchers could start to come with a plan for combined usage of the RGO and WHCH, to their optimum level. WHCH could be opted for faster locomotion and RGO for more accessibility in places where slower locomotion is preferred.

Note: The important values from the above papers are given in Table 1.

#### Comparison between RGO and other Orthosis available in the market

There were totally thirteen articles that made evaluation between an RGO and other orthoses, ten articles addressing energy expenditure and three regarding gait parameters. The RGO was compared with various orthosis like, a non-reciprocating orthosis (KAFO, HKAFO and Non-RGO) or a medially linked orthosis with de-coupled hip joints (WO, PW, HGO) or other RGO models (ARGO, IRGO). With the non-reciprocating orthosis the subjects tend to ambulate using a swing-through or swivel motion with the help of a crutch. Whereas with the other types of orthosis the subjects perform a reciprocating gait motion with the help of a crutch or rollator.

The RGO's mean energy expenditure vary from 2.85 to 5.80 (beats/m) in terms of PCI [7, 27-30], 0.711 to 2.54 (ml/kg m) in terms of VO2 cost [6, 23, 27-29, 31-33]. From the studies that compare RGO against non-reciprocating orthosis the outcome is quite puzzling, in some studies the RGO has lower VO2 cost compared to non-reciprocating gait orthosis [32, 33], there is also evidence of HKAFO being more energy efficient compared to RGO [31] and there were also results with no significant difference between the two in terms of VO2 cost [23, 28, 32]. Katz found out that there is only significant difference in the VO2 cost between the RGO and HKAFO only for the subjects with thoracic lesion level, where as there was no significant difference for the high lumbar patients [32]. If we take the VO2 consumption into account, in two studies the HKAFO was significantly higher than the RGO [23, 31] and in the other studies, there was no significant difference between the RGO and Non-reciprocating gait orthosis [28, 32]. Two studies reported about PCI, one had a non-significant result [28] and the other reported that the IRGO had significantly lower PCI compared to a bilateral KAFO [30]. But in terms of HR both of the studies reported that there was no significant difference [28, 30]. For the comparison between RGO and medially linked orthosis with decoupled hip joints, the evidence suggest that (I)RGOs are better than the WO in both VO2 cost and PCI [29, 33]. There were two more articles which compared RGO and HGO (PW), but no conclusion could be derived from them due to insufficient data [6, 7]. It was also found in literature that the IRGO has a significantly lower PCI level compared to a LSU-RGO [27].

### Table 1. Comparison between RGO and Wheelchair/Normal Gait

The following table contains the results of the important parameters from some of the studies for a quick reference. For more details check the references

Author,		Sample	_	Male	Type of	Lesion	Types of	#
Year	Study Design	size	Age	population %	paraplegia <sup>\$</sup>	level	ambulation	Results <sup>#</sup>
	Uncontrolled						RGO, HGO,	
Bowker,	Comparative				SB - 18		WHCH, and	PCI (beats/m): RGO 5.0 , HGO 4.1, WHCH 0.7, Normal 0.21
1992	Study	28	17.1	74.29%	Traumatic - 10	NA	Normal	Vel. (m/min): RGO 14.3, HGO 15.6, WHCH 60, Normal 65
	Uncontrolled							
Bernardi,	Comparative				Praplegic - 10		RGO and	WEC (J/kg m): RGO 11 (4), Normal @ slow speed 10(0.3)
1995	Study	17	NA	58.82%	Normal - 7	T4 - T12	Normal	Vel. (m/sec): RGO 0.26 (0.16), Normal @ slow speed 0.82(0.13)
	Controlled							
Bernardi,	Comparative				Praplegic - 6		RGO and	VO <sub>2</sub> cost (ml/kg min): RGO 10.8 (0.8), WHCH 10(0.3)
1995	Study	12	NA	50.00%	Normal - 6	NA	WHCH	Vel. (m/sec): RGO 0.17 (0.08), WHCH 1.28(0.17)
	Uncontrolled							
Tyler,	Comparative						RGO, HKAFO	VO <sub>2</sub> cost (ml/kg m): RGO 0.81 (0.34), HKAFO 0.54 (0.12), Normal 0.22 (0.073)
1997	Study	26	3.7-15	NA	SB	T12-L4	and Normal	Vel. (m/sec): RGO 0.27 (0.11), HKAFO 0.68 (0.20), Normal 1.05 (0.16)
1337	Study	20	3.7 13	14/1	35	112 54	una reorma	Ver. (11) See). 1100 0.27 (0.11), 110 110 0.00 (0.20), 110 1110 1.05 (0.10)
	Uncontrolled							PCI (beats/m): RGO 17.67 (9.4), Normal @ regular speed 1.47(0.26)
Bernardi,	Comparative				SCI - 11		RGO and	WEC (J/kg m): RGO 27.2 (9.9), Normal @ regular speed 3.53(0.46)
1999	Study	96	NA	45.45%	Normal - 18	NA	Normal	Vel. (m/sec): RGO 0.26 (0.16), Normal @ regular speed 0.82(0.13)
								Orthosis
								HR (beats/min): PW 150(13), RGO 131(21), RGO-FES 155(23)
								VO <sub>2</sub> cost (ml/kg min): PW 71.8(7.3), RGO 76.5(21.3), RGO-FES 62.3(12.2)
								Vel. (km/h): PW 0.59(0.2), RGO 0.67(0.1), RGO-FES 0.57(0.3)
								WHCH
	Controlled						PW, RGO,	HR (beats/min): PW 160(16), RGO 155(31), RGO-FES 154(31)
Merati,	Comparative						RGO-FES and	VO <sub>2</sub> cost (ml/kg min): PW 63.8(24.0), RGO 68.9(27.1), RGO-FES 67.6(23.9)
2000	Study	14	31.4(10.2)	92.86%	SCI - 14	C7-T10	WHCH	Vel. (km/h): PW 6.2(2.0), RGO 5.4(1.3), RGO-FES 5.2(1.6)

<sup>\$</sup>SB-Spina Bifida, SCI-Spinal cord injury

The above table does not have the "Years after injury, Training time" column since all the values were "NA"

<sup>&</sup>lt;sup>¿</sup> RGO-Reciprocating Gait Orthosis, HGO-Hip Guidance Orthosis, WHCH-Wheelchair, HKAFO-Hip Knee Ankle Foot Orthosis, PW-ParaWalker, FES-Functional Electrical Stimulation

<sup>&</sup>lt;sup>#</sup> PCI-Physical Cost Index, Vel.-Velocity, WEC- Walking Energy Cost, VO<sub>2</sub> Cost-Oxygen Cost, HR-Heart Rate,

The mean velocity of the RGO users varied from 5.435 to 20.4 m/min [6, 7, 23, 27-35]. When compared against the other orthosis available in the market, the RGO are faster than the WO and KAFO [29, 30, 32-34]. But the there is also evidence of the HKAFO being faster than the RGO [23, 31]. The higher velocity was achieved because the subjects used swing-through motion while using the HKAFO. With the HKAFO the subject's velocity improved over time and regular usage, but not in the case of the RGO [23]. It is also said that the hip flexion contracture has a positive correlation with the walking velocity [32]. In terms of cadence there was no significant difference recorded between the orthoses in literature and the average cadence ranged between 30-40 steps/min [27, 28, 35]. Likewise for stride length, there was no significant difference found, and the paraplegic had the stride length nearly between 0.9-1.0 m [28, 35]. The normal person's cadence range from 90-135 steps/min and stride length between 1.25-1.85 m [35]. This clearly shows the paraplegic take shorter steps compared to a normal person, and since the paraplegic's cadence is also low, their velocity is also low compared to a normal person.

Some of the negative aspects of RGO are, the subjects find the RGO to be heavy/bulky and in fact it is one of the reason why the users have abandoned the RGO [6, 23, 31, 32]. The weight of the orthosis could have some impact over the VO2 cost [30, 31]. The energy expenditure of an orthosis doesn't have a impact over the acceptance rate [6], but it would be better to design a RGO with better strength to weight ratio, so that it will have a positive impact with the end users [30]. Compared to a WO or KAFO, the RGO has a thoracolumbar corset; therefore the RGO lacks the appeal in the beginning and the patients find it hard to change diapers [29, 32]. One could also think of perspiration problems, since the patient's lower torso is covered by a plastic corset. It was mentioned in one of the studies that the IRGO doesn't fit properly in the regular WHCH available in the market [34]. On the contrary it was also mentioned the HGO has parts only for kids above 5 years old [21].

On the bright side, due to the coupling of the bowden cable or isocentric bars, the RGOs give better stability and postural control, compared to the KAFO or WO [30, 33]. The RGOs also provide better hip flexion compared to the (H)KAFO or WO, so the RGO user have better hip joint stability and have lesser hip contracture [23, 29, 32, 33]. The corset is believed to improve the static balancing of the subjects [33]. Due to the improved stability, the IRGO give more independent gait compared to a WO [34].

Since the RGO has a lower VO2 compared to the HKAFO [23, 31], it is suggested that the RGO would be better for long distance ambulation compared to a conventional HKAFO [31]. The question is, why the HKAFO having higher VO2 consumption? Is it due to extra strain on the upper limbs or due to the higher velocity reached during swing-through motion? There is evidence of people who are performing well with both the orthosis and also people performing bad [23, 29-31]. So, is it the mechanical system we need to optimize or the training method? Non-users have more or less the same performance level compared to the users, still they reject the RGO [20]. So In order to find out an improved way to quantify what is the overall performance level (patient + orthosis) and the effort exerted by the human (physical and mental load), would it be better if we start to see the overall system using system identification techniques? By this way, we can have a better understanding of the patient's limitations, and improve the design of the RGO accordingly. Even if we succeed designing the best orthosis, what about the money cost? In literature it is mentioned that

the RGO is 50% more expensive than the HGO or WO [7, 34, 36]. So does the extra money spent on the orthosis worth the cost? It is up to the patient as a customer to decide, what he/she values more. Is it energy cost or economic cost?

The problem with these studies is that there are various methods and units for measuring the energy expenditure of the subjects. The authors say the reason why their results conflict with the previous studies might be due to the different experimental procedure or different parameters used [23, 27, 31]. This makes it difficult to compare the results of all the studies together. All the studies couldn't be grouped together and compared. Then the sample sizes of these studies are small, that the author themselves claim there is no clear conclusion from their results due to the small sample size [23, 27, 28, 32]. There is a huge amount of non-significant results reported, and there was no power analysis either to support the argument that the compared orthoses have the same energy expenditure. The variations in results could be due to the different types of gaits performed by the subjects. In some studies the subjects used a swing-through motion, in other the subjects used swivel motion. The skill level of the subjects plays an important role too; there is evidence of outliers who either perform really well or bad with their orthosis [23, 29-31].

The WO is the least energy efficient orthosis, but there is no clear conclusion from the studies when comparing RGO against the other orthoses. Therefore, future studies should have a standardized experimental procedure in order to have a clear conclusion.

Note: The important values from the above papers are given in Table 2

#### Comparison between RGO and Hybrid RGO

Hybrid RGO systems is a conventional RGO system that is being augmented by means of mechanical, pneumatic, hydraulic or electrical system in order to improve the overall performance. The hybrid RGO system is not similar to an exoskeleton or a PGO. The hybrid RGO still derives the driving force from the user, whereas an exoskeleton can produce its own driving force.

RGO+FES system is one of the hybrid RGO systems, it aids the subjects to contract and extend their muscles with a help of an electrical stimulations. The electrodes can either be internal or external. Five articles contained data related to RGO+FES performance, 4 out of 5 compared the regular RGO with the RGO+FES [6, 37-40]. Most of the results were nonsignificant. The only significant results that were recorded were, the HR was increased during without FES condition at velocities 0.1 and 0.2 m/s [39] and the slope difference of HR/VO2 curves between the orthosis and WHCH, was significantly lower for the RGO+FES system compared to RGO [6]. Yet the RGO+FES has a high energy consumption compared to the wheelchair [6, 40]. The authors of these studies say the RGO+FES performs better than the RGO [38-40], but none of the study has a proper significant result to prove that. The functional parts of the muscles react to a proper nerve impulse asynchronously, whereas is completely opposite for external stimulation. The motor units are activated synchronously to FES stimulation. Due to usage of FES there might be arousal of muscle fatigue. So the question is how does the FES system influence the condition of the muscle in long run? The other questionable factor about these studies is the sample size, 3 out of 5 studies had a sample size equal to 1 [37, 38, 40]. As per the patient, they don't like to spend more time, just to get the electrodes stuck around their body [37, 39].

**Table 2. Comparison between RGO and Other Orthosis** 

Author,		Years after	Training	Commis		Male	Tuno of	Lesion	Tymes of	
Year	Study Design	injury	Time	Sample size	Age	population %	Type of paraplegia <sup>\$</sup>	level	Types of ambulation <sup>c</sup>	Results <sup>#</sup>
Jefferson, 1990	Controlled Comparative Study	5 yrs	NA	1	33	100.00%	SCI	T5	RGO, ARGO and HGO	Cadence (steps/min): RGO 39-35, ARGO 39-37, HGO 34-37 Stride length(m): RGO 0.99-1.02, ARGO 0.99, HGO 0.84-0.98 Vel. (m/s): RGO 0.32-0.30, ARGO 0.31, HGO 0.24-0.30
Bowker, 1992	Uncontrolled Comparative Study	NA	NA	28	17.1	74.29%	SB - 18 SCI - 10	NA	RGO and HGO	PCI (beats/m): RGO 5.0 , HGO 4.1 Vel. (m/min): RGO 14.3, HGO 15.6
Winchester, 1993	Controlled Comparative Study	min 2 yrs	35 (7.5)hrs	4	24-36	100%	SCI	T5-T10	RGO and IRGO	PCI (beats/m): RGO 3.6 (0.7), IRGO 2.6 (0.5) VO <sub>2</sub> cost (ml/kg m): RGO 1.1 (0.3), IRGO 1.0 (0.1) Vel. (m/min): RGO 12.7 (1.9), IRGO 13.5 (2.1)
Tyler, 1997	Uncontrolled Comparative Study	NA	NA	26	3.7-15	NA	SB	T12-L4	RGO and HKAFO	VO <sub>2</sub> cost (ml/kg m): RGO 0.81 (0.34), HKAFO 0.54 (0.12) Vel. (m/sec): RGO 0.27 (0.11), HKAFO 0.68 (0.20)
Izerman, 1997	Controlled Comparative Study	NA	4 weeks	6	38.7(10.9)	100%	SCI	T4-T12	ARGO and NRO	PCI: ARGO 5.4, NRO 5.8 VO <sub>2</sub> cost : ARGO 1.55, NRO 1.63 Vel. (m/sec): ARGO 0.24(0.11), NRO 0.23(0.13)
Katz,	Controlled Comparative								HKAFO and	$VO_2$ cost thoracic level (ml/kg m): HKAFO 1.85, RGO 0.72 $VO_2$ cost upper lumbar level (ml/kg m): HKAFO 1.23, RGO 0.75 $Vel.$ thoracic level(m/min): HKAFO 6.52 RGO 12.70
1997	Study	NA	7 weeks	8	2-11	37.50%	SB	NA	RGO	Vel. upper lumbar level(m/min): HKAFO 17.32, RGO 16.37
Harvey, 1998	Controlled Comparative Study	4-19 yrs	8 weeks	9	max 55	100%	SCI	T9-T12	WO and IRGO	PCI: WO 8.4-10.3, IRGO 4.3-7.0 VO₂ cost : WO 3.95-4.91, IRGO 1.65-1.80 Vel. (m/min): WO 5.2-5.7, IRGO 10.9-11.5
Merati, 2000	Controlled Comparative Study	NA	NA	14	31.4(10.2)	92.86%	SCI	C7-T10	PW and RGO	HR (beats/min): PW 150(13), RGO 131(21) VO <sub>2</sub> cost (ml/kg min) : PW 71.8(7.3), RGO 76.5(21.3) Vel. (km/h): PW 0.59(0.2), RGO 0.67(0.1)

**Table 2. Comparison between RGO and Other Orthosis** 

Author, Year	Study Design	Years after injury	Training Time	Sample size	Age	Male population %	Type of paraplegia <sup>\$</sup>	Lesion level	Types of ambulation	Results <sup>#</sup>
										O2 cost (ml/kg m) Yr.1: RGO 0.787(0.34), HAKFO 0.657(0.31) O2 rate (ml/kg min) Yr.1: RGO 11.51(1.9), HAKFO 21.13 (3.1) Vel (m/s) Yr.1: RGO 0.28(0.11), HAKFO 0.6(0.2)
										O2 cost (ml/kg m) Yr.2: RGO 0.711(0.27), HAKFO 0.759(0.51) O2 rate (ml/kg min) Yr.2: RGO 12.67(3.8), HAKFO 23.67 (9.7) Vel (m/s) Yr.2: RGO 0.32(0.10), HAKFO 0.62(0.22)
Thomas, 2001	Uncontrolled Comparative Study	NA	Min 1 yr usage	23	4-15 (8)	56.52%	SB	T12-L4	RGO and HKAFO	O2 cost (ml/kg m) Yr.3: RGO 0.841(0.30), HAKFO 0.847(0.39) O2 rate (ml/kg min) Yr.3: RGO 14.75(2.6), HAKFO 18.23 (4.3) Vel. (m/s) Yr.3: RGO 0.33(0.15), HAKFO 0.43(0.2)
Abe, 2006	Controlled Comparative Study	NA	167-180 days	2	33-66	50%	SCI-1 Tumor-1	T9-T12	KAFO, WO and RGO	VO2 cost (ml/kg m) : KAFO 5.25, WO 3.03, RGO 2.54 Vel (m/min): KAFO 3.525, WO 5.06, RGO 5.435
Leung, 2009	Controlled Comparative Study	32-281 months	8 weeks	6	19-46	33.33%	SCI	T12-L1	IRGO and KAFO	PCI (beats/min): KAFO 6.77(3.28), IRGO 2.85(0.77) Vel. (m/min): KAFO 5.5(4.3), IRGO 10.46(2.00)

<sup>\$</sup> SB-Spina Bifida, SCI-Spinal cord injury

<sup>&</sup>lt;sup>è</sup> RGO-Reciprocating Gait Orthosis, ARGO-Advanced Reciprocating Gait Orthosis, HGO-Hip Guidance Orthosis, IRGO-Isocentric Reciprocating Gait Orthosis, HKAFO-Hip Knee Ankle Foot Orthosis, NRO-Non Reciprocal Orthosis, WO-Walkabout Orthosis, PW-ParaWalker, KAFO-Knee Ankle Foot Orthosis

<sup>&</sup>lt;sup>#</sup> Vel.-Velocity, PCI-Physical Cost Index, VO<sub>2</sub> Cost-Oxygen Cost, HR-Heart Rate,

In literature it was mentioned that the subjects went for an extra training for the FES system in order to condition their muscles, meaning that is going to be extra cost of both time and money. So, is the RGO+FES system worth it? More research with proper experimental protocol needs to be conducted, in order to get a clear conclusion.

There are more hybrid RGO systems described in literature, namely the RGO+FES combined with an Auditory Feedback System (AFS) [41], or a RGO+FES with a Variable Hip Coupling Mechanism (VHCM) [42-44], or a RGO+FES with a Stance-Control Knee Mechanism (SCKM) [45]. It was found that the AFS was helpful only during medium walking velocity (1.22km/h) and in fact it worsened the performance of the subject if used during higher velocity (1.8km/h) [41]. There were four articles related to the VHCM, two of them were introductory design articles, another article enumerating further about an add-on development like the Finite-State Postural Controller (FSPC) [44], one out of the four articles had to be rejected since all the test subjects were able bodied persons. It was denoted that the VCHM provides minimum resistance to the motion of the hip joints [44]. With the SCKM study it was reported that the SCKM system reduces the upper limb forces on the walking aid and also the muscle stimulation, thereby allowing the subject to walk longer distances [45].

Note: The important values from the above papers are given in Table 3a

Apart from the hybrid RGOs, there is research done on new RGO designs, which have new mechanical alterations, like a RGO having a Stance Control Orthosis (SCO) [46], an ARGO with a dorsiflexion assist AFO [47] or using a trunk extension along with an ARGO [48]. With the SCO it was found out that the stance control system does improve the gait pattern of the patient, both the velocity and the stride length was doubled [46]. It was evident that both the velocity and stride length were significantly higher when the dorsiflexion assist AFO was used compared to the regular solid AFO [47]. Similarly with the additional trunk extension it was noted that there was a significant improvement in the walking speed, trunk and hip movement [48].

Note: The important values from the above papers are given in Table 3b

It is evident these hybrid RGO or mechanically altered RGO do improve the gait parameters from these results [44-48]. But what about their energy cost? More research needs to be done in terms of energy cost. Then issue with some of these studies is that there is only one test subject and these hybrid orthosis are in their prototype phases, so they have their own short comings [44, 45]. In fact in the SCKM study the subject performed better with only the FES system compared to the hybrid orthosis, the reason being the subject has used only the FES for the past 24 years [45]. So the subjects need time to learn and adapt to a new system, but how long? Regarding to the use of the trunk extension, how it is going to have impact with the subject in terms of ergonomic factors. We know that the subject tend to prefer the orthosis without a thoracolumbar corset, so how well would the patients appreciate a thoracolumbosacral orthosis, which is going to be strapped over more parts their body and also in terms of the extra time required for donning and doffing it.

## Table 3a. Comparison between RGO Vs Hybrid Orthosis

Author, Year	Study Design	Years after injury	Training Time	Sample size	Age	Male population %	Type of paraplegia <sup>\$</sup>	Lesion level	Types of ambulation <sup>¿</sup>	Results <sup>#</sup>
Isakov, 1992	Controlled Comparative Study	6 years	NA	1	40	0.00%	SCI	T4-5	RGO and RGO+FES	PCI (beats/m): RGO 2.55, RGO+FES 1.54 Cadence (steps/min): RGO 39, RGO+FES 42 Step length(m): RGO 0.61, RGO+FES 0.59 Vel. (m/min): RGO 23.9, RGO+FES 25.2
Beillot, 1996	Controlled Comparative Study	4-77 months	6 weeks	14	19-42	92.86%	complete dorsal spastic paraplegia	T2-T10	RGO and RGO+FES	HR@0.1 m/s (beats/min) : RGO 147, RGO+FES 121 HR@0.2 m/s (beats/min) : RGO 155, RGO+FES 123
Merati, 2000	Controlled Comparative Study	NA	NA	14	31.4	92.86%	SCI	C7-T10	RGO and RGO+FES	HR (beats/min): RGO RGO 131(21), RGO+FES 155(23) $VO_2$ cost (ml/kg min): RGO 76.5(21.3), RGO+FES 62.3(12.2) Vel. (km/h): RGO 0.67(0.1), RGO+FES 0.57(0.3)
Spadone, 2003	Controlled Comparative Study	2 years	195 hrs	1	28	100.00%	SCI	Т5-Т6	ARGO, ARGO-FES, Parastep, and WHCH	HR @ Self Chosen Vel. (beats/ min): ARGO 142, ARGO-FES 108, Parastep 124, WHCH 133  HR @Max Vel. (beats/ min): ARGO 145, ARGO-FES 165, Parastep 124, WHCH 156  VO <sub>2</sub> cost @ Self Chosen Vel. (ml/kg min): ARGO 0.79, ARGO-FES 0.94, Parastep 1.33, WHCH 0.9  VO <sub>2</sub> cost @ Max Vel. (ml/kg min): ARGO 1.15, ARGO-FES 1.22, Parastep 1.33, WHCH 1.22  Self Chosen Vel. (km/h): ARGO 0.52, ARGO-FES 0.53, Parastep 0.2, WHCH 3.35  Max Vel. (km/h): ARGO 1.01, ARGO-FES 1.05, Parastep 0.2, WHCH 4.38
CS To, 2012	Controlled Comparative Study	·		1	70	100.00%	SCI	Т9	IRGO, FES, HNPO and	Cadence Left(steps/min): IRGO 31, FES 60, HNPO 34, HNP 26 Cadence Right(steps/min): IRGO 36, FES 60, HNPO 36, HNP 34  Step length Left(m): IRGO 0.24, FES 0.41, HNPO 0.21, HNP 0.23  Step length Right(m): IRGO 0.31, FES 0.42, HNPO 0.36, HNP 0.36  Vel. (m/s): IRGO 0.12, FES 0.43, HNPO 0.15, HNP 0.14

## Table 3b. Comparison between RGO Vs Hybrid Orthosis

Author, Year	Study Design	Years after injury	Training Time	Sample size	Age	Male population %	Type of paraplegia <sup>\$</sup>	Lesion level	Types of ambulation <sup>¿</sup>	Results <sup>#</sup>
Rasmussen, 2007	Uncontrolled Comparative Study	17 months	1 month	1	30	100%	SCI	T10	RGO with Locked Knee and SCO	Cadence (steps/min): Locked 38.4(17.6), SCO 30.37(1.32) Stride length(m): Locked 0.44(0.27), SCO 0.92(0.05) Vel. (m/s): Locked 0.11(0.04), SCO 0.23(0.02)
Bani, 2013	Controlled Comparative Study	12-36 months	6-10 weeks	4	24-29	75%	SCI	T8-T12	DA-AFO and solid AFO	Cadence (steps/min): DA-AFO 42(3.09), solid AFO 40(2.38) Stride length(cm): DA-AFO 100(9.48), solid AFO 94.50(9.25) Vel. (m/s): DA-AFO 0.35(0.01), solid AFO 0.32(0.02)
Arazpour, 2014	Controlled Comparative Study	24-45 months	6-8 weeks	4	20-32	75%	SCI	T8-T12	ARGO and ARGO+TLSO	Cadence (steps/min): ARGO 54(3.77), ARGO+TLSO 55(3.59) Step length(cm): ARGO 36(0.95), ARGO+TLSO 38(1.63) Vel. (m/s): ARGO 0.33(0.02), ARGO+TLSO 0.35(0.02)

<sup>\$</sup> SCI-Spinal cord injury,

<sup>&</sup>lt;sup>è</sup> RGO-Reciprocating Gait Orthosis, FES-Functional Electrical Stimulation, ARGO-Advanced Reciprocating Gait Orthosis, WHCH-Wheelchair, IRGO-Isocentric Reciprocating Gait Orthosis, HNP-Hybrid-NeuroProsthesis, SCO-Stance Control Orthosis, DA-AFO-Dorsiflexion Assist Ankle Foot Orthosis, AFO-Ankle Foot Orthosis, TLSO-Thoracolumbosacral Orthosis

<sup>&</sup>lt;sup>#</sup> PCI-Physical Cost Index, Vel.-Velocity, HR-Heart Rate, VO<sub>2</sub> Cost-Oxygen Cost

#### Comparison between RGO and PGO

The powered gait orthosis (PGO) are mechanical exoskeletons or orthosis, where the main driving power is derived from an external source. There is a lot of literature regarding PGO; all of them were not included in this study since it is beyond the scope of this study. Four articles comparing the RGO and PGO were taken into consideration [49-52]. The results from these studies clearly point to the fact that the PGO helps to reduce the vertical and lateral compensatory motion, also the cadence, stride length and walking velocity seemed to improve with the PGO [49-52]. None of the four articles had any information about the energy cost. So it is really not sure if these improvements in the gait parameters happen at extra or same or low energy cost. It was also reported in a review article that more studies needs to be done regarding the PGO efficiency and the current results are not substantial enough [19].

#### Other Facts and Correlations regarding RGO

These articles were not exclusive or comparative study of a RGO model. Some of the studies were how the RGO training has impact over the subject or correlational studies [53-65]. These studies were not discussed in the above section because they were not completely in line with those studies, but these articles are related to the RGOs energy expenditure or gait dynamics.

In terms of walking dynamics the subjects ambulated in a consistent pattern; the trunk extension was generated due to moments at the shoulder and trunk flexion due the hip moments; an opposing extension moment over hip was observed during the beginning of the swing phase which contradicted the intent of the reciprocal coupling [58]. In another study it was found out that the front cable in the LSU-RGO doesn't aid flexion of the swinging leg [60]. It is suggested that the reciprocal coupling contribute lesser than the trunk and pelvis motion during the swing phase of the gait. They also suggest the patient's trunk posture might affect the arm loading and the RGO's reciprocal links action. This in turn will affect the overall energy expenditure [58]. So a patient's posture depends on his/her physical limitations, but the posture can be changed to a certain extent with the help of supporting devices and proper training. It was found that orthotic training has influence over the EMG activity of the ankle extensor soleus muscle. It is believed with proper training, the tibialis anterior muscle activity could be induced [56]. Walking with orthosis influence the bone mineral density, most part of the axial loading is transmitted by the body and the flexion/extension moment was transmitted by the bone [59]. In short, training with an orthosis helps to improve the spinal locomotor neuronal activity and also reduce bone osteoporosis [56, 59]. The use of a treadmill in orthotic training has been found to improve the walking ability of a patient [53]. It was recorded that the WEC after the treadmill training was significantly lower compared to the WEC before the training. The issue here to be speculated in this study is that, there was no control group to properly verify the effect. Then some subjects were trained for 2 months and some for 6 months. So did the patients have an improved performance because of the treadmill or was it just because they improved in due time.

These were the following correlations found from literature, it was found out that oxygen uptake and oxygen cost is dependent on walking speed [54]. The PCI was a valid measure for changes in within-patient oxygen uptake [55]. In a cross-sectional study to find how the performance of the paraplegic patients vary depending upon their lesion level. The results denoted that there was a strong positive correlation between lesion level and energy cost (r=0.85), velocity also had a strong positive correlation with the lesion level (r=0.74) but peak crutch force had a strong negative correlation with lesion level (r=-0.78) [57]. Even though there are these various correlations made with lesion levels and energy costs, these studies doesn't gives us a clear picture what parameter one has to improve in his/her RGO design, so that the patient is going to be benefited in the end.

In order to get better understanding of what exactly happens to the body while walking with a RGO, in the last decade mathematical model analysis are done by few groups of researchers [61-65]. With mathematical models one could overcome the problems of small and diverse sample population of an experimental analysis. One could run these simulations and get better understanding before recruiting subjects for experimental analysis [63]. Yet there are some limitations to this approach, the accuracy of the results from the simulations depends on how well the mathematical model is designed. The current models have some limitations like constant stiffness and constrains of the rigid bodies or numerical errors due to multiple spring damper systems or unable to change the lesion level of the model [61-65]. These were the findings from the mathematical models; the constant hip coupling in the IRGO limits the stride length and this could be overcome by using a hybrid orthosis (RGO+FES) with coordinated joint locking system. The patients will also encounter less muscle fatigue while using a hybrid orthosis compared to FES-only system [61, 62]. In another research it was hypothesised that a modified gait patter, with larger trunk movement and no axial rotation could reduce the upper body loading and energy cost [64]. It was suggested that increasing the hip stiffness could increase the gait velocity [65]. The only conclusion from the above articles would be more research needs to be done in order to check whether these hypotheses are true.

#### **RGO Usage**

There were totally five follow-up studies [5, 20-22, 36], who's primary aim was to study the usage of the reciprocal gait orthosis. Three studies where done is a single centre and two where multi-centred. There were two more articles that were included [6, 24], since they contained data about ergonomic parameters and user preference as secondary information. From the seven articles it was observed that the abandonment of the reciprocal gait orthoses vary from 9.09% to 78.57%. The factors that influence the abandonment of an orthosis are as follows;

The time taken to don/ doff an orthosis does affect the probability of abandonment [6, 22]. When compared between HGO and RGO, patients find it difficult to don/doff the RGO [20, 36]. This doesn't mean majority of the patients prefer HGO. Only 4 out of 22 (18.18%) preferred the HGO as it was easier to don/doff [36].

Functionality of the orthosis has a huge impact over the acceptance rate of the orthosis. This factor is like a double edged sword and it depends on the patient's perspective. The non-users say they find it hard to use the RGO [5, 6, 36] or they don't see the functional gain in using a RGO [20]. On the other hand RGO users say they chose the RGO because of its ease

to stand up with free hands [36] and the use of RGO creates a greater feeling of personal moral [5]. The ability to climb stairs at the time of discharge affects the probability of RGO rejection rate at follow-up. Only 14.3 % of climbers abandoned at follow up but 43.5% non-climbers abandoned at follow up [22]. So it is not only the RGO but it depends on how far the patient is willing and able to put effort. Youngsters (age <18) denoted that it is difficult to use the lavatory while wearing the RGO [5]. Patients should be aware of the limitations of the RGO and they should not think RGO as an alternative for wheelchair [5, 20, 22, 36].

For some patients the ergonomic factors like cosmesis, comfort and control plays a role in their orthosis acceptance rate. 12 out of 22 patients chose RGO compared to HGO due to its improved cosmesis [36]. At the same time 1 out of 27 rejected the ARGO due to its lack of cosmesis [20]. Comfort factor is more important than cosmetic factor [36]. In terms of control, the HGO is resists the hip adduction more compared to RGO [36]. HGO users were unable to climb curbs/stairs [20, 36]. So this might increase the probability of HGO rejection rate. But youngsters (<18) with spina bifida prefer this less flexible HGO, as they can concentrate less about standing upright [21]. The youngsters felt the orthosis is less reliable when there is a breakage, as it took them more time to adjust to the repaired orthosis, compared to adults (18+) [5]. On the contrary Franceschini claims breakage doesn't influence the rate of abandonment [22].

The external factor like moral support by parents, spouse, or friends is vital. Nearly 50% of the users said they would have abandoned the orthosis if they didn't have the encouragement and help from the people around them [5]. Likewise the community users are the ones who can stand up and sit down independently [21]. The geographical distance between the subject's home and rehab center could be a factor for abandonment [5, 22]. A product might have a good design, but still fail in the market due to improper promotion [3].

Some patients had stopped using the RGO either due to clinical improvement or problem. One out of 22 [21], 3 out of 85 [5] improved and progressed to KAFO after some time. One out of 27 [20], 6 out of 85 [5] were advised not to use the RGO surgical/medical reasons. There are also instances where the subject dies and thus the RGO is abandoned [21]. Finally there are a bunch of subjected who lost contact with the rehab centres, thus considering them as non-users [5, 6] or they were excluded from the studies [22].

So in short the overall conclusion from the above studies is that there is no clear conclusion regarding which orthosis is mostly preferred. Subjects do give importance to comfort level, cosmesis and effort required to use the orthosis. Yet there is no statistically significant correlation between actual energy expenditure and RGO abandonment rate. It is more of a subjective analysis. If the subjects have the confidence that they can use the RGO by themselves or they get enough support from the people around them, they tend to use the orthosis. There was only one controlled comparative study. The selection criteria for these different groups that were formed, is quite absurd. It is mentioned that the patient should have high motivational skills and should be aware of the limitation of a RGO. So meaning, no matter how bad the orthosis is; if the patient has perseverance to use it, he/she won't abandon the orthosis. So there is a huge influence of psychological factors than mechanical and physiological factor that influence the rejection rate of a RGO. So maybe future studies should run something like a NASA TLX test for both the subject and also the person who

helps the patients, on regular intervals of 2-4 months, as part of the experiment. This might give a more insight about what the psychological state of the patient and the people around. More research needs to be done on how a user and a non-user sees the RGO in terms of the psychological aspects, like if the patient is a satisficer or a maximiser and how does the environment they live in affect their motivation level.

Note: The important values from the above papers are given in Table 4

#### **DISCUSSION**

As mentioned earlier the aim of this paper is to do a literature review regarding RGO. Around 60 articles were used in this review to have an overall look about the performance characteristics and rejection rates of a RGO. A most common problem found in some of these studies was the sample size was small, that too some of them had only single subject for the case study [35, 37, 38, 40, 45, 50, 51]. Due to the lack of subjects, now the question would be how valid are their results? It is tough to generalize the results from these studies, with such small sample size we don't know for sure, if the effect is due to a specific cause or due to some random cause. In fact some researchers claimed that they got non-significant result due to the lack of sample size [23, 27, 28, 32]. None of the study had a power analysis performed to support how strong their finding is. Therefore it only leads us to say there is no clear conclusion and further research needs to be done.

Then speaking about the experimental procedure, the method of doing these experiments needs to be standardised. The performance metric varies between studies. Even though the researchers of two different studies try to measure the same variable, they measure them with a completely different metric and this makes it complicated to compare the results of all the studies together. Even if the metric remain the same, at times the researchers get conflicting results to that of the previous paper. They claim this might be due to the variation in the experimental procedures [23, 27, 31]. Therefore a standardized experimental procedure needs to be followed. In some the studies that were made, normal people were used as control group [8, 25]. Using a normal person in the study is fine for case-control study where we want to find the effect of disease, but if our intension is to find the effectiveness of the treatment/intervention, then using a normal person as the control group and the paraplegic using RGO as the experimental group, doesn't really help.

In a few other studies there were some outliers who performed extremely well. The reason that particular patient performed really well to some set of conditions because he/she is well trained and experienced in those conditions [44, 45]. It is something similar to comparing a normal person skating in an ice rink and a professional athlete who skates for speed skating. The subjects should be classified not only by their lesion level and age, but also by their level of efficiency before the experiment and after the experiment, E.g. the garrett score used by Franceschini [22]. The hours of training and practice does make the human learn how to use a tool at the optimum efficiency. In order to reach the optimum efficiency what would be the required hours of training and what type of regime should be followed?

## **Table 4. Rejection Rate**

Author, Year	Study Design	Sample size	Muliti- Centered	Types of ambulation <sup>¿</sup>	Follow-up or Usage Time	Rejection rate %	Community User %	Specific model Acceptance rate	Usage Hours	Traning hours
Whittle,	Controlled							RGO - 12/22		
1991	Comparitive	22	No	RGO and HGO	2X 4 months	27.27%	NA	HGO - 4/22	NA	3hrs X (4-5) days
Lotta, 1994	Uncontrolled Comparitive	28	Yes	RGO, ARGO and HGO	6 months	25.00%	14.29%	RGO - 10/12 ARGO - 8/11 HGO - 3/4	0.5 - 3 hrs/day	3 - 16 weeks
Phillips, 1995	Uncontrolled Comparitive	22	No	RGO and HGO	3 months to 6 years (Usage time)	9.09%	59.09%	RGO - 12/13 HGO - 7/7	1 - 6.5 hrs/day	NA
Sykes, 1995	Exclusive	85	No	RGO	2 to 7 years (Usage time)	71.00%	25.88%	NA	Kids (<18): 15 hrs/week Adults (+18): 7 hrs/week	NA
Bernardi, 1995	Exclusive	33	No	RGO	3 years	33.33%	15.15%	NA	2 hrs/day	NA
Franceschini, 1997	Uncontrolled Comparitive	74	Yes	RGO, ARGO and HGO	6 months	32.43%	12.16%	NA	NA	39 days
Merati, 2000	Uncontrolled Comparitive	14	No	RGO, PW and RGO+FES	4 years	78.57%	NA	RGO - 3/6 RGO+FES - 0/4 PW - 0/4	NA	NA

<sup>&</sup>lt;sup>1</sup> RGO-Reciprocating Gait Orthosis, HGO-Hip Guidance Orthosis, ARGO-Advanced Reciprocating Gait Orthosis, PW-ParaWalker, FES-Functional Electrical Stimulation

Just because one has the skill it doesn't mean everyone will perform better, this where the factor of motivation comes into play. There is no standard tool to measure the motivation level of an individual or the people around him. The training time, psychological health of a person and the external support he/she gets also has a strong influence. It was also mentioned in literature that there is quite a difference in rejection rates between people who are able to climb stairs with the help of a RGO at the end of their training program and those who can't [22].

Speaking about rejection rates, there are various factors come in to the picture, some of the factors are functionality, ergonomics, time to don/doff, reliability, peer pressure etc. A product might have a good design, but it can still fail in the market due to improper promotion[3]. There might be instance where the customer might have a higher expectation. Since the orthosis doesn't meet their level of expectations, it might be discarded or it can also be abandoned for no reason.

It is clear that the subject's performance doesn't purely depend on the RGO, there are other factors like training time, and type of training, psychological factors, other physical factors like the lesion level, patient's upper body strength, weight of the patient does have influence over the performance characteristics. Some of the studies do give information about the patient's lesion level, hours of training or usage, etc. but they don't take these factors into account. We should start to use system identification techniques, and try to solve the problem with open system approach.

In recent times mathematical models and new (hybrid) orthotic solutions are experimented and these RGOs seem improve the gait parameters [44-48, 63-65]. These designs are still in prototyping stage. Some of their outcomes do seem promising, but further investigation is required to learn more about their energy cost, endurance level, and price. There is no point in selling a new RGO to a customer/patient that would allow him to walk with the same speed, comfort and energy cost of the previous RGO models, but only with a higher initial and maintenance cost.

#### **CONCLUSION**

In order to give a precise overall picture about the current state of RGOs is quite a complex and puzzling task. In terms of rejection rates and performance characteristics of a RGO there is no clear conclusion. One could say the patient is likely to abandon the RGO due to the high energy demand; at times the aspect of cosmesis and comfort also comes into play, but there is no statistical proof for that. The patients see the RGO more of a therapeutic device and the wheelchair as a conventional way to ambulate. The orthosis is an assistive device, in a man-machine system it's not only the machine that should be taken into account, so the human factor does plays an important role. More standardized experiments need to be conducted, so that they could be used to compare with other studies and a proper conclusion could be achieved in future. In the end the aspiration is to have a better quality of life. In order to do those, as designer we need to improve the device to meet the customer needs, at the same time the customer should also be made aware of the limitations of what one could achieve with the current technology.

#### **REFERENCES**

- 1. Cooper, R.A., H. Ohnabe, and D.A. Hobson, *An introduction to rehabilitation engineering*. 2006: CRC Press. isbn. 0849372224.
- 2. Lin, V.W. and C.M. Bono, *Spinal cord medicine: principles and practice*. 2010: Demos Medical Publishing. isbn. 1935281771.

Literature Review 85

- 3. Stallard, J. and R. Major, *A review of reciprocal walking systems for paraplegic patients: factors affecting choice and economic justification.* Prosthetics and orthotics international, 1998. **22**(3): p. 240-247.
- 4. Robb, J., L. Gordon, D. Ferguson, Z. Dunhill, R. Elton, and R. Minns, *A comparison of hip guidance with reciprocating gait orthoses in children with spinal paraplegia: results of a ten-year prospective study.* European Journal of Pediatric Surgery, 1999. **9**(S 1): p. 15-18.
- 5. Sykes, L., J. Edwards, E.S. Powell, and E.R.S. Ross, *The reciprocating gait orthosis: long-term usage patterns.* Archives of physical medicine and rehabilitation, 1995. **76**(8): p. 779-783.
- 6. Merati, G., P. Sarchi, M. Ferrarin, A. Pedotti, and A. Veicsteinas, *Paraplegic adaptation to assisted-walking:* energy expenditure during wheelchair versus orthosis use. Spinal cord, 2000. **38**(1): p. 37-44.
- 7. Bowker, P., N. Messenger, C. Ogilvie, and D. Rowley, *Energetics of paraplegic walking*. Journal of biomedical engineering, 1992. **14**(4): p. 344-350.
- 8. Bernardi, M., I. Canale, V. Castellano, L. Di Filippo, F. Felici, and M. Marchetti, *The efficiency of walking of paraplegic patients using a reciprocating gait orthosis.* Paraplegia, 1995. **33**(7): p. 409-415.
- 9. Ditunno, J., W. Young, W. Donovan, and G. Creasey, *The international standards booklet for neurological and functional classification of spinal cord injury.* Spinal Cord, 1994. **32**(2): p. 70-80.
- 10. Sandler, A., *Living with spina bifida: A guide for families and professionals*. 2004: Univ of North Carolina Press. isbn. 0807855472.
- 11. Rosenbaum, P., N. Paneth, A. Leviton, M. Goldstein, M. Bax, D. Damiano, B. Dan, and B. Jacobsson, *A report:* the definition and classification of cerebral palsy April 2006. Dev Med Child Neurol Suppl, 2007. **109**(suppl 109): p. 8-14.
- 12. Emery, A.E., *The muscular dystrophies*. The Lancet, 2002. **359**(9307): p. 687-695.
- 13. Hart, D., Orthoses or prostheses for coordinating limb movement. 1990, Google Patents.
- 14. Poplawski, C., *Hip-reciprocating apparatus*. 1990, Google Patents.
- 15. Dall, P. and M. Granat, *The function of the reciprocal link in paraplegic orthotic gait.* JPO: Journal of Prosthetics and Orthotics, 2001. **13**(1): p. 10-13.
- 16. Moore, P., *The ParaWalker: walking for thoracic paraplegics.* Physiotherapy Theory and Practice, 1988. **4**(1): p. 18-22.
- 17. Rose, G., J. Stallard, and M. Sankarankutty, *Clinical evaluation of spina bifida patients using hip guidance orthosis*. Developmental Medicine & Child Neurology, 1981. **23**(1): p. 30-40.
- 18. Saitoh, E., T. Suzuki, S. Sonoda, J. Fujitani, Y. Tomita, and N. Chino, *Clinical Experience With A New Hip-Knee-Ankle-Foot Orthotic System Using A Medial Single Hip Joint for Paraplegic Standing and Walking1*. American journal of physical medicine & rehabilitation, 1996. **75**(3): p. 198-203.
- 19. Arazpour, M., M.A. Bani, and S.W. Hutchins, *Reciprocal gait orthoses and powered gait orthoses for walking by spinal cord injury patients*. Prosthetics and orthotics international, 2013. **37**(1): p. 14-21.
- 20. Lotta, S., A. Fiocchi, R. Giovannini, R. Silvestrin, L. Tesio, A. Raschi, L. Macchia, V. Chiapatti, M. Zambelli, and C. Tosi, *Restoration of gait with orthoses in thoracic paraplegia: a multicentric investigation.* Paraplegia, 1994. **32**(9): p. 608-15.
- 21. Phillips, D., R. Field, N. Broughton, and M. Menelaus, *Reciprocating orthoses for children with myelomeningocele*. *A comparison of two types*. Journal of Bone & Joint Surgery, British Volume, 1995. **77**(1): p. 110-113.
- 22. Franceschini, M., S. Baratta, M. Zampolini, D. Loria, and S. Lotta, *Reciprocating gait orthoses: a multicenter study of their use by spinal cord injured patients.* Archives of physical medicine and rehabilitation, 1997. **78**(6): p. 582-586.
- 23. Thomas, S.S., C.E. Buckon, J. Melchionni, M. Magnusson, and M.D. Aiona, *Longitudinal assessment of oxygen cost and velocity in children with myelomeningocele: comparison of the hip-knee-ankle-foot orthosis and the reciprocating gait orthosis.* Journal of Pediatric Orthopaedics, 2001. **21**(6): p. 798-803.
- 24. Bernardi, M., I. Canale, F. Felici, A. Macaluso, P. Marchettoni, and E. Sproviero, *Ergonomy of paraplegic patients working with a reciprocating gait orthosis.* Spinal Cord, 1995. **33**(8): p. 458-463.

- 25. Bernardi, M., A. Macaluso, E. Sproviero, V. Castellano, D. Coratella, F. Felici, A. Rodio, M. Piacentini, M. Marchetti, and J. Ditunno Jr, *Cost of walking and locomotor impairment*. Journal of Electromyography and Kinesiology, 1999. **9**(2): p. 149-157.
- 26. Jagacinski, R.J. and J.M. Flach, *Control theory for humans: Quantitative approaches to modeling performance*. 2002: CRC Press. isbn. 1135690227.
- 27. Winchester, P., J. Carollo, R. Parekh, L. Lutz, and J. Aston, *A comparison of paraplegic gait performance using two types of reciprocating gait orthoses.* Prosthetics and Orthotics International, 1993. **17**(2): p. 101-106.
- 28. Ijzerman, M., G. Baardman, H. Hermens, P. Veltink, H. Boom, and G. Zilvold, *The influence of the reciprocal cable linkage in the advanced reciprocating gait orthosis on paraplegic gait performance.* Prosthetics and orthotics international, 1997. **21**(1): p. 52-61.
- 29. Harvey, L.A., G.M. Davis, M.B. Smith, and S. Engel, *Energy expenditure during gait using the walkabout and isocentric reciprocal gait orthoses in persons with paraplegia.* Archives of physical medicine and rehabilitation, 1998. **79**(8): p. 945-949.
- 30. Leung, A.K., A.F. Wong, E.C. Wong, and S.W. Hutchins, *The Physiological Cost Index of walking with an isocentric reciprocating gait orthosis among patients with T(12) L(1) spinal cord injury.* Prosthet Orthot Int, 2009. **33**(1): p. 61-8.
- 31. Cuddeford, T.J., R.P. Freeling, S.S. Thomas, M.D. Aiona, D. Rex, H. Sirolli, J. Elliott, and M. Magnusson, *Energy consumption in children with myelomeningocele: a comparison between reciprocating gait orthosis and hip–knee–ankle–foot orthosis ambulators*. Developmental Medicine & Child Neurology, 1997. **39**(4): p. 239-242.
- 32. Katz, D.E., N. Haideri, K. Song, and P. Wyrick, *Comparative study of conventional hip-knee-ankle-foot orthoses versus reciprocating-gait orthoses for children with high-level paraparesis.* Journal of Pediatric Orthopaedics, 1997. **17**(3): p. 377-386.
- 33. Abe, K., Comparison of static balance, walking velocity, and energy consumption with knee-ankle-foot orthosis, walkabout orthosis, and reciprocating gait orthosis in thoracic-level paraplegic patients. JPO: Journal of Prosthetics and Orthotics, 2006. **18**(3): p. 87-91.
- 34. Harvey, L.A., M.B. Smith, G.M. Davis, and S. Engel, *Functional outcomes attained by T9-12 paraplegic patients with the walkabout and the isocentric reciprocal gait orthoses.* Archives of physical medicine and rehabilitation, 1997. **78**(7): p. 706-711.
- 35. Jefferson, R. and M. Whittle, *Performance of three walking orthoses for the paralysed: a case study using gait analysis.* Prosthetics and Orthotics International, 1990. **14**(3): p. 103-110.
- 36. Whittle, M.W., G.M. Cochrane, A.P. Chase, A.V. Copping, R.J. Jefferson, D.J. Staples, P.T. Fenn, and D.C. Thomas, *A comparative trial of two walking systems for paralysed people.* Paraplegia, 1991. **29**(2): p. 97-102.
- 37. Phillips, C., *Electrical muscle stimulation in combination with a reciprocating gait orthosis for ambulation by paraplegics*. Journal of biomedical engineering, 1989. **11**(4): p. 338-344.
- 38. Isakov, E., R. Douglas, and P. Berns, *Ambulation using the reciprocating gait orthosis and functional electrical stimulation*. Spinal Cord, 1992. **30**(4): p. 239-245.
- 39. Beillot, J., F. Carre, G. Le Claire, P. Thoumie, B. Perruoin-Verbe, A. Cormerais, A. Courtillon, E. Tanguy, G. Nadeau, and P. Rochcongar, *Energy consumption of paraplegic locomotion using reciprocating gait orthosis.* European journal of applied physiology and occupational physiology, 1996. **73**(3-4): p. 376-381.
- 40. Spadone, R., G. Merati, E. Bertocchi, E. Mevio, A. Veicsteinas, A. Pedotti, and M. Ferrarin, *Energy consumption of locomotion with orthosis versus Parastep-assisted gait: a single case study.* Spinal cord, 2003. **41**(2): p. 97-104.
- 41. Phillips, C., J. Gallimore, and D. Hendershot, *Walking when utilizing a sensory feedback system and an electrical muscle stimulation gait orthosis.* Medical engineering & physics, 1995. **17**(7): p. 507-513.
- 42. To, C., R. Kobetic, and R. Triolo. *Hybrid orthosis system with a variable hip coupling mechanism*. in *Engineering in Medicine and Biology Society, 2006. EMBS'06. 28th Annual International Conference of the IEEE*. 2006. IEEE.

Literature Review

87

- 43. To, C.S., R. Kobetic, J.R. Schnellenberger, M.L. Audu, and R.J. Triolo, *Design of a variable constraint hip mechanism for a hybrid neuroprosthesis to restore gait after spinal cord injury.* Mechatronics, IEEE/ASME Transactions on, 2008. **13**(2): p. 197-205.
- 44. Kobetic, R., C.S. To, J.R. Schnellenberger, M.L. Audu, T.C. Bulea, R. Gaudio, G. Pinault, S. Tashman, and R.J. Triolo, *Development of hybrid orthosis for standing, walking, and stair climbing after spinal cord injury.* J Rehabil Res Dev, 2009. **46**(3): p. 447-62.
- 45. To, C.S., R. Kobetic, T.C. Bulea, M.L. Audu, J.R. Schnellenberger, G. Pinault, and R.J. Triolo, *Sensor-Based Stance Control With Orthosis and Functional Neuromuscular Stimulation for Walking After Spinal Cord Injury.* JPO: Journal of Prosthetics and Orthotics, 2012. **24**(3): p. 124-132.
- 46. Rasmussen, A.A., K.M. Smith, and D.L. Damiano, *Biomechanical evaluation of the combination of bilateral stance-control knee-ankle-foot orthoses and a reciprocating gait orthosis in an adult with a spinal cord injury.* JPO: Journal of Prosthetics and Orthotics, 2007. **19**(2): p. 42-47.
- 47. Bani, M.A., M. Arazpour, F.T. Ghomshe, M.E. Mousavi, and S.W. Hutchins, *Gait evaluation of the advanced reciprocating gait orthosis with solid versus dorsi flexion assist ankle foot orthoses in paraplegic patients*. Prosthet Orthot Int, 2013. **37**(2): p. 161-7.
- 48. Arazpour, M., M. Gharib, S.W. Hutchins, M.A. Bani, S. Curran, M.E. Mousavi, and H. Saberi, *The influence of trunk extension in using advanced reciprocating gait orthosis on walking in spinal cord injury patients: A pilot study.* Prosthet Orthot Int, 2014.
- 49. Ohta, Y., H. Yano, R. Suzuki, M. Yoshida, N. Kawashima, and K. Nakazawa, *A two-degree-of-freedom motor-powered gait orthosis for spinal cord injury patients*. Proceedings of the Institution of Mechanical Engineers, Part H: Journal of Engineering in Medicine, 2007. **221**(6): p. 629-639.
- 50. Arazpour, M., A. Chitsazan, S.W. Hutchins, F.T. Ghomshe, M.E. Mousavi, E.E. Takamjani, G. Aminian, M. Rahgozar, and M.A. Bani, *Evaluation of a novel powered hip orthosis for walking by a spinal cord injury patient: a single case study.* Prosthetics and Orthotics International, 2012. **36**(1): p. 105-112.
- 51. Arazpour, M., A. Chitsazan, S.W. Hutchins, M.E. Mousavi, E.E. Takamjani, F.T. Ghomshe, G. Aminian, M. Rahgozar, and M.A. Bani, *Evaluation of a novel powered gait orthosis for walking by a spinal cord injury patient.* Prosthetics and orthotics international, 2012. **36**(2): p. 239-246.
- 52. Arazpour, M., M.A. Bani, R.V. Kashani, F.T. Ghomshe, M.E. Mousavi, and S.W. Hutchins, *Effect of powered gait orthosis on walking in individuals with paraplegia*. Prosthetics and orthotics international, 2013. **37**(4): p. 261-267.
- 53. Felici, F., M. Bernardi, A. Rodio, P. Marchettoni, V. Castellano, and A. Macaluso, *Rehabilitation of walking for paraplegic patients by means of a treadmill*. Spinal cord, 1997. **35**(6): p. 383-385.
- 54. Ijzerman, M.J., G. Baardman, H.J. Hermens, P.H. Veltink, H.B. Boom, and G. Zilvold, *Speed dependence of crutch force and oxygen uptake: implications for design of comparative trials on orthoses for people with paraplegia*. Archives of physical medicine and rehabilitation, 1998. **79**(11): p. 1408-1414.
- 55. Ijzerman, M.J., G. Baardman, M.A. van't Hof, H.B. Boom, H.J. Hermens, and P.H. Veltink, *Validity and reproducibility of crutch force and heart rate measurements to assess energy expenditure of paraplegic gait.*Archives of physical medicine and rehabilitation, 1999. **80**(9): p. 1017-1023.
- 56. Nakazawa, K., W. Kakihana, N. Kawashima, M. Akai, and H. Yano, *Induction of locomotor-like EMG activity in paraplegic persons by orthotic gait training.* Exp Brain Res, 2004. **157**(1): p. 117-23.
- 57. Kawashima, N., D. Taguchi, K. Nakazawa, and M. Akai, *Effect of lesion level on the orthotic gait performance in individuals with complete paraplegia*. Spinal Cord, 2006. **44**(8): p. 487-94.
- Johnson, W.B., S. Fatone, and S.A. Gard, *Walking mechanics of persons who use reciprocating gait orthoses.*Journal of Rehabilitation Research and & development, 2009. **46**(3): p. 435-446.
- 59. Karimi, M.T., O. Esrafilian, A. Esrafilian, M.J. Sadigh, and P. Amiri, *Determination of the influence of walking with orthosis on bone osteoporosis in paraplegic subjects based on the loads transmitted through the body.* Clinical Biomechanics, 2013.

- 60. Dall, P., B. Müller, I. Stallard, J. Edwards, and M. Granat, *The functional use of the reciprocal hip mechanism during gait for paraplegic patients walking in the Louisiana State University reciprocating gait orthosis.*Prosthetics and orthotics international, 1999. **23**(2): p. 152-162.
- 61. To, C., R. Kirsch, R. Kobetic, and R. Triolo. *The feasibility of a functional neuromuscular stimulation powered mechanical gait orthosis with coordinated joint locking*. in *Engineering in Medicine and Biology Society, 2004. IEMBS'04. 26th Annual International Conference of the IEEE*. 2004. IEEE.
- 62. To, C.S., R.F. Kirsch, R. Kobetic, and R.J. Triolo, *Simulation of a functional neuromuscular stimulation powered mechanical gait orthosis with coordinated joint locking*. Neural Systems and Rehabilitation Engineering, IEEE Transactions on, 2005. **13**(2): p. 227-235.
- 63. Johnson, W., S. Fatone, and S. Gard. *Modeling the walking patterns of reciprocating gait orthosis users with a novel lower limb paralysis simulator*. in *Engineering in Medicine and Biology Society, EMBC, 2011 Annual International Conference of the IEEE*. 2011. IEEE.
- 64. Nakhaee, K., F. Farahmand, and H. Salarieh, *Studying the effect of kinematical pattern on the mechanical performance of paraplegic gait with reciprocating orthosis.* Proceedings of the Institution of Mechanical Engineers, Part H: Journal of Engineering in Medicine, 2012: p. 0954411912447717.
- 65. Johnson, W.B., S. Fatone, and S.A. Gard, *Modeling effects of sagittal-plane hip joint stiffness on reciprocating gait orthosis-assisted gait.* J Rehabil Res Dev, 2013. **50**(10): p. 1449-56.

Literature Review

89